博士論文

Dynamics of Terrigenous Dissolved Organic Matter in the Marine Environments

（海洋環境中における陸起源溶存態有機物の動態）

Chia-Jung Lu

呂 佳蓉

東京大学大学院新領域創成科学研究科

Graduate School of Frontier Science

The University of Tokyo

2016 年 9 月

ACKNOLEDGEMENTS

I am deeply thankful to my doctoral advisor Assoc. Prof. Hiroshi Ogawa who introduced me to an exciting science and opened up many opportunities to broaden my expertise. Marine Biogeochemistry was new to me and I truly appreciate Assoc. Prof. Ogawa offered this wonderful opportunity.

I also wish to thank Assoc. Prof. Hideki Fukuda (AORI, The University of Tokyo) for his kind help, support and wonderful suggestions to improve my dissertation. Moreover, I would like to thank Prof. Toshi Nagata, Assoc. Prof. Hajime Obata and Assoc. Prof. Juichiro Ashi (AORI, The University of Tokyo) for being a part of my dissertation committee and providing me the constructive advice.

In addition, this study would not have been possible without the help from Prof. Ronald Benner, Dr. Cédric G. Fichot and Mr. Yuan Shen (Dept. of Biological Sciences and Marine Science Program, University of South Carolina), and Assoc. Prof. Youhei Yamashita (Faculty of Environmental Earth Science, Hokkaido University). I also thank them for their support and for always answering my frequent questions.

Furthermore, I would like to express my gratitude to the members of Marine Biogeochemistry Group, AORI, The University of Tokyo. I am grateful for their support, expertise and helpfulness.

Finally, I would like to thank my family for their warmhearted support throughout my life.

TABLE OF CONTENTS

Chapter 1
General Introduction

1.1. Terrigenous dissolved organic matter (tDOM) in the ocean

Dissolved organic matter (DOM) in the ocean presents one of the largest reservoirs of organic material and exchangeable carbon (ca. 662 ± 32 Pg C) at the Earth's surface (Carlson and Hansell, 2015). It is operational defined as organic matter that passes through a given pore size filter such as 0.7-µm Whatman® GF/F filter or 0.2-µm plastic filters (typically track-etched polycarbonate) (Ogawa and Tanoue, 2003; Carlson and Hansell, 2015). DOM plays an important role in marine biogeochemical cycles, and it contains many biologically identifiable classes of compounds such as sugars, amino acids and humics (Hansell and Carlson, 2001). Understanding the role of DOM in marine environment can advance our knowledge in the global carbon cycle. Fig 1-1 shows sources and sinks of DOM in the ocean, DOM is controlled by several factors including biological, chemical, and physical parameters, but biotic removal process is the primary consumption process of DOM in marine environment (Carlson and Hansell, 2015). Generally, the sources of DOM in the ocean include marine and terrestrial origins. Marine DOM is widely defined as organic matter that is produced by biological processes throughout water column in the ocean. Terrigenous DOM (tDOM) is terrestrial derived material which is transported through river into to the ocean (Fig. 1-1).

The annual global riverine flux of particle and dissolved organic carbon is ~0.4 Pg C (Schlesinger and Melack, 1981), and the annual marine POC (at 100 m) is ~7 Pg C (Hedges, 1992). Although those are the small fractions compared with the global net primary production (~50 Pg C year^{-1}) in marine environment, tDOM represents a huge source of reduced carbon to the ocean, integrates drainage basin processes, and incorporates bioactive elements whose cycling modulates the biosphere over geological time (Hedges 1992; Hedges et al., 1997). Previous studies suggested tDOM is humic-like substance and accompanied with high fluorescence, photosensitive, high molecular

weight and relatively resistant to microbial degradation (compare with photodegradation) (Coble, 1996; Hernes and Benner, 2003; Helmns et al., 2008; Yamashita and Tanoue, 2008; Spencer et al., 2009; Benner and Kaiser, 2011). It is well known that tDOM usually has high C/N molar ratios and high concentrations of aromatic carbon, and depleted stable carbon isotope ratios ($\delta^{13}C$) compared with marine DOM (Benner at al., 1992; Opsahl and Benner, 1997), however, these information of chemical characteristics are deficient in quantifying terrigenous origins within marine DOM because regional variability in DOM sources and diagenesis are unclear (Opsahl and Benner, 1997). Therefore, a direct evidence of tDOM, such as lignin phenols, is very important to distinguish the "real terrestrial matter" in the ocean. Lignin is a biopolymer found only in terrestrial vascular plant and its chemical characteristic is not influenced by other marine DOM in waters. Numerous studies used lignin phenols as the tracer of tDOM and found lignin is susceptible to photochemical process (Spencer et al., 2009; Hernes and Benner, 2003; Fichot and Benner, 2012). However, the recent lignin investigations have demonstrated biodegradation is the main removal process in rivers and river-influenced ocean margins (Ward et al., 2013; Fichot and Benner, 2014). Furthermore, regardless of photodegradation and biodegradation, previous lignin studies suggested tDOM is rapidly removed in the ocean margin regions (Opsahl and Benner, 1997; Hedges et al., 1997). The regeneration nutrients, which were caused by tDOM consumption processes, often limit primary production in the coastal ocean and it accounts for ~25% of global ocean productivity (Opsahl and Benner, 1997). Numerous investigations suggested tDOM is chromorphoic chemical components and found the good relations between tDOM and optical data (including absorption and fluorescence) (Coble 1996; Fichot and Benner, 2012; Spencer et al., 2012; Yamashita and Tanoue, 2008), therefore, study DOM optical properties can help us to have a better understanding of tDOM in the ocean. DOM optical properties were also measured in this study to investigate the relationships between tDOM, lignin and DOM optical properties. On the other hand, tDOM accompanied with bioactive trace metals and discharge to the ocean. This indicates that although tDOM is a small fraction of bulk DOM in the ocean (Opsahl and Benner, 1997), tDOM still plays an important role in global biogeochemical cycles.

1.2. What is lignin?

Lignin is a phenolic polymer and only occurs in cell walls of vascular plants. Lignin is essentially absent from all other living organism in the ocean, therefore, lignin has potential for indicating the presence of land-derived organic matter in the marine environments (Hedges and Mann, 1979; Meyers-Schulte and Hedges, 1986; Opsahl and Benner, 1998). Lignin is the most abound biopolymers on land, and it contains 15–40% carbon in vascular and woody plant. Although tannin is another unique biomarker of vascular plant, the carbon amount in tannin is less than 20% and 45% in vascular and woody plants, respectively (Whitehead, 2008).

Lignin-derived phenols are characterized on the basis of cupric oxide (CuO) oxidation products as shown in Fig. 1-2, and those can reflect the amount and sources of parent polymer. Nine major phenols include *p*-hydroxy, vanillyl and syringyl groups in the forms of aldehydes, ketones and carboxylic acid (Hedges and Mann, 1979; Hedges et al., 1988). Cinnamyl phenols, including ferulic and *p*-coumaric acids, are also produces by CuO oxidation from nonwoody vascular plant tissues (Hedges and Mann, 1979; Kaiser and Benner, 2011). The benzene ring of lignin structure units (a phenolic ring and three-carbon side chain) are substituted by 0, 1 or 2 methoxy ($-OCH_3$) groups as like *p*-hydroxy (P), vanillyl (V) and syringyl (S) phenols, respectively (Fig. 1-2). Two cinnamyl phenols (C) are the original lignin structure and terminate in zero or one carboxyl (Fig. 1-2).

Because almost all gymnosperms produce only vanillyl phenols, and angiosperms (flowering plants) produce syringyl phenols and also vanillyl counterparts, S/V ratios is used to distinguish between gymnosperm and angiosperm sources (Hedges and Mann, 1979). C/V ratios are used to discriminate between woody and non-woody vascular plants tissues due to only non-woody plant produces significant amount of cinnamyl phenols (Hedges and Mann, 1979). The compound 3,5-dihydrobenzoic acid (DiOHBA) (Fig. 1-2) was included in the open-ocean study because it is a major CuO oxidation product in humic matter and was proposed to be an indicator of soil organic matter in marine and freshwater environment (Dickens et al., 2007; Benner and Kaiser, 2011; Kaiser and Benner, 2011). Ratios of lignin phenols are also used as the indicators of

tDOM degradation. Previous studies of incubation experiment of river samples suggested photochemical and biological processes increase or decrease the ratios of lignin phenols (Opsahl and Benner, 1998; Spencer et al., 2009; Benner and Kaiser, 2011).

1.3. What is chromophoric dissolved organic matter (CDOM)?

Chromorphoric dissolved organic matter (CDOM) is the fraction of DOM that adsorbs ultraviolet (UV) and visible light, and it is ubiquitous in marine waters and plays an important role in marine biogeochemical cycles (Helms et al., 2008; Nelson et al., 2010; Yamashita et al., 2013). CDOM has been widely studied in the sources and sinks of DOM in the ocean (Nelson et al., 1998; Cobles 2007; Helms et al., 2008; Yamashita and Tanoue, 2009), and it is recognized as allochthonous or autochthonous inputs in the marine environment (Stedmon and Nelson, 2015). Figure 1-3 represents the primary sources and sinks of CDOM in the ocean. River is the most important source of terrestrial humic materials and it dominates CDOM "concentrations" (the absorption intensity of CDOM) in estuarine and coastal regions. Sediment releasing may be significant local sources of CDOM in coastal regions, but deep sea sediment is not a significant source (Blought and Del Vecchio, 2002; Nelson and Siegel, 2012). In additional, upwelling of subsurface water is a possible transport pathway of CDOM in coastal regions (Coble, 2007). However, CDOM does not significantly correlate with chlorophyll in coastal waters, but *in-situ* productivity is the primary CDOM sources in open ocean regions. Phytoplankton are not the directly sources of CDOM, these are transformed to CDOM due to microbial decomposition of heterotrophic bacteria (Nelson et al., 1998; Coble, 2007; Blough and Del Vecchio; 2002). The removal pathways of CDOM in the ocean include photobleaching and microbial processes. Photobleaching acts as a significant sink of CDOM, and microbial decomposition is lesser importance (Blough and Del Vecchio, 2002; Coble, 2007; Helms et al., 2008). In addition, physical mixing of river waters and seawater is another factor controlling CDOM distribution and conservative behavior in coastal regions (Blough and Del Vecchio, 2002; Stedmon and Markager, 2003; Coble, 2007).

Estimates of the CDOM contribution to total DOC in the ocean have ranged from 20–70%, which are highest values in coastal regions and that is dominant by river input, and values at the lower end of the range are in open ocean areas (Coble, 2007). However, we still poorly understand the chemical structure and dynamics of CDOM in seawater. It is well known that CDOM is the optical properties of most natural water and CDOM provides us with the information of the bulk DOM, which undergoes chemical, biological and even physical processes (Coble, 2007; Helms et al., 2008).

CDOM absorption spectra decrease exponentially with increasing wavelength and those vary depending on its source (Fig. 1-4). CDOM absorption spectra have typically fitted these spectra to an exponential function (1):

$$a(\lambda) = a(\lambda_i)e^{-S(\lambda-\lambda_i)} \quad (1)$$

where $a(\lambda)$ and $a(\lambda_i)$ are the absorption coefficients at wavelength λ and reference wavelength λ_i (m^{-1}), respectively. S is the spectral slope coefficients (nm^{-1}) over the corresponding spectral range (λ-λ_i). Absorption coefficients $a(\lambda)$ are calculated from the equation (2):

$$a(\lambda) = 2.303A(\lambda)/r \quad (2)$$

where A is the optical density measured at wavelength λ across pathlength, r (m). The fitting of absorption data to Eq. (1) has proved quite useful as a simple means to characterize CDOM spectral rapidly (Blough and Del Vecchio, 2002).

CDOM spectral slope (S) is usually calculated because of predominant loss of absorption at shorter wavelength and decreased steepness in the spectrum (Coble, 2007), higher S values infer absorption decline rapidly with longer wavelength. Difference in S values can indicate CDOM origin, with generally lower S values in freshwater or coastal water than in marine environment (Coble, 2007; Helms et al., 2008; Yamashita et al., 2013). In addition, numerous studies found difference in S values also indicate DOM photobleaching transformation in waters (Helms et al., 2008, Fichot and Benner, 2012; Yamashita et al., 2013).

1.4. Relationship between tDOM, lignin and CDOM

To our knowledge, little is known regarding the connections between tDOM and CDOM. tDOM was investigated by lignin phenols in river, river-influenced coast area and open ocean because lignin is unique of terrestrial organic matter, and numerous studies found lignin is susceptible to solar irradiation (Opsahl and Benner, 1997; Hernes and Benner, 2002, 2003; Spencer et al., 2009; Amon et al., 2012; Fichot and Benner, 2012, 2014; Ward et al., 2013). CDOM was used to trace terrestrial and marine DOM and DOM alteration processes in marine environment (Swan et al., 2009; Yamashita and Tanoue, 2008, 2013), even though the compounds of CDOM are still unclear. CDOM optical properties were also investigated in Arctic rivers and found CDOM absorption is strongly corrected to DOC concentrations (Spencer et al., 2008, 2009). Additionally, the linear relationship was also observed between CDOM absorption and lignin concentrations in river-influenced margin (Hernes and Benner, 2003; Fichot and Benner, 2012). Fichot et al. (2011, 2016) utilized CDOM absorption to establish the models for predicting DOC and lignin concentrations in coastal ocean. Numerous studies found the good correlations between lignin and CDOM optical properties (Hernes and Benner, 2003; Spncer et al., 2008, 2009; Fichot and Benner, 2012), but those results only highlighted lignin is chromophore, the compounds of CDOM are still unclear. Stubbins et al. (2010) measured dissolved organic matter in the Congo River and also its photochemical alternation. Their results showed that a 90% loss in aromatic compounds (including lignin, tannin, and aromatic) and the photo-resistant fraction were aliphatic compounds. Therefore, tDOM and CDOM are overlap in some features but they are not completely same, and it needs more investigations to have a better understanding of the relationship between tDOM and CDOM.

1.5. Objectives of this study

On the basis of lignin is measured as tDOM in this study, the following questions will be discussed in each chapter,

(1) Numerous of tDOM studies have focused on the plumes of the major rivers in the world and found lignin is highly related with CDOM absorption in coastal regions (Opsahl et al., 1999; Benner and Opsahl, 2001; Amon et al., 2012; Fichot and Benner,

2014; Ward et al., 2013; Mann et al., 2014). In addition, tDOM transformation in coastal ocean is dominated by photodegradation and it is based on the trends of lignin ratios and CDOM parameters (Hernes and Benner, 2003; Fichot and Benner, 2012, 2016). However, most of the estuarine environments are not in large spatial scale as like the major large rivers systems. In this chapter, lignin phenols and CDOM optical properties were measured in Otsuchi Bay, where is a typical ria coastal environment and the terrestrial original is dominant by river input. Three rivers in this catchment are also included to investigate the dynamics of tDOM in a small spatial scale environment. It is crucial to distinguish the removal mechanism of tDOM in this bay such as photodegradation, biodegradation and/or other factors (see Chapter 2).

(2) Some previous river water incubation studies have pointed out that photodegradation is primarily responsible for losses of the lignin phenols components of tDOM (Opsahl and Benner, 1998; Herne and Benner, 2003; Stubbins et al., 2010; Benner and Kaiser, 2011). However, recent studies have demonstrated biodegradation is the main removal process of lignin phenols in rivers and river-influenced ocean margin (Ward et al., 2013; Fichot and Benner, 2014). Those investigations results imply the effect of biodegradation is possibly ignored or underestimated in previous incubation experiments, especially when the water residence time in *in-situ* environment is longer than laboratory incubation time. Additionally, the strong relationships between lignin and CDOM are based on lignin concentrations and CDOM optical properties results (Hernes and Benner, 2003; Fichot and Benner, 2012, 2016). However, it is still unclear regarding the removal pathways between lignin and CDOM, especially lignin is a chemical compound and CDOM is an optical property of the bulk DOM. In Chapter 3, photochemical and microbial processes of lignin and CDOM were investigated in decomposition experiment with river water and *in-situ* microbial assemblage exposed to natural sunlight or kept in the dark. Meanwhile, this incubation experiment was conducted with "considerable incubation time" (longer than the water residence time in real environment) to understand the complete processes of tDOM decomposition. This decomposition experiment can provide more evidence of lignin and CDOM undergoing photodegradation and biodegradation, and also include the degradation pathways (see Chapter 3).

(3) Although previous studies have suggested ocean margin is the major and important hot spot for tDOM transformation because the concentrations of lignin, the direct evidence of tDOM, is very low in the open ocean (0.7–2.4%), and that couples with a much shorter oceanic residence time (Atlantic: 21–93 year, Pacific: 29–132 year) compared with marine DOM (Hedges et al., 1997; Opsahl and Benner, 1997). However, once tDOM sinks quickly into deeper layer after exporting to the ocean, tDOM could reside in the ocean and transport for a long distance. Because solar irradiance effect is minor and temperature is low in deep seawater layer, tDOM is protected from photodegradation and biodegradation. Therefore, tDOM can transport to more open-ocean environment.

It is well known that North Pacific Intermediate water (NPIW) is the terrestrial water mass and its original terrestrial source is from the Amur River (Tally, 1991; Yasuda, 2004, Nishioka et al., 2014). Numerous studies found the chemical characteristics of terrestrial matter in NPIW including rich contains in organic carbon, humic substance, and dissolved Fe (Nakatsuka et al., 2004; Yamashita and Tanoue, 2008; Nishiola et al., 2013), however, it still lacks the direct terrestrial evidence, such as lignin phenols. Lignin and CDOM were measured to investigate NPIW in the western North Pacific Ocean, and those two tracers can indicate the distribution of NPIW and also the diagenesis of tDOM in the ocean (see Chapter 4). In additional, a notable hypothesis of tDOM is organic ligands for trace metal in the ocean (Rue et al., 1995). However, the direct evidence of organic ligands is lacking. The terrestrial chemical characters in NPIW (Nakatsuka et al., 2004; Yamashita and Tanoue, 2008; Nishiola et al., 2013) imply tDOM may act as organic ligands with bioactive trace metals in the ocean. Therefore, lignin analysis can help us have a better understanding of this hypothesis (see Chapter 4)

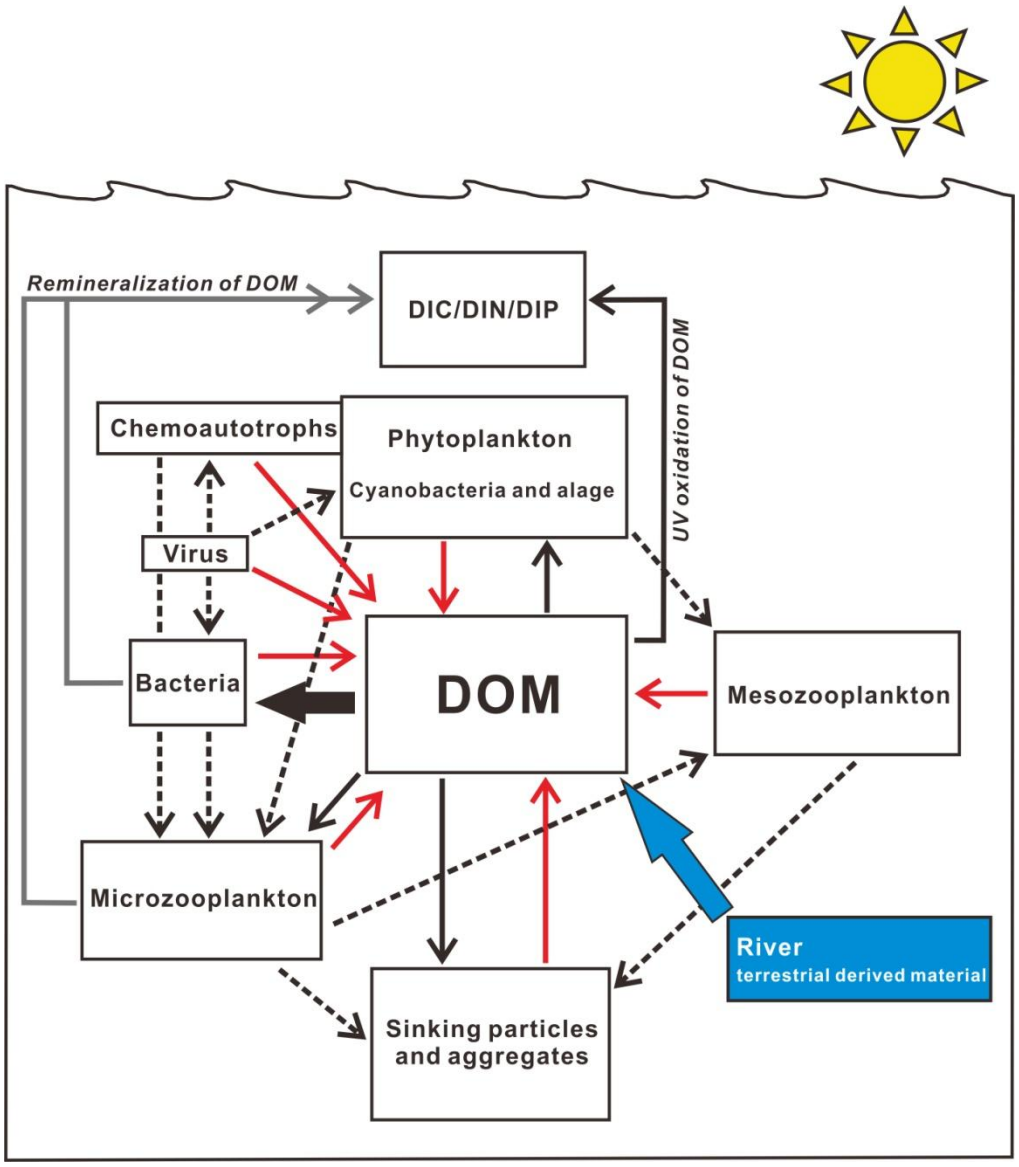

Fig. 1-1 Schematic diagram indicating sources and sinks of dissolved organic matter (DOM) in marine system. Dashed lines represent food wed interactions. Red and black solid arrows represent DOM production and consumption, respectively. The large black arrow is the dominant biotic removal, uptake by heterotrophic prokaryotes. Blue solid arrow and shade represent allochthonous input from terrestrial environment, and that is terrestrial derived materials input by river. Modified from Carlson and Hansell (2015).

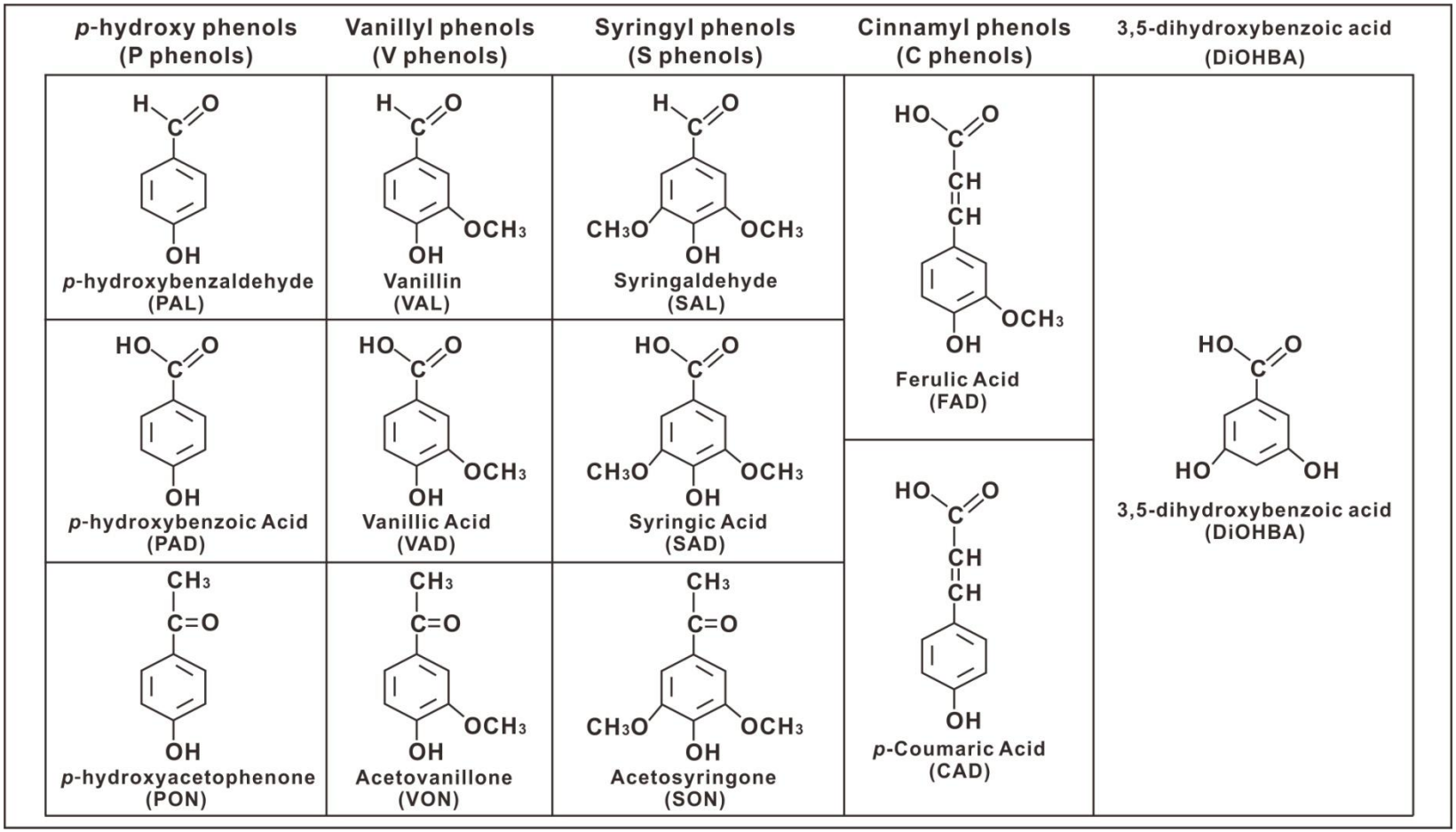

Fig. 1-2 Names, structures, and abbreviations of *p*-hydroxy, vanillyl, syringyl and cinnnmyla phenols derived from alkaline CuO oxidation method. Modified from Hedges et al. (1988) and Opsahl and Benner (1998).

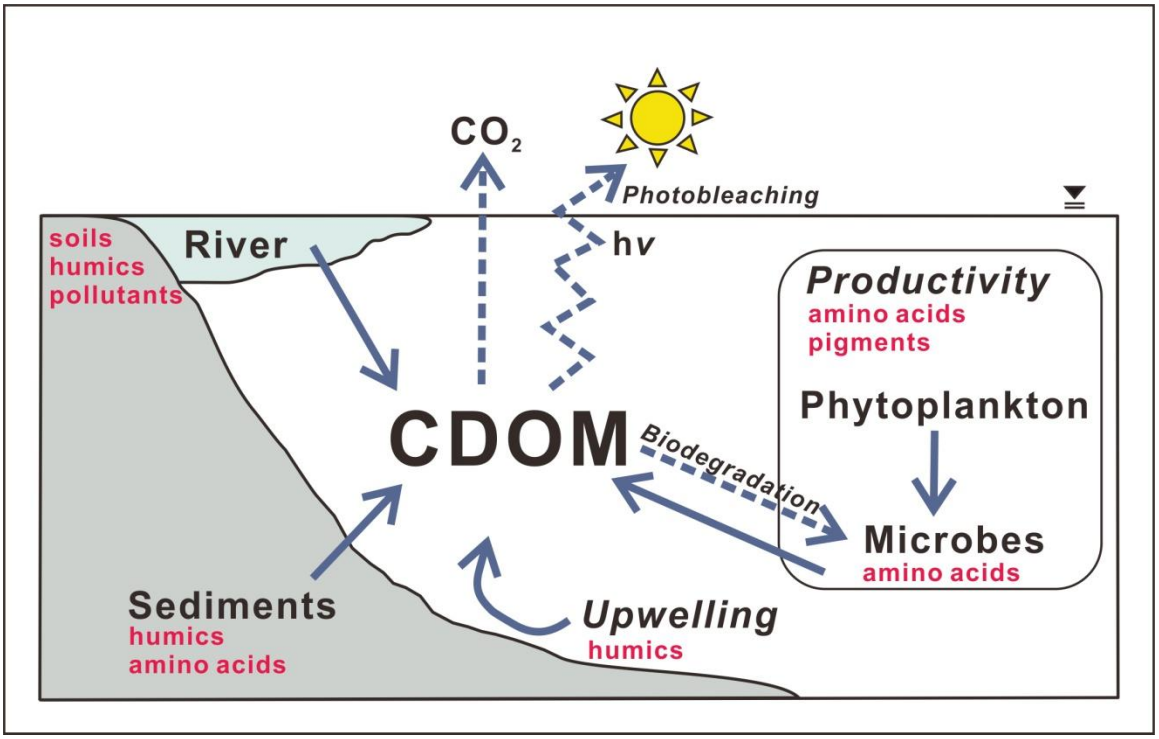

Fig. 1-3 Schematic diagram indicating sources and sinks of chromorphoric dissolved organic matter (CDOM) to the ocean. The solid arrows represent the sources including river input, sediment releasing and *in-situ* productivity. The dashed arrows represent the removal pathways of CDOM including photobleaching and biodegradation. Modified from Coble (2007).

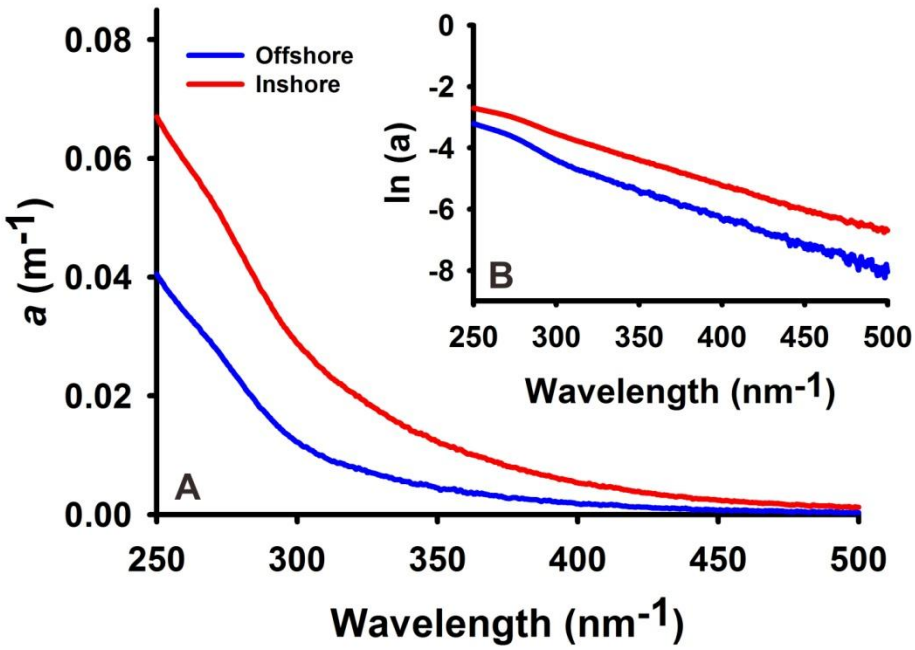

Fig. 1-4 Typical absorption spectrum in offshore and inshore waters those were collected in Otsuchi Bay, Japan, in July 2013 **(A)** on a linear scale and **(B)** on a logarithmic scale.

Chapter 2

The River-Influenced Coastal Area: tDOM in Otsuchi Bay, Japan

2.1. Introduction

The global riverine flux of particulate and dissolved organic carbon to the ocean is ~0.4 Pg C year^{-1} (Schlesinger and Melack, 1981). Dissolved organic carbon (DOC) comprises more than half of this flux and is an important component of the global carbon cycle (Hedges et al., 1997). Lignin is a phenolic polymer common to all vascular plants (Hedges and Mann, 1979) and a useful biomarker of terrigenous dissolved organic matter (tDOM) in the ocean (Meyers-Schulte and Hedges, 1986; Opsahl and Benner, 1997). Low concentrations of lignin phenol were observed in the Atlantic and Pacific oceans and the oceanic residence times of tDOM ranged from decades to a century (21–132 year) (Opsahl and Benner, 1997). These results highlighted tDOM is an important source of inorganic nutrients regeneration in the coastal ocean and also suggested ocean margins could be important sites for tDOM transformations (Opsahl and Benner, 1997; Hedges et al., 1997). Biodegradation and photodegradation of tDOM are major processes in the remineralization of tDOM in ocean margins (Miller and Zepp, 1995; Benner and Opsahl, 2001; Fichot and Benner, 2014). Photochemical processes play an important role in the degradation of lignin phenols in seawater (Hernes and Benner, 2003; Fichot and Benner, 2012). Recent studies have demonstrated that biodegradation is also an important removal process of lignin phenols in rivers and river-influenced ocean margins (Ward et al., 2013; Fichot and Benner, 2014). Photochemical processes have been shown to enhance the microbial degradation of tDOM, thereby contributing to its remineralization (Miller and Moran, 1997; Moran et al., 2000; Mopper and Kieber, 2002; Obernosterer and Benner, 2004; Fichot and Benner, 2014).

Chromophoric dissolved organic matter (CDOM) is ubiquitous in marine waters and plays a significant role in marine biogeochemical cycles (Nelson et al., 2010; Yamashita et al., 2013). CDOM absorption coefficients and spectral slopes (*S*) are useful

indicators for estimating DOC concentrations and sources, tDOM molecular weight and the extent of photochemical alteration (Del Vecchio and Blough, 2002; Helms et al., 2008; Fichot and Benner, 2011, 2012; Spencer et al., 2012; Yamashita et al., 2013). Hydrophobic constituents, including lignin, are the important chromophore in tDOM because of the high correlation between hydrophobic constituents and CDOM absorption (Spencer et al., 2012; Hernes and Benner, 2003; Fichot and Benner, 2012; Shen et al., 2015). In addition, CDOM $S_{275\text{-}295}$ is related to DOM origin, molecular weight and transformations; hence, $S_{275\text{-}295}$ is a good indicator of tDOM in the ocean (Helms et al., 2008; Fichot and Benner, 2012). The applicability of this optical tracer of tDOM relies on a strong nonlinear relationship between $S_{275\text{-}295}$ and the DOC-normalized lignin yield in rivers and along the freshwater-marine continuum in river-influenced ocean margins (Fichot and Benner, 2012; Fichot et al., 2013). The ratio of absorption at 250 nm and 365 nm (E_2/E_3) is another optical property that strongly correlates with aromatic content, molecular weight and degradation of DOM (de Haan, 1972; Lou and Xie, 2006; Helms et al., 2008; Bouillon et al., 2014; Spencer et al., 2012; Santos et al., 2014).

Previous studies suggested a narrow range of the global riverine DOC flux; however, it is rather coarse ranging from 0.20–0.36 Pg C year^{-1} measured from 40–164 rivers (Meybeck, 1993; Aitkenhead and McDowell, 2000; Dai et al., 2012; Raymond and Spencer, 2015). These riverine DOC flux results imply the uncertainty (~20–30%) in the global river flux and point out the importance to advance in the global/regional river export estimates (Raymond and Spencer, 2015). In additional, numerous studies investigated the top 30 rivers on the Earth's surface and estimated those rivers contribute 51% of the total annual global discharge and provide vast quantities of tDOM to the ocean (Raymond and Spencer, 2015), in other words, the status of tDOM in the remain 49% small estuarine area is unclear.

Previous studies used lignin-derived phenols and CDOM to trace tDOM in the plumes of the Mississippi River, Amazon River and the six major Arctic rivers (Opsahl et al., 1999; Benner and Opsahl, 2001; Amon et al., 2012; Fichot and Benner, 2014; Ward et al., 2013; Mann et al., 2014). Understanding the amount and removal mechanism of tDOM can improve our knowledge of the global carbon cycles in marine system. However, tDOM removal mechanism should be variable and it should depend on the

environment condition, especially most of the estuarine environments are not in large spatial scale as like above rivers. Except river delta, such as the Mississippi River system, ria is another major estuarine environment and that is incised valleys where estuarine zone can remove according to climatic changes (Evans and Prego, 2003). The geological term *ria* is defined as a downed river valley, which has been formed by a relative rise of sea level either because of eustatic changes, tectonic change or a combination of both (Evans and Prego, 2003). Now, the general definition of ria is that occurs at a river mouth and is formed with drowned river valley and opens to the sea. Although ria coast is common and highly relates with human activity, the tDOM removal mechanism is still unclear. The present study investigated the riverine sources and transformations of lignin and CDOM in a typical ria coast, Otsuchi Bay, on the Pacific Ocean coast of Japan. Measurements of lignin phenols and CDOM in the river and bay waters can indicate the direct injection of river-transported tDOM to adjacent coastal waters and also imply the tDOM transformation.

2.2 Study site

Otsuchi Bay is a semi-closed coastal area along the Sanriku ria coast in northern Japan, and is one of the areas struck by a massive tsunami associated with the 2011 Tohoku earthquake. The tsunami caused considerable damage along the Pacific side of the Tohoku Region and the northern part of the Kanto Region (Kazama and Noda, 2012). The Otsuchi River, Kozuchi River and Unosumai River flow into Otsuchi bay. The catchments of these three rivers are 116, 66 and 150 km^2, respectively (Coastal Oceanography of Japanese Island, 1985). The total freshwater discharge into the bay ranges from 3–35 m^3 s^{-1}. Approximately 55% of the freshwater entering the bay comes from the Unosumai River, with 30% and 15% freshwater coming from the Otsuchi and Kozuchi Rivers, respectively (Anbo et al., 2005). Water exchange between the bay and coastal ocean is rapid, with water residence time within the bay estimated to be on the order of a week to a month based on the residual current (3–5 cm s^{-1}; Otobe et al., 2009) and the physical dimensions of the bay (length 7 km; wide 2–4 km; depth 9–60 m) (Fukuda et al., 2015). Water circulation changes on a seasonal basis in Otsuchi Bay. The

density current is affected by river discharge, tide-induced residual current and seasonal changes in wind (Otobe et al., 2009). Recent studies directly pointed out that the baroclinic circulation in this bay has a three-layer structure and this circulation is a seasonal variation, however, the surface outflow are fresh and buoyant water discharging form rivers (Tanaka et al., 2015). Fukuda et al. (2015) recently investigated nutrient dynamics in the water column following the 2011 Tohoku earthquake and noticed three distinct periods: (1) a stratified period (stratification between Tsugaru current with high salinity and river water: May-September), (2) a mixing period (October-January), and (3) an Oyashio current intrusion period (low salinity and low temperature: February-April). Although water is frequently flushed out of the bay to the coastal zone, previous studies also indicated that river inflow is the key factor controlling water exchange and nutrient concentrations in this bay and suggested river inflow has a major influence on DOM dynamic (Furuya et al., 1993; Kawamiya et al., 1996; Anbo et al., 2005; Fukuda et al., 2007).

2.3. Material and Method

2.3.1. Sampling overview

Samples were collected from the three rivers and along a transect in Otsuchi Bay during 2012–2013 (Fig. 2-1A). Water samples from the rivers were collected using a bucket, and water samples from the bay were collected at the surface (1 m) and near the bottom using a Niskin bottle (maximum depth of 78 m at station L0). In order to assess the vertical distribution of tDOM in the middle of the bay, seawater samples were collected at different depths at station L3 in November 2013. The depths of each station were: 78 m at L0, 44 m at L1, 41 m at L2, 35 m at L3, 26 m at L4, 18 m at L5, 7 m at L6, and 17 m at L8, respectively. The average salinity values (mean ± 1-standard division, 1-SD) were 32.39 ± 0.26 (n = 6) and 33.60 ± 0.08 (n = 4) in September and November 2012; 33.57 ± 0.08 (n = 12), 33.25 ± 0.64 (n = 18), 32.62 ± 1.63 (n = 22) and 33.34 ± 0.35 (n = 5) in March, May, July and November 2013, respectively. These data

demonstrate that the freshwater volume represented a small fraction of the total water volume of the bay during all seasons.

In Otsuchi Bay, the water exchange rate can be very rapid with dramatic salinity increases over a short distance from river mouths to the bay. This often makes it difficult to interpret an accurate mixing model. In order to overcome this issue, additional samples were collected in the limited area of mid-salinity range around the Unosumai River mouth at station U1–U8 (Fig. 2-1B) in November 2014 for optical analyses, and the average salinity was 29.77 ± 5.17 (1-SD, n = 14).

2.3.2. Lignin extraction and analysis

Water samples were filtered through Whatman® polycarbonate filter (1-µm pore size) and then acidified to ca. pH 2.5 using sulfuric acid. tDOM fraction including lignin was extracted by solid phase extraction (SPE) on a C18 cartridge (Varian MegaBond Elut) at a flow rate of ~50 mL min^{-1} using a peristaltic pump (Masterflex L/S tubing pump, Cole-Parmer) (Louchouarn et al., 2000; Hernes and Benner, 2002). Before extraction, 50 mL of methanol was passed through the cartridges followed by 1 L of acidified Milli-Q water (pH = 2.5). After extraction, the cartridges were stored at 4˚C until elution with 30 mL methanol. The eluate was then stored at -20˚C until derivatized with BSTFA/TMCS [N,O-bis(trimethylsilyl)trifluoroacetamide containing 1% trimethylchlorosilane] before GC/MS analysis. Eleven lignin phenols were produced by the CuO oxidation method, and those phenols and two spikier, trans-cinnamic acid (CiAD) and ethyl-vanillin (EVAL), were identified and quantified using an Agilent 7890 gas chromatograph equipped with a Varian DB5-MS capillary column and an Agilent 5975 mass selective detector (Kaiser and Benner, 2011). The GC/MS analysis in this study was carried out in full scan mode (range *m*/*z* 50–650) and SIM mode (a characteristic ion for quantification with 2 qualifier ions) (Table 2-1). The SIM ions were selected based on overall abundance and characteristic fragmentation pattern (Kaiser and Benner, 2011). Chromatogram of eleven lignin phenols and two spikier on GC/MS are shown in Fig 2-2. Comparing with a standard mixture, the small coelution was observed in some *in-situ* samples, such as the surface seawater at station L0 (Fig. 2-2C–2D). The clean chromatograms were found in the DOM extract of the surface seawater in Otsuchi Bay

and the Unosumai River (Fig. 2-2A–2B), this result indicated the quantification of lignin analysis is efficiency in this method.

Total dissolved lignin concentrations were calculated as the sum of 9 lignin phenols ($TDLP_9$) (nmol L^{-1}) from three phenol families: *p*-hydroxy phenols (*p*-hydrobenzaldehyde (PAL), *p*-hydroxybenzoic acid (PAD), *p*-hydroxyacetophenone (PON)), vanillyl phenols [vanillin (VAL), vanillic acid (VAD), acetovanillone (VON)], syringyl phenols [syringaldehyde (SAL), syringic acid (SAD), acetosyringone (SON)]. The sum of eleven phenols ($TDLP_{11}$), including PAL, PAD, PON, VAL, VAD, VON, SAL, SAD, SON and cinnamyl phenols [*p*-coumaric acid (CAD) and ferulic acid (FAD)], was also presented in this study. Finally, the ratios of *p*-hydroxy to vanillyl phenols (P/V), syringyl to vanillyl phenols (S/V), cinnamyl to vanillyl phenols (C/V), acid/aldehyde ratios of *p*-hydroxy [$(Ad/Al)_P$], acid/aldehyde ratios of vanillyl [$(Ad/Al)_V$] and acid/aldehyde ratios of syringyl phenols [$(Ad/Al)_S$] were also calculated. S/V and C/V ratios were calculated to distinguish the taxonomic origins of lignin such as angiosperm, gymnosperm, woody and non-woody plants. P/V, S/V and acid/aldehyde ratios of two lignin phenols were calculated to imply tDOM transformations in the waters (Table 2-2).

2.3.3. Chl. *a* and CDOM analysis

Samples were gravity-filtered directly from the Niskin bottle and through pre-combusted Whatman® GF/F filters (0.7-µm pore size). The GF/F filters were immediately stored at -20˚C in the dark for chlorophyll *a* (Chl. *a*) measurements (Suzuki and Ishimaru, 1990). The filtrate was collected in pre-combusted glass vials (teflon-lined cap), and stored frozen in the dark for CDOM analysis. CDOM absorbance was measured from 200 nm to 800 nm of wavelength at 0.5 nm intervals using a dual-beam spectrophotometer (UV-1800, Shimadzu). A Mili-Q was used as the blank, and this blank scan was subtracted from each spectrum. Spectral absorption coefficient $a(\lambda)$ (m^{-1}) was conserved using baseline-corrected that was entire spectrum subtracted average values ranging from 590 nm to 600 nm (Green and Blough, 1994; Yamashita and Tanoue, 2009). The 5-cm or 3-cm quartz cells were used for all *in-situ* samples and that was depended on the sample size. The quartz cell was rinsed by Milli-Q water and stored in 1 mol L^{-1}

hydrochloric acid after measuring. The method of Yamashita and Tanoue (2009) was used to convert absorbance to Napierian absorption coefficient.

Absorption coefficients of CDOM decreased with increasing wavelength and were fit to the following exponential equation (3):

$$a(\lambda) = a(\lambda_i)e^{-S(\lambda-\lambda_i)} \quad (3)$$

where $a(\lambda)$ and $a(\lambda_i)$ are the absorption coefficients at wavelength λ and reference wavelength λ_i (m^{-1}), respectively, and S is the spectral slope coefficients (nm^{-1}) over the corresponding spectral range (λ-λ_i). The typical absorption spectrum is shown in Fig. 2-3, CDOM absorption coefficients are declining exponentially with increasing wavelength. Absorption spectrum obtained for a variety of sampling site and indicated levels of CDOM is positive related with tDOM sources (Fig 2-3). The reproducibility is half of range of duplicated samples and it is ± 0.02 (2σ), and a noise level is less than 0.00004. The CDOM absorption coefficients at 250 nm [a(250)] and 350 nm [a(350)], and the spectral slope coefficients between 275–295 nm ($S_{275\text{-}295}$) and between 350–400 nm ($S_{350\text{-}400}$), and the slope ratio (S_R) of $S_{275\text{-}295}$ to $S_{350\text{-}400}$ were reported in this study. The ratio of absorption coefficient at 250 nm to that at 365 nm (E_2/E_3) was also calculated. The index of relative values of CDOM spectral slope $S_{275\text{-}295}$, S_R, and absorption coefficient ratio, E_2/E_3, are showed in Table 2-3. Those CDOM indicators imply the sources, characteristics and photobleaching of DOM in waters (Table 2-3).

2.3.4. Calculated DOC concentrations from CDOM

The DOC concentrations were retrieved from CDOM absorption coefficients, [a(λ), at λ = 275 nm and 295 nm] using a multiple linear regression approach to calculate DOC concentration ($[DOC]_{ca}$) in coastal waters following the equation (Fichot and Benner 2011):

$$\ln[\mathrm{DOC}]_{\mathrm{ca}} = \alpha + \beta \ln[a(275)] + \gamma \ln[a(295)] \quad (4)$$

where α, β and γ are regression coefficients and the unit was μmol. In this study α, β and γ are the coefficients following Fichot and Benner (2011) from the north Gulf of Mexico. Here, when $a(275) \leq 3.5\ m^{-1}$, α = 3.4707, β = 1.8591 and γ = -1.2421; otherwise $a(275) > 3.5\ m^{-1}$, α = 2.9031, β = 2.7703 and γ = -2.0400. In Fichot and Benner (2011)

method, DOC concentrations estimated were within ± 4.2% of the measured DOC concentrations ranging from 60 µmol L^{-1} to 300 µmol L^{-1}.

2.4. Results

2.4.1. Dissolved lignin phenols and CDOM in river waters

Lignin phenol concentrations varied from 2–5-fold among rivers and on a seasonal basis. Overall, $TDLP_9$ ranged from 5.97–80.7 nmol L^{-1} (Table 2-4), and $TDLP_{11}$ ranged from 7.09–87.0 nmol L^{-1} (Appendix 2-1). The Otsuchi River consistently exhibited the lowest concentrations, whereas the Unosumai River consistently exhibited the highest concentrations. Lignin concentrations for all three rivers were several-fold higher in July 2013, following a period of heavy rainfall (Table 2-4). In contrast, lignin phenol composition exhibited little seasonal variability. Lignin phenol ratios (P/V, S/V, C/V, (Ad/Al)p, (Ad/Al)v, (Ad/Al)s) were slightly higher in the Otsuchi River and lower in the Unosumai River. The P/V ranged from 0.52–1.16, S/V ranged from 0.61–0.87, C/V ranged from 0.17–0.50 (Table 2-4). The $(Ad/Al)_P$, $(Ad/Al)_V$ and $(Ad/Al)_S$ ranged from 1.00–1.69 in $(Ad/Al)_P$; 0.64–1.11 in $(Ad/Al)_V$ and 0.50–0.78 in $(Ad/Al)_S$, respectively (Table 2-4, Appendix 2-1).

The absorption coefficients of CDOM at *a*(250) and *a*(350) in the rivers ranged several-fold from 1.79–7.08 m^{-1} and from 0.32–1.88 m^{-1}, respectively (Table 2-4, Appendix 2-1). The spectral slope coefficients, $S_{275\text{-}295}$ and $S_{350\text{-}400}$, ranged from 0.0068–0.0165 and 0.0105–0.0167 nm^{-1}, respectively, and the slope ratio, S_R, ranged from 0.65–1.14 (Table 2-4, Appendix 2-1). The lowest $S_{275\text{-}295}$, $S_{350\text{-}400}$ and S_R values were all observed in March 2013. The E_2/E_3 ratios ranged from 3.78–7.23 (Appendix 2-1).

2.4.2. Dissolved lignin phenols and CDOM in bay waters

The changes in chlorophyll *a* concentrations, lignin phenol concentrations, and CDOM absorption coefficients along the river-ocean continuum in Otsuchi Bay are shown in Fig. 2-4. Chlorophyll *a* concentrations ranged from 0.23 to 9.96 µg L^{-1}, peaking at mid-salinities in July 2013 and dropping to relatively low concentrations at salinities

>32 (Fig. 2-4A). $TDLP_9$ and CDOM absorption in surface waters decreased with increasing salinity, which was consistent with their terrigenous origin (Fig. 2-4B–4C; Tables 2-5, Appendix 2-2). $TDLP_9$ and the CDOM absorption coefficient $a(350)$ were significantly linearly correlated (R^2 = 0.63, p < 0.001, n = 32). $TDLP_9$ concentrations ranged from 1.47–24.5 nmol L^{-1} in surface waters and 2.46–14.3 nmol L^{-1} in subsurface waters, respectively (Table 2-5). The CDOM absorption coefficient, $a(350)$, ranged from 0.17 to 0.55 m^{-1} in surface water (Table 2-5) and 0.12 to 0.38 m^{-1} in subsurface waters.

Seasonal variations in lignin phenol composition were minimal, whereas composition varied significantly across the salinity gradient (p < 0.001). In surface waters, P/V, S/V and $(Ad/Al)_V$ changed rapidly at salinities >32 (Fig. 2-5A–5C). The P/V, S/V, and $(Ad/Al)_V$ in surface waters ranged from 0.59–2.71, 0.40–0.75 and 0.79–1.25, respectively (Fig. 2-5A–5C; Table 2-5). The $S_{275\text{-}295}$ also increased at salinities >32 (Fig. 2-5D). No clear trends were observed between salinity and C/V (range 0.16–0.28), $(Ad/Al)_P$ (range 1.16–2.40), and $(Ad/Al)_S$ (range 0.48–0.75) (Table 2-5, Appendix 2-2). In surface and subsurface waters, $S_{275\text{-}295}$ ranged from 0.0213–0.0319 nm^{-1} and 0.0243–0.0331 nm^{-1} (Table 2-5, Appendix 2-2), $S_{350\text{-}400}$ ranged from 0.0135–0.0177 nm^{-1} and 0.0125–0.0176 nm^{-1}, S_R ranged from 1.23–2.25 and 1.49–2.24, and E_2/E_3 ranged from 7.16–13.0 and 8.16–14.6, respectively (Appendix 2-2). $TDLP_9$ concentrations were strongly correlated with $S_{275\text{-}295}$ in surface and subsurface waters (R^2 = 0.91, p < 0.001, n = 23 in surface water; R^2 = 0.72, p < 0.01, n = 9 in subsurface water).

Variations in lignin phenol composition (C/V, S/V, P/V) and $S_{275\text{-}295}$ among river and surface seawater samples are shown in Fig. 2-6. Lignin phenols in rivers had elevated S/V and C/V compared to the surface waters of Otsuchi Bay, and bay waters with salinities <32 had S/V and C/V values that clustered between the river and high salinity (>32) (Fig. 2-6A). These observed trends were consistent with the rivers being the major source of lignin in the bay, and with physical mixing and decomposition processes shaping the parameters. The P/V and $S_{275\text{-}295}$ were relatively low in the rivers and increased in the bay, and confirmed the riverine source of the tDOM and CDOM and the role of physical mixing and decomposition processes (Fig. 2-6B). Five of the lower salinity (<32) samples had P/V values similar to those in river water. These samples had $S_{275\text{-}295}$ values that were intermediate between those in river and higher salinity bay waters.

These five lower salinity samples indicated that physical mixing effect was higher than alternation processes at low and mid salinities. At higher salinities (>32), there was a broad range in P/V (0.8–2.7), indicative of mixing and alteration processes (Fig. 2-6B).

A vertical profile at station L3 in November 2013 revealed the variations in physical properties, lignin concentrations, and CDOM with depth in the water column (Fig. 2-7). A vertical density gradient was observed in the upper few meters of the water column (Fig. 2-7A). $TDLP_9$ concentrations were maximal (8.41 nmol L^{-1}) near the surface and declined rapidly to 3.91 nmol L^{-1} at 20 m (Fig. 2-7A). The *a*(350) tracked lignin phenol concentrations and decreased rapidly with depth, whereas the P/V and $S_{275-295}$ increased rapidly with depth from 1.32 to 2.82 and 0.0281 to 0.0327 nm^{-1}, respectively (Fig. 2-7B). The P/V, S/V and C/V values in surface water were 1.32, 0.68 and 0.24, respectively; and 2.82, 0.57, and 0.22, respectively, at 20 m depth (Table 2-5). The observed vertical trends in lignin phenols and CDOM were consistent with physical mixing being a dominant process shaping the observed distributions of tDOM concentration and composition in the upper 20 m of the water column. Similar results in concentrations and compositions of lignin phenols and CDOM data in surface and bottom waters at each station in other seasons (Table 2-5, Appendix 2-2).

2.4.3. CDOM distribution and physical mixing across a salinity gradient

During November 2014, water samples were collected near the mouth of the Unosumai River and adjacent bay waters to investigate CDOM distributions and mixing across a salinity gradient (Fig. 2-1B, Appendix 2-3). A simple conservative mixing model was constructed using CDOM values from the Unosumai River as a freshwater end member and coastal seawater from station L6 as a marine end member (Fig. 2-8). The conservative mixing curve was obtained between salinity and *a*(350) (Fig. 2-8A), because behavior of CDOM optical properties are following the conservative behavior as like other dissolved chemical elements in coastal area (Stedmon and Markager, 2003; Hernes and Benner, 2003; Fichot and Benner, 2012). However, a conservative behavior with non-linear curve was expected between salinity and CDOM slope $S_{275-295}$ (Fig. 2-8B) based on previous studies including investigations and laboratory model studies (Stedmon and Markager, 2003; Hernes and Benner, 2003; Fichot and Benner, 2012;

Dixon et al., 2014). Measured values of *a*(350), a proxy for lignin phenol concentrations, were consistently below the conservative mixing line at mid salinities indicating some removal (<25%) of CDOM across the salinity gradient in upper Otsuchi Bay (Fig. 2-8A). Most values of $S_{275\text{-}295}$ were below the mixing line at salinities <28, with values closer to the mixing line at higher salinities (Fig. 2-8B), which is consistent with the cumulative effects of photochemical alteration of CDOM.

2.5. Discussion

2.5.1. Riverine sources of lignin and CDOM

The Unosumai River is the source of more than half of the freshwater, CDOM and lignin entering Otsuchi Bay from continental runoff. Lignin concentrations in the Unosumai River were typically several-fold higher than those in the Otsuchi and Kozuchi rivers. Concentrations of lignin phenols and CDOM absorption were highest during July when precipitation was the highest recorded during this study. This observation is consistent with other observations of high lignin concentrations and CDOM absorption coefficients values during major precipitation events in other river systems (Spencer et al., 2009; Amon et al., 2012; Shen et al., 2012). High lignin concentrations and CDOM absorption coefficients values accompanying with high precipitation were because rainfall leached more humic substances releasing from soils into river water. A different pattern was observed in November 2012, when higher precipitation was associated with lower lignin concentrations compared with November 2013, potentially due to snowmelt in November 2013 (Baker et al., 2000). Snowmelt also increased in runoff volume on land and leached more humic substances from soils into river water.

The S/V (0.73 ± 0.07) and C/V (0.33 ± 0.10) values indicated the lignin in these rivers originated primarily from non-woody angiosperm tissues (Hedges and Mann, 1979). The P/V, S/V and C/V values were similar to those in the Mississippi River (Shen et al., 2012), but the S/V and C/V were higher than those in large Arctic rivers, which have greater contributions from gymnosperm vegetation (Amon et al., 2012). Although lignin phenol compositions in rivers draining into Otsuchi Bay were similar to those

observed in the Mississippi River, the $TDLP_{11}$ concentrations in the Mississippi River ($TDLP_{11}$ = 146.2 ± 56.3 nM; $TDLP_9$ is not reported; Shen et al., 2012) were three to nine times higher than the average $TDLP_{11}$ in the rivers flowing into Otsuchi Bay.

Lignin concentrations were not strongly coupled with discharge in the Otsuchi and Kozuchi rivers indicating other factors influence lignin concentrations and CDOM properties. High discharge was associated with lower lignin concentrations and *a*(350) in the Otsuchi River. This result inferred the mechanisms controlled lignin concentrations were multiple factors, and it was not only affected by rainfall and discharge in other studies (Spencer et al., 2009; Amon et al., 2012; Shen et al., 2012). Previous investigation found strontium isotope value, $^{87}Sr/^{86}Sr$, in the Otsuchi River was higher (ca. 0.7094–0.7080) than that in the Kozuchi and Unosumai River (ca. 0.7080–0.7053) (Nakano, 2016). Sr isotope ratio has been used as a tracer in hydrogeologic studies because of the predominance of geologically derived Sr (Blum et al., 1992; Nakano et al., 2010). The highest $^{87}Sr/^{86}Sr$ ratio in the Otsuchi River is correspondent to the bedrock of the watershed (Kicheol et al., 2015). In addition, groundwater is abundant in the downstream of the Otsuchi River, and this highlights other processes may affect tDOM transformation in waters. Previous studies pointed out that the sorption onto minerals and microbial degradation shaped the concentration and compositions of tDOM during its passage through the soil column to the saturated zone of groundwater or river waters (Ward et al., 2013; Shen et al., 2015), therefore, $TDLP_9$ was the lowest in the Otsuchi River. Other factors influence lignin concentrations could include human activities and land use, considering the river sampling site is located downstream of the city of Otsuchi and many people migrated here after the 2011 Tohoku earthquake (The questionnaire survey report for temporary housing residents in Otsuchi area, Japan, 2012). Previous studies have observed that land use, vegetation cover and hydrology play important roles in shaping the quantity and quality of CDOM and DOM in rivers (Yamashita et al., 2011; Walker et al., 2013; Mann et al., 2014). Strong relationships were observed between lignin phenol concentrations and CDOM absorption coefficients *a*(250) (R^2 = 0.88, $p < 0.001$, n = 15) and *a*(350) (R^2 = 0.87, $p < 0.001$, n = 15), indicating the potential for using these optical parameters as tracers of lignin in river.

2.5.2. Retrieved DOC concentrations from CDOM

The estimated $[DOC]_{ca}$ concentrations ranged from 48.8 to 93.7 µmol in this bay (Fig. 2-9). The high $[DOC]_{ca}$ values were observed in the surface layer and those declined with increasing depth excluding the extremely low value (48.8 µmol) at 20 m station L3 collected in March. Other unexpected results were found in September 2012, the extremely high DOC concentrations were obtained and those ranged from 90 to 94 µmol in surface water, and those were higher than the previous long-term observation result (Fukuda et al., 2007). Otherwise, the maximum $[DOC]_{ca}$ (87.8 µmol) was observed in July 2012 with high precipitation event in July 2013. Previous investigation in Otsuchi Bay found DOC concentration was significantly with Chl. *a*, salinity and temperature (Fukuda et al., 2007), and the $[DOC]_{ca}$ were consistent with previous DOC concentrations measured in Otsuchi Bay (Fukuda et al., 2007).

The calculated $[DOC]_{ca}$ model from Fichot and Benner (2011) did not useful to approach DOC concentration in river waters. Based on Fukuda et al. (2007) data, DOC concentration was ca. 86 µmol in freshwater (salinity = 0). However, the values of $[DOC]_{ca}$ in river waters (36.26–110.34 µmol) were anomalous compared with Fukuda et al. (2007) results.

In the present study, although DOC concentrations was retrieved from CDOM absorption coefficients, $[DOC]_{ca}$ values were consistence with previous observation results (72.6 ± 4.9 µmol L^{-1} at depth 0–2 meter, 1-SD, n = 20) (Fukuda et al., 2007). However, the unexpected $[DOC]_{ca}$ values in September 2012 were caused by bottle effects, that was from the brown vial and only used in September 2012, and somehow the low value (< 60 µmol L^{-1}) in March 2013 implied the necessary to re-parameterize the [DOC]-retrieved model with local data even though the general approach of Fichot and Benner (2011) should work well in river-influenced coastal area. In addition, the anomalous values in river water also highlighted the necessity to re-parameterize the [DOC]-retrieved model with local data.

2.5.3. Transformations of lignin and CDOM in Otsuchi Bay

The physical mixing of river and coastal seawater played an important role in controlling the distributions and concentrations of lignin and CDOM in Otsuchi Bay. Our

seasonal data in Otsuchi Bay were limited, but a simple mixing curve for *a*(350) indicated some lignin removal (up to 25%) across mid salinities in the upper bay. Evidence indicated photochemical and biological processes both played a role in the decomposition of lignin and CDOM in the bay. Molecular indicators of lignin transformations, including P/V, S/V and $(Ad/Al)_V$, provided strong evidence of the oxidation and decomposition of lignin at higher salinities (>32) in surface and subsurface waters. Lignin molecular indicator of biological transformation, $(Ad/Al)_S$, was slightly increased even at higher salinities. This pattern indicated the influence of microbial degradation was minor in this bay. Likewise, the spectral slope ($S_{275\text{-}295}$) indicated transformations of tDOM and CDOM were evident at higher salinities in surface and subsurface waters of Otsuchi Bay. Photobleaching increased $S_{275\text{-}295}$ values was observed in the higher salinity and rivers samples (Fig. 2-6B), Indeed, previous studies (Helms et al., 2008; Fichot and Benner, 2012; Yamashita et al. 2013) and our upper bay (near the mouth of the Unosumai River and salinity <28) results have shown that the photochemical degradation of CDOM, unlike microbial degradation, effectively increases $S_{275\text{-}295}$. Assuming photochemical processes were largely responsible for spectral slope ($S_{275\text{-}295}$) transformations (Helms et al., 2008; Fichot and Benner, 2012), the elevated spectral slopes observed in deeper waters indicated previous exposure to solar radiation (Fig. 2-7).

2.6. Conclusion

The present study investigated the removal mechanism of tDOM in a ria coast. In Otsuchi Bay, lignin phenols were river-derived and physical mixing of river and coastal water shaped the lignin distributions and parameters. In addition, lignin composition ratios suggested tDOM decomposition processes in this bay including photochemical and microbial transformations, but the contributions of those two removal mechanisms were unclear in *in-situ* data. The similar results were also observed in CDOM optical properties. Physical mixing and photochemical processes played an important role in CDOM results. However, CDOM slope $S_{275\text{-}295}$ was primary responsible for photobleaching, the influence of biodegradation was unknown in CDOM patterns.

Therefore, those results highlighted the necessity of decomposition experiment to better understand the mechanism of tDOM removal.

In addition, this study results suggested lignin concentrations were not only associated with river discharge and precipitation in terrestrial environment, but also affected by other factors such as water residence time as like the lignin results in the Otsuchi River. Previous study found tDOM were relatively depleted in groundwater DOM and coupled with relatively lower molecular weight, and biological process dominated tDOM decomposition (Shen et al., 2015). Therefore, this highlights the potential to better understand tDOM decomposition mechanism in terrestrial environment by studying tDOM in these three rivers, especially in the Otsuchi River.

Table 2-1 Symbols, retention times, and characteristic mass fragments for CuO oxidation products. Data are from Kaiser and Benner (2011).

Compound	Symbol	RRT_{DBS}*	Major ions (*m/z*)**
Cinnamic acid	CiAD	1	131,*161*,205,*220*
Ethyl-vanillin	EVAL	1.106	167,179,*195*,*238*
p-hrdroxybenzaldehyde	PAL	0.672	151,*179*,*194*
p-hydroxyacetophenone	PON	0.586	193,*194*,*208*
p-hydroxybenzoic acid	PAD	1.172	193,*223*,267,*282*
Vanilllin	VAL	0.986	193,194,*209*,*224*
Acetovanillone	VON	1.153	193,*208*,223,*238*
Vanillic acid	VAD	1.441	223,267,*282*,297,*312*
Syringaldehyde	SAL	1.315	224,*239*,*254*
Acetosyringone	SON	1.448	223,238,*253*,*268*
Syringic acid	SAD	1.692	253,297,*312*,327,*342*
3,5-dihydroxy-benzoic acid	DiOHBA	1.558	28,*311*,*355*,370
p-coumaric acid	CAD	1.749	*219*,249,293,*308*
Ferulic acid	FAD	2.014	*249*,293,308,*323*,338

*Retention times are relative to CiAD on an Agilent DB-5 column.
** Underlined ions are used for SIM quantification. Italicized ions were used to assess peak purity.

Table 2-2 Lignin composition ratios [P/V, S/V, $(Ad/Al)_V$ and $(Ad/Al)_S$] indicate tDOM transformations in the waters.

Lignin composition ratio	Transformation		Description	Reference
	Photochemical	Biological		
P/V	Increasing	—	Methoxy substitution increased photoreactivity of lignin phenols	Benner and Kaiser, 2011
S/V	Decreasing	—		Opsahl and Benner, 1998
$(Ad/Al)_V$	Increasing	Increasing	Oxidation of propyl side-chain and increasing the carboxyl content of the remaining lignin	Hedges et al., 1988; Benner et al., 1991; Opsahl and Benner, 1995
$(Ad/Al)_S$	—	Increasing		Hedges et al., 1988; Opsahl and Benner, 1995

Table 2-3 The index of relative values of CDOM spectral slope $S_{275\text{-}295}$, S_R and the ratio of absorption coefficient at 250 nm and that at 365 nm (E_2/E_3).

Indicator	Values of $S_{275\text{-}296}$, S_R, E_2/E_3	
	Shallower (lower values)	Steeper (higher values)
DOM origin	Terrestrial	Marine
Molecular weight of DOM	Higher	Lower
Aromatic content	Higher	Lower
Photobleaching	Lower	Higher

de Hann, 1972; Helms et al., 2008: Fichot and Benner, 2011, 2012; Spencer et al., 2012; Yamashita et al., 2013; Bouillon et al., 2014

Table 2-4 Dissolved lignin phenol concentrations ($TDLP_9$), composition ratios (P/V, S/V, C/V and $(Ad/Al)_V$) and CDOM absorption coefficient at 350 nm ($a(350)$) and spectral slope 275–295 nm ($S_{275\text{-}295}$) in the rivers.

Month	[1]Rainfall (mm)	Sampling site	[2]$TDLP_9$ (nmol L^{-1})	P/V	S/V	C/V	$(Ad/Al)_V$	$a(350)$ (m^{-1})	$S_{275\text{-}295}$ (nm^{-1})
Nov 2012	29.5	Otsuchi River	5.97	0.74	0.81	0.50	0.64	0.32	0.0160
		Kozuchi River	12.2	0.73	0.81	0.45	0.68	0.68	0.0165
		Unosumai River	26.3	0.69	0.76	0.43	0.70	1.03	0.0132
Mar 2013	17.5	Otsuchi River	6.43	1.16	0.77	0.37	1.11	0.38	0.0068
		Kozuchi River	12.3	0.80	0.77	0.37	0.80	0.47	0.0113
		Unosumai River	31.4	0.65	0.64	0.24	0.79	1.05	0.0105
May 2013	11.5	Otsuchi River	6.90	0.65	0.67	0.24	0.91	0.49	0.0115
		Kozuchi River	11.6	0.74	0.75	0.44	0.74	0.46	0.0151
		Unosumai River	35.1	0.57	0.69	0.28	0.73	1.33	0.0136
July 2013	186.5	Otsuchi River	37.6	0.52	0.73	0.22	0.78	0.78	0.0138
		Kozuchi River	57.3	0.59	0.69	0.22	0.76	1.26	0.0133
		Unosumai River	80.7	0.52	0.61	0.17	0.79	1.88	0.0136
Nov 2013	18.5	Otsuchi River	16.0	0.88	0.87	0.39	0.77	0.58	0.0127
		Kozuchi River	22.3	0.85	0.75	0.27	0.69	0.79	0.0129
		Unosumai River	34.9	0.75	0.68	0.29	0.79	1.22	0.0130

[1]Rainfall data is from Japan Meteorological Agency (http://www.jma.go.jp/jma/index.html). It is the cumulative rainfall results for 10 days before sampling date at station Tsukimoushi.
[2]$TDLP_9$: sum of syringyl phenols, vanillyl phenols and *p*-hydroxy phenols.
P/V: molar ratio of *p*-hydroxy phenols to vanillyl phenols.
S/V: molar ratio of syringyl phenols to vanillyl phenols.
C/V: molar ratio of cinnamyl phenols to vanillyl phenols.

Table 2-5 Dissolved lignin phenol concentrations ($TDLP_9$), composition ratios (P/V, S/V, C/V and $(Ad/Al)_V$) and CDOM parameters ($a(350)$ and $S_{275-295}$) in Otsuchi Bay.

Month	Sampling site	Depth (m)	Salinity	Temp. (℃)	$TDLP_9$ (nmol L^{-1})	P/V	S/V	C/V	$(Ad/Al)_V$	$a(350)$ (m^{-1})	$S_{275-295}$ (nm^{-1})
Sep 2012	L1	1	32.72	22.37	4.44	0.89	0.68	0.20	0.79	0.32	0.0313
	L2	1	32.56	22.30	4.50	0.82	0.72	0.19	0.88	0.34	0.0306
	L3	1	32.38	22.20	4.98	0.89	0.67	0.19	0.82	0.33	0.0305
	L4	1	31.96	21.89	5.31	0.79	0.67	0.18	0.80	0.36	0.0289
	L5	1	32.29	22.05	5.83	0.83	0.70	0.20	0.82	0.35	0.0294
	L6	1	32.44	22.22	6.14	0.85	0.74	0.21	0.81	0.39	0.0286
Nov 2012	L0	1	33.66	15.34	1.47	1.22	0.60	0.23	1.25	0.17	0.0319
	L1	1	33.51	14.82	1.85	1.08	0.57	0.23	1.01	0.19	0.0302
	L5	1	33.56	15.07	2.55	1.04	0.66	0.24	0.94	0.19	0.0299
	L6	1	33.67	15.27	2.72	0.98	0.75	0.27	0.85	0.20	0.0295
Mar 2013	L0	1	33.61	5.69	4.83	2.57	0.40	0.16	1.06	No data	No data
	L1	1	33.56	5.83	4.93	2.18	0.48	0.16	1.14	No data	No data
	L3	1	33.50	5.80	5.54	2.71	0.43	0.17	1.00	No data	No data
	L5	1	33.34	6.19	5.75	1.98	0.51	0.19	1.03	0.19	0.0283
	L6	1	33.51	6.30	5.37	2.23	0.49	0.17	1.08	No data	No data
May 2013	L0	1	32.75	11.92	7.39	2.25	0.56	0.22	1.03	No data	No data
	L0	78	33.72	8.73	5.20	3.93	0.54	0.27	1.17	No data	No data
	L1	1	33.31	10.77	6.44	2.69	0.55	0.22	1.05	0.22	0.0299
	L3	1	32.82	12.16	7.15	2.19	0.60	0.23	1.00	0.19	0.0297
	L3	35	33.62	8.75	6.19	3.46	0.53	0.21	1.10	0.18	0.0302
	L5	1	33.29	10.71	9.02	2.21	0.58	0.23	0.97	0.21	0.0302
	L6	1	33.02	12.20	11.7	1.51	0.65	0.25	0.89	0.24	0.0281
	L6	7	33.39	9.49	6.88	1.68	0.63	0.23	0.98	0.22	0.0287
	L8	1	30.93	14.74	10.7	1.34	0.66	0.28	0.92	0.26	0.0265
July 2013	L0	1	32.24	18.16	6.62	1.22	0.63	0.21	1.07	0.22	0.0297
	L0	78	33.99	11.39	2.46	3.06	0.52	0.30	1.08	0.16	0.0303
	L1	1	30.20	18.25	20.4	0.59	0.60	0.18	0.89	0.44	0.0237

(*Continues*)

Table 2-5 (*Continued*)

Month	Sampling site	Depth (m)	Salinity	Temp. (℃)	$TDLP_9$ (nmol L^{-1})	P/V	S/V	C/V	$(Ad/Al)_V$	*a*(350) (m^{-1})	$S_{275-295}$ (nm^{-1})
July 2013	L3	1	31.16	18.29	19.6	0.65	0.61	0.18	0.89	0.45	0.0231
	L3	35	33.74	15.63	4.55	2.61	0.64	0.26	1.08	0.22	0.0293
	L5	1	29.45	18.95	24.5	0.59	0.61	0.19	0.84	0.48	0.0226
	L6	1	28.76	19.26	23.1	0.65	0.63	0.20	0.87	0.55	0.0213
	L6	7	33.22	17.30	14.3	0.83	0.64	0.21	0.87	0.34	0.0253
	L8	1	29.69	18.33	20.9	0.69	0.64	0.22	0.84	0.38	0.0237
Nov 2013	L3	1	32.71	14.98	8.41	1.32	0.68	0.24	0.88	0.27	0.0281
	L3	5	33.46	15.17	6.03	1.60	0.66	0.23	0.98	0.24	0.0296
	L3	10	33.49	15.08	4.58	2.45	0.57	0.20	1.17	0.20	0.0318
	L3	20	33.51	15.02	3.91	2.82	0.57	0.22	1.22	0.17	0.0329
	L3	35	33.53	15.03	4.13	2.64	0.55	0.19	1.15	0.17	0.0327

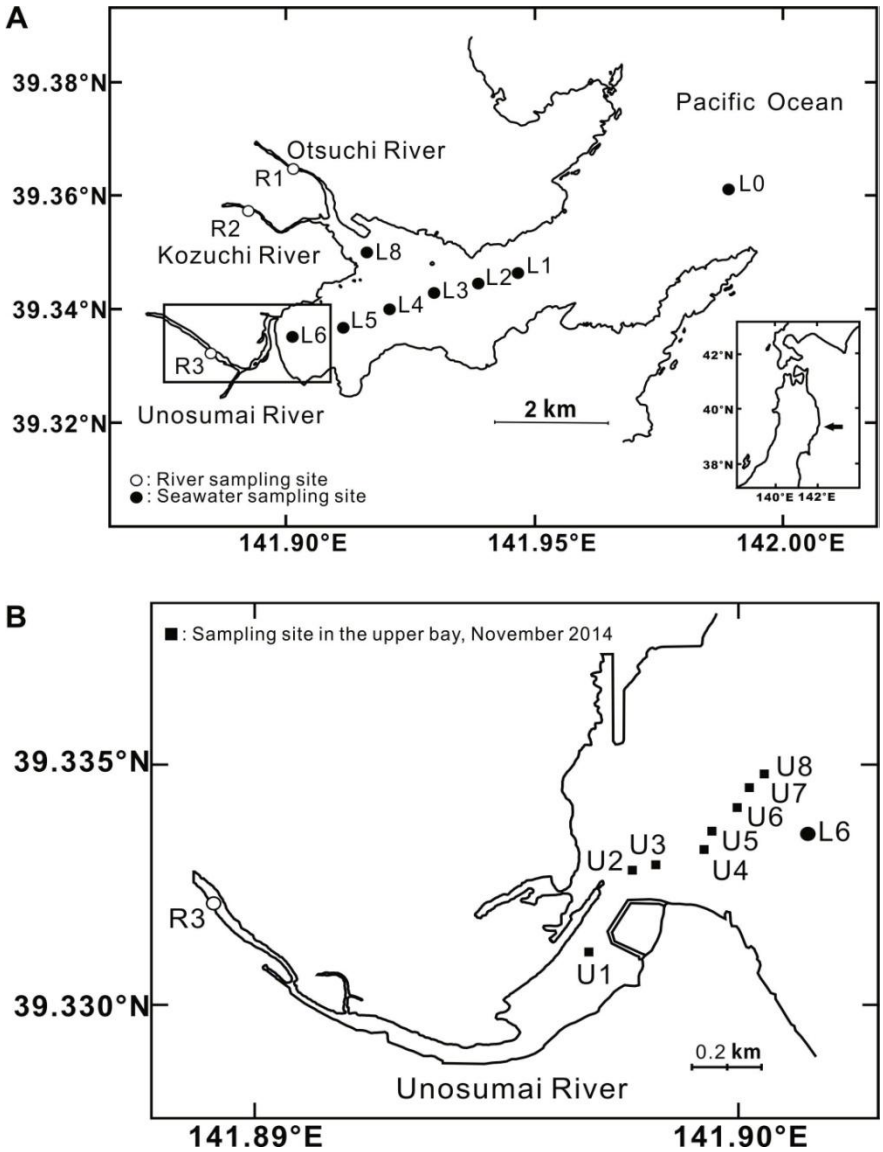

Figure 2-1 (A) Sampling sites in the three rivers in the catchment basin and in Otsuchi Bay **(B)** mid-salinity stations in the upper bay near the mouth of the Unosumai River.

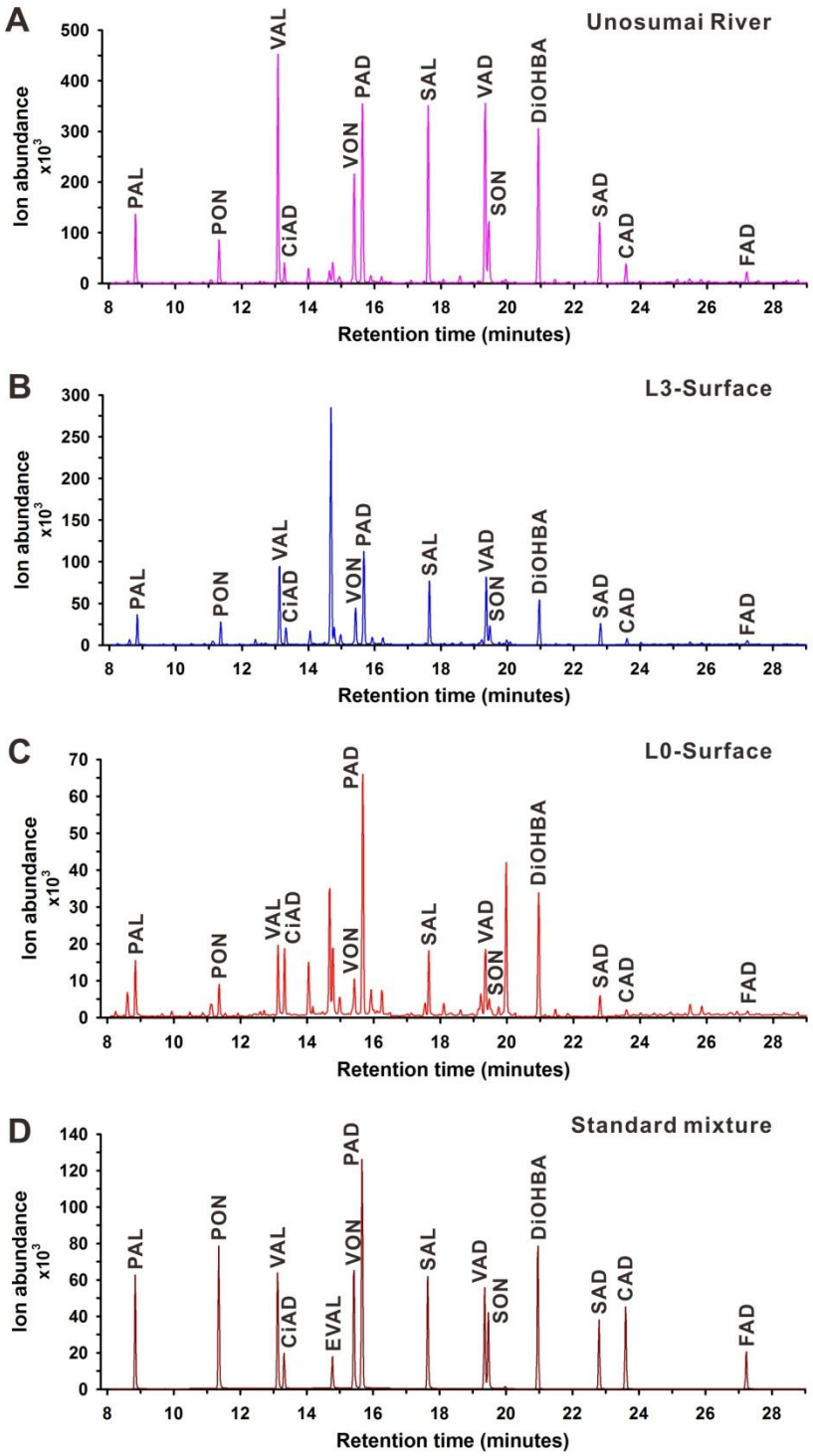

Figure 2-2 Selected chromatograms of **(A)** the Unosumai River, **(B)** surface water at station L3, **(C)** surface water at station L0, and **(D)** a 80 *p*mol μL^{-1} standard mixture. Those three samples were collected in July, 2013. Abbreviations are explained in Table 2-3.

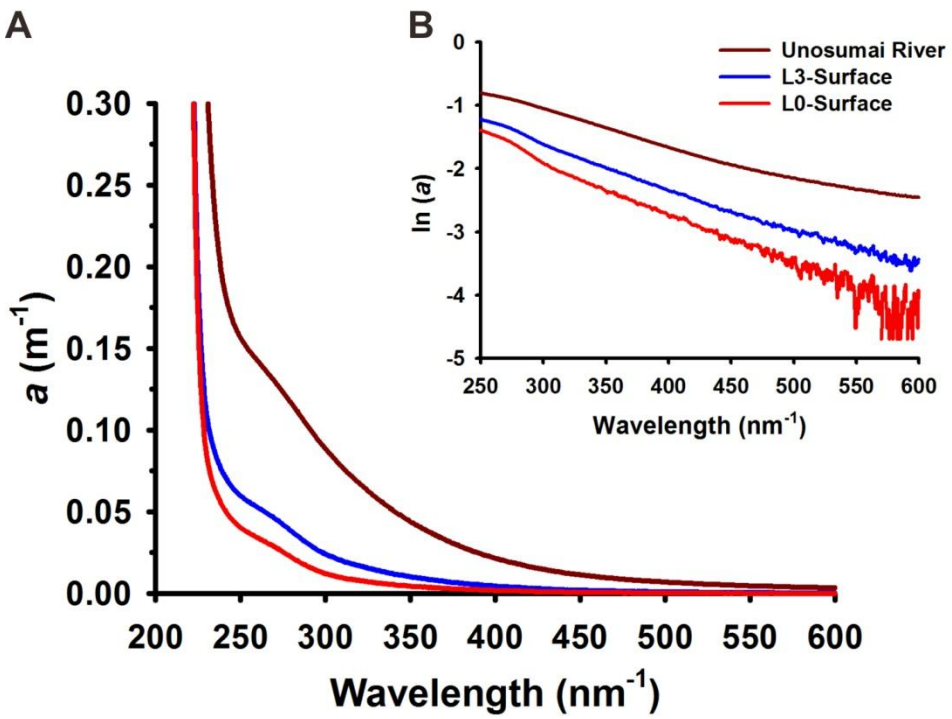

Figure 2-3 Typical absorption spectrum in the surface water at station L0 and L3 and the Unosumai River **(A)** on a linear scale and **(B)** on a logarithmic scale.

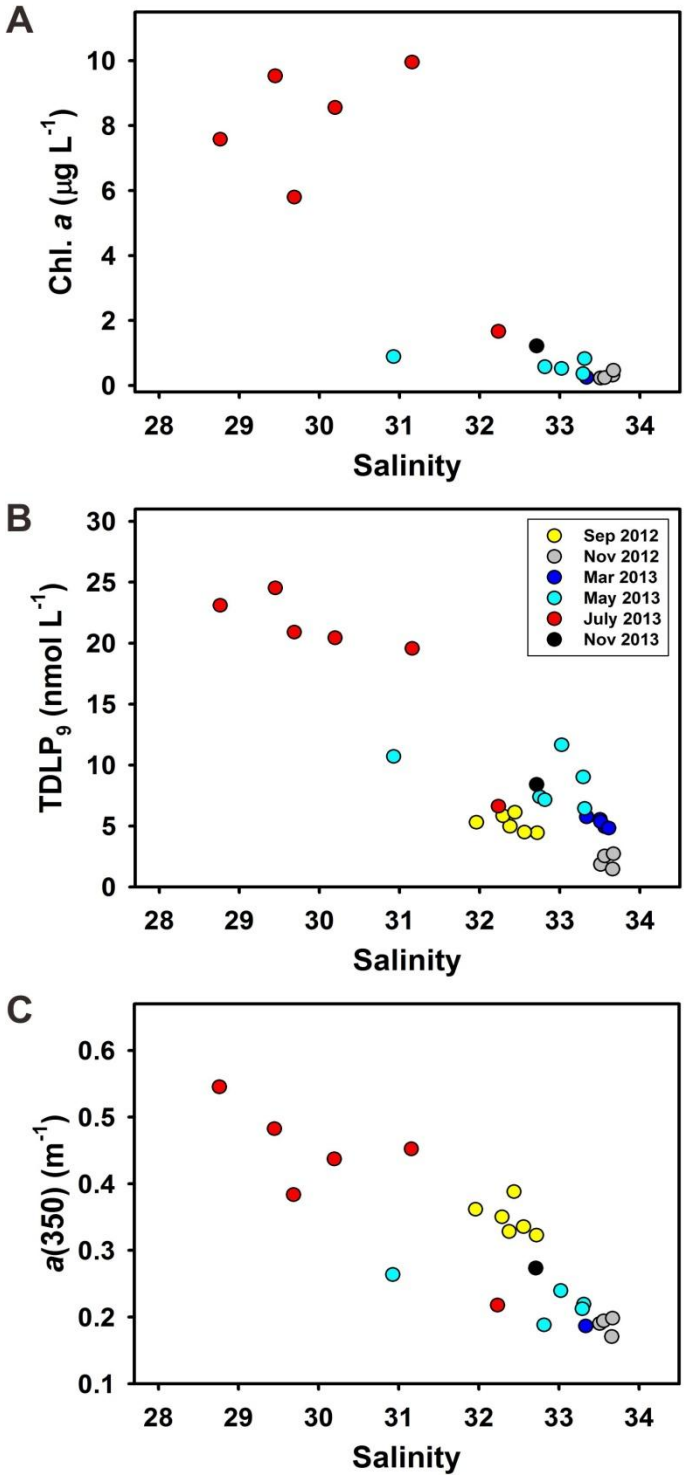

Figure 2-4 Relationships between salinity and **(A)** chlorophyll *a* (Chl. *a*), **(B)** dissolved lignin phenol concentrations ($TDLP_9$), and **(C)** CDOM absorption coefficients [*a*(350)] in surface waters of Otsuchi Bay.

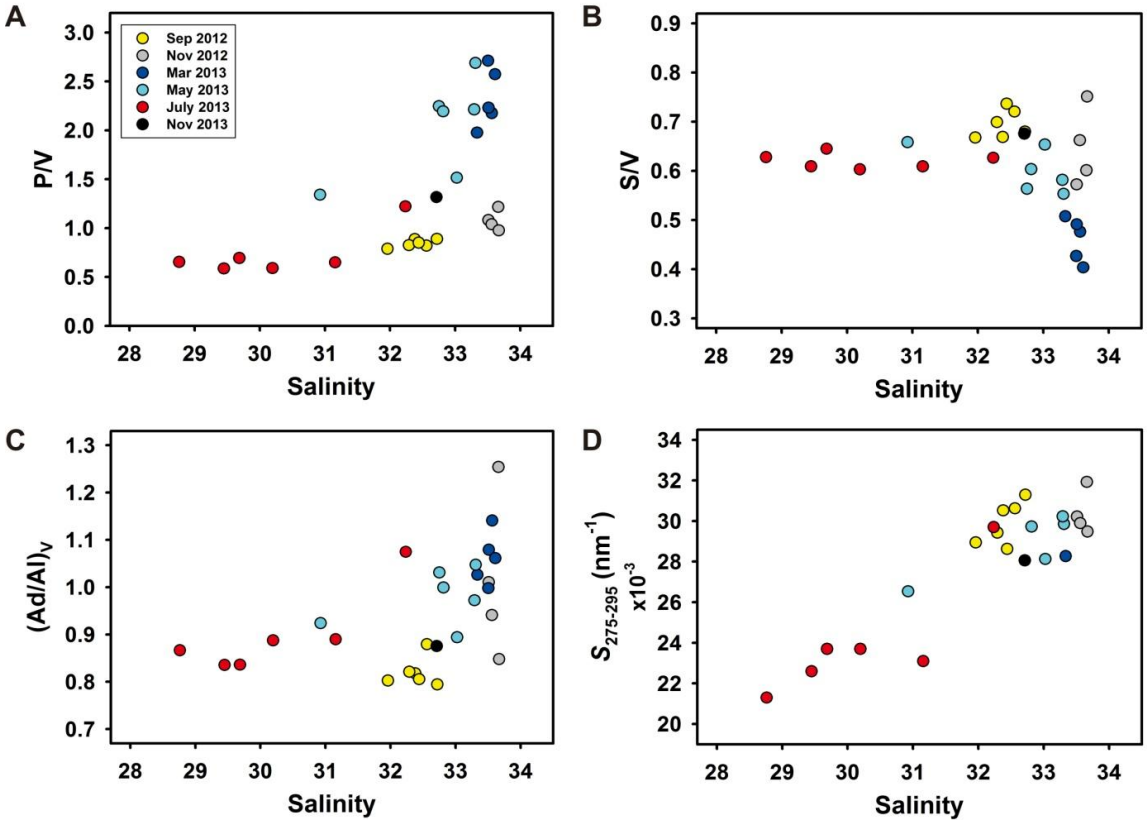

Figure 2-5 Relationships between salinity and lignin phenol compositions **(A)** molar ratio of *p*-hydroxy phenols to vanillyl phenols (P/V), **(B)** molar ratio of syringyl phenols to vanillyl phenols (S/V), **(C)** molar ratio of vanillic acid to vanillin phenols [$(Ad/Al)_V$], and **(D)** the spectral slope coefficient of CDOM absorption coefficient spectrum between 275 and 295 nm ($S_{275\text{-}295}$) in surface waters of Otsuchi Bay.

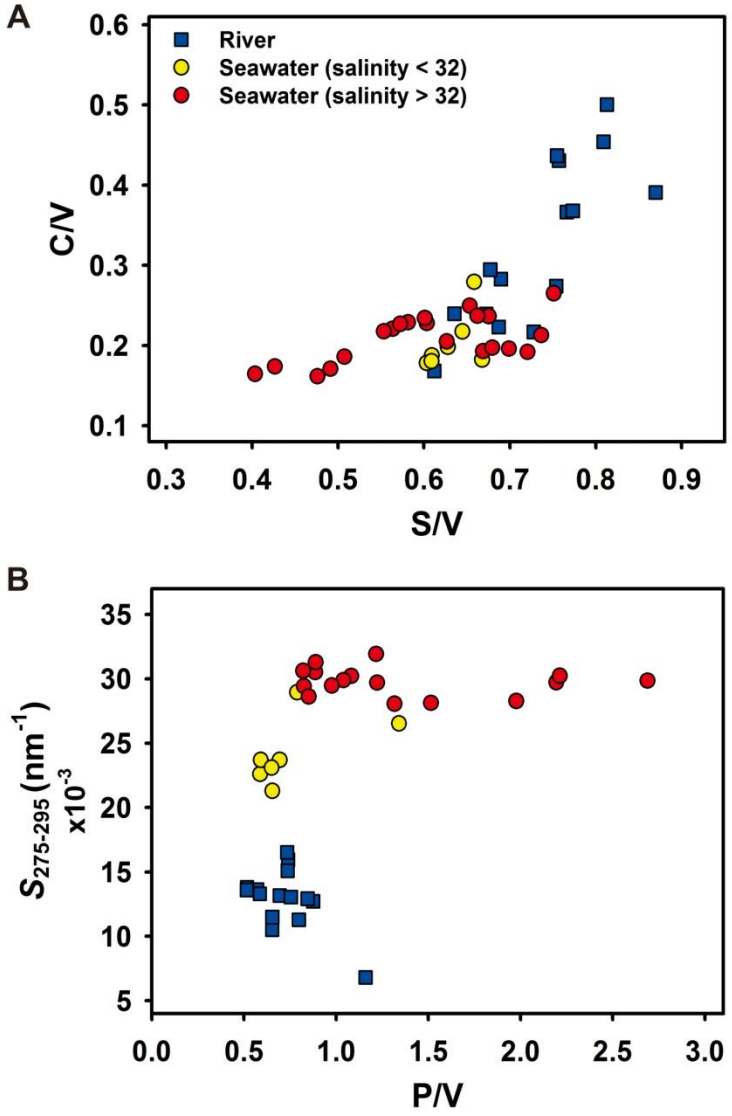

Figure 2-6 Scatter plots of lignin phenol compositions **(A)** S/V ratio versus C/V ratio, **(B)** P/V ratio versus spectral slope $S_{275-295}$ in river (blue squares) and surface waters (red circles).

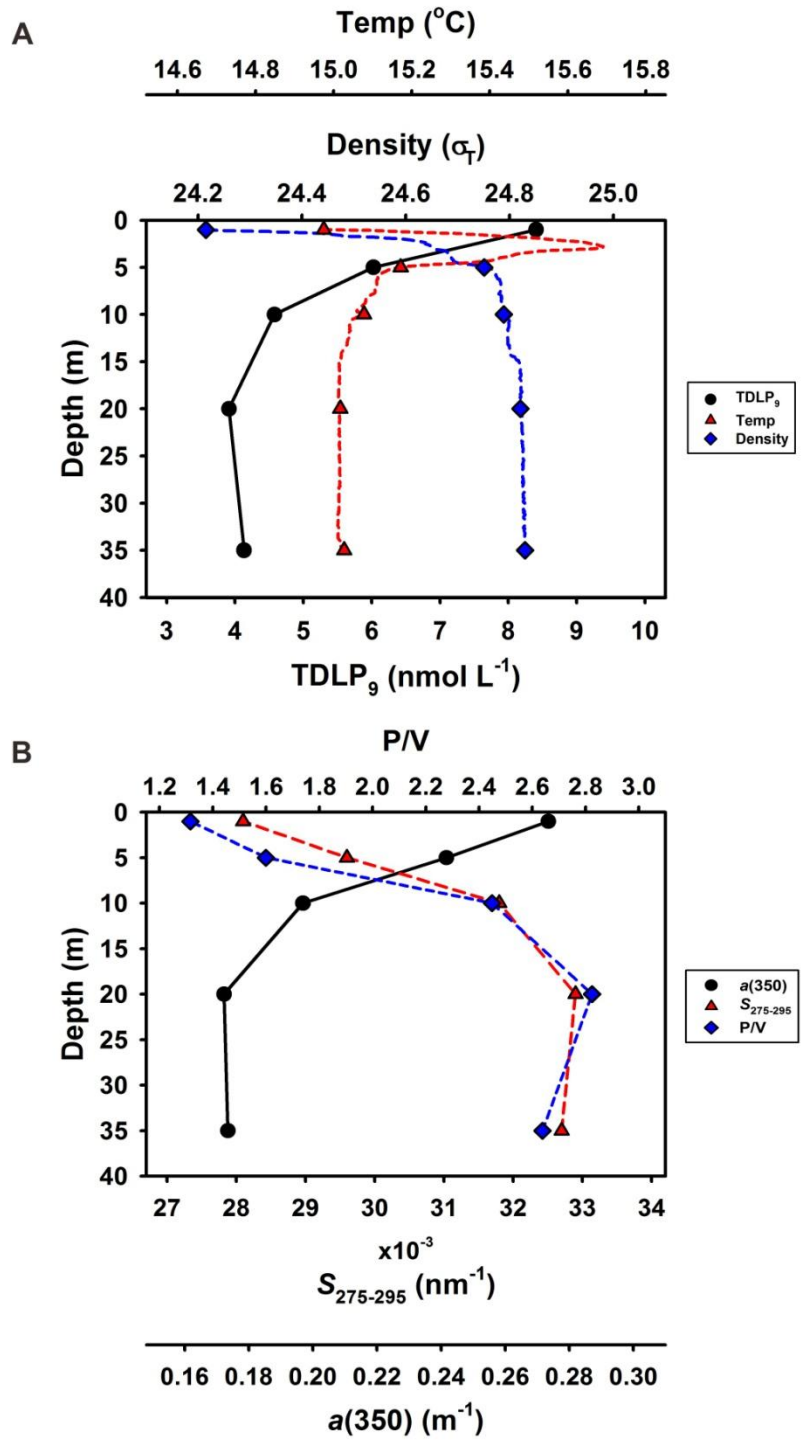

Figure 2-7 Vertical profiles of **(A)** lignin phenol concentrations ($TDLP_9$), temperature and density (σ_T), **(B)** CDOM absorption coefficient *a*(350), spectral slope $S_{275\text{-}295}$ and lignin compositions P/V at station L3 in November 2013. Temperature and density data are form conductivity-temperature-depth (CTD) sensors at each 0.1 meter.

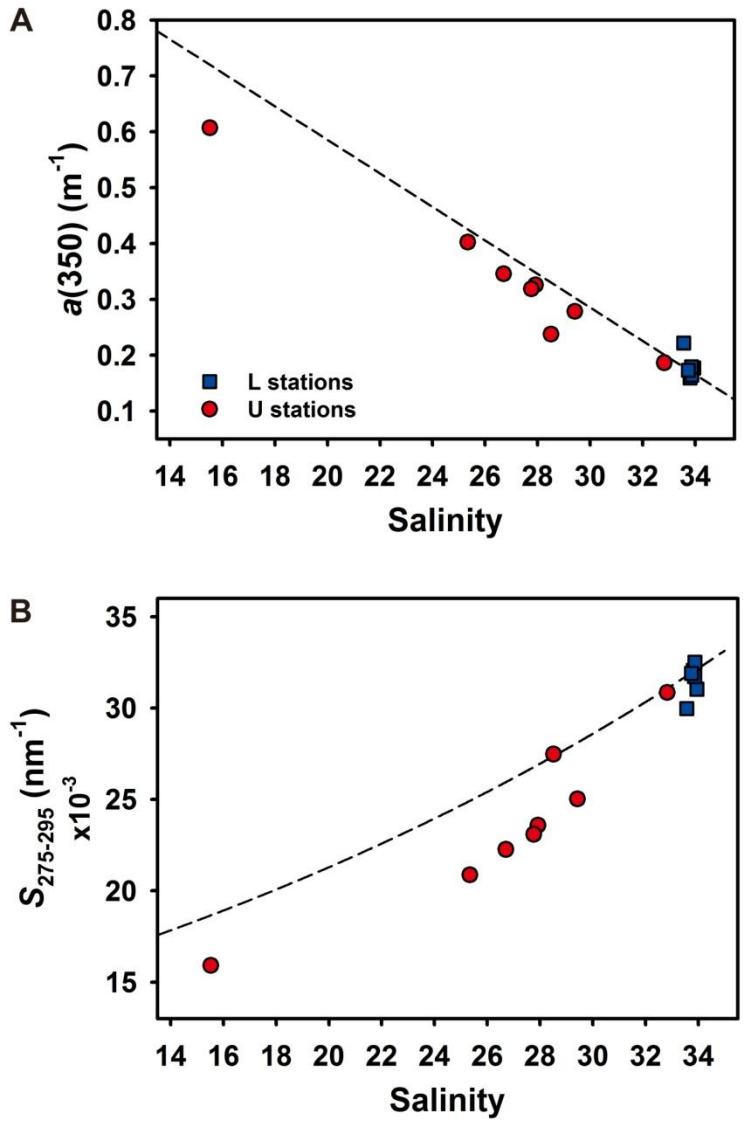

Figure 2-8 Relationships between salinity and **(A)** *a*(350) and **(B)** salinity and $S_{275\text{-}295}$ in surface waters including mid salinity (U stations, red circles) and high salinity (L stations, blue squares) samples in November 2014. Dashed lines are conservative mixing curves constructed using the Unosumai River as the riverine end-member and station L6 as the marine end-member.

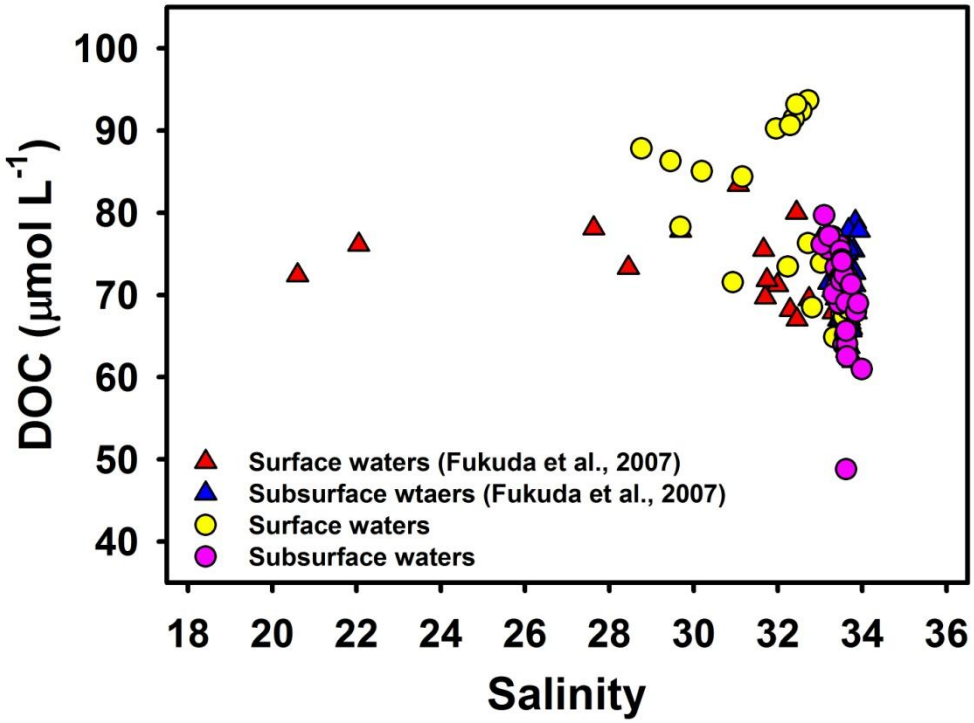

Figure 2-9 Relationship between salinity and DOC concentration retrieved from CDOM absorption coefficients *a*(275) and *a*(295). Surface waters were at 1 m (yellow circles) and subsurface waters (pink circles) were at 6–78 m in this study. Triangles present dissolved DOC concentrations in surface waters (0–2 m, red triangles) and subsurface waters (5–75 m, blue triangles) in the previous study (Fukuda et al., 2007).

Chapter 3
Decomposition Experiment of tDOM in River Water

3.1. Introduction

Photochemical and biological processes are the major degradations of lignin and CDOM in natural environment. Previous studies pointed out that lignin is photosensitive and susceptible to solar radiation indicating photodegradation is primarily responsible for losses of the lignin phenol components of tDOM (Opsahl and Benner, 1998; Herne and Benner, 2003; Stubbins et al., 2012; Benner and Kaiser, 2011). The photodegradation rate of lignin phenols is influenced by the presence of methoxy groups on the aryl ring (such as S/V and P/V ratios) or the oxidation of propyl side-chains which increases the carboxyl content of the remaining lignin (such as Ad/Al ratios) (Ertel and Hedges, 1984; Opsahl and Benner, 1995; McNally et al., 2005; Benner and Kaiser, 2011). Additionally, the slowly microbial oxidation rate of lignin phenols was inferred lignin is relatively high resistance to biodegradation (Hedges et al., 1985; Opsahl and Benner, 1995, 1998). Therefore, it is well recognized that photodegradation preferentially removes lignin from riverine DOM, and biodegradation preferentially removes carbohydrates and amino acids (Benner and Kaiser 2011). Photochemical processes have been shown to enhance the microbial degradation of tDOM, thereby, contributing to its remineralization (Miller and Moran, 1997; Moran et al., 2000; Mopper and Kieber, 2002; Obsernosteret and Benner, 2004; Fichot and Benner, 2014). However, the recent studies have demonstrated biodegradation is the main removal process of lignin phenols in rivers and river-influenced ocean margin (Ward et al., 2013; Fichot and Benner, 2014). Those investigations results imply the effect of biodegradation is possible ignored or underestimated in previous incubation experiments. Meanwhile, CDOM has been widely studied in the sources and sinks of DOM and pointed out the terrestrial origin and photobleaching in the ocean (Coble 2007; Helms et al., 2008; Nelson et al., 2010; Fichot and Benner 2011, 2012; Spencer et al., 2012; Yamashita et al., 2013). Numerous studies

found lignin phenols strongly correlated with CDOM absorbance *a*(350) (Hernes and Benner, 2003; Fichot and Benner, 2012; Fichot et al., 2013; Mann et al., 2016), and another strong nonlinear relationship between DOC-normalized lignin yield and spectral slope $S_{275\text{-}295}$ in rivers and river-influenced ocean margin (Fichot and Benner, 2012; Fichot et al., 2013). This strong relationship between dissolved lignin and CDOM parameters indicated lignin is an important chromophore and consisted with that lignin is photoreactive. However, the good linkage between lignin and CDOM is based on lignin phenol concentrations and CDOM optical properties. It is still unclear regarding the linkage of removal or degradation pathway between lignin and CDOM, especially the analysis is difference due to lignin is a chemical characteristic and CDOM is an optical property.

In this study, a lignin decomposition experiment was used to determine the susceptibility of riverine DOM to photochemical and biological degradation. Photodegrdation and biodegradation of lignin and CDOM were investigated in decomposition experiment with river water and *in-situ* microbial assemblage exposure to natural sunlight or kept in the dark. These experiments demonstrate relationships between lignin phenols and CDOM optical properties and provide a framework for interpreting the transformations of tDOM in bay waters as described in Chapter 2. The riverine water was incubated for two months which was longer than the real residence time in *in-situ* environment to investigate the story of tDOM degradation. The removal pathway between lignin phenols and CDOM properties is further compared in this decomposition experiment.

3.2. Material and Method

3.2.1. Sample collection

The riverine water was collected in the Unosumai River, Iwate, Japan in July 2013 in order to investigate the photochemical and microbial degradation of tDOM. River water was collected using a bucket and filtered through a Whatman® polycarbon membrane (1-µm pore size), collected in an acid-washed Nalgene carboy. Although river

water was be filtered immediately and the filtrate was stored in low temperature (4˚C) and dark condition for 22 days. Nearly 10% of the initial lignin concentrations in this experimeny, compared with the Unosumai River data in July 2012, were consumed during the period because of microbial oxidation. Four polycarbonate containers (30 L) were filled with the filtrate and incubated in a water bath (24 ± 5 ˚C) for 62 days on the roof of a building at the University of Tokyo. Two containers were covered with quartz plate and exposed to natural sunlight. The other two containers were wrapped with aluminum foil and used as a dark treatment. A photo-radiometer (Delta OHM, spectral range: 315~400 nm) was equipped to monitor UVA irradiance. Subsamples (5L) were collected after 3, 10, 20, 41 and 62 days of incubation, and subsamples were filtered through 1-µm filter before the extraction of lignin and CDOM measurements.

3.2.2. Lignin extraction and analysis

Water samples were filtered through Whatman® polycarbonate filter (1-µm pore size) and then acidified to ca. pH 2.5 using sulfuric acid. tDOM fraction including lignin phenols was extracted following the method as described in Chapter 2. Total dissolved lignin concentrations (nmol L^{-1}) were calculated as the sum of 9 lignin phenols ($TDLP_9$) from three phenol families including P, V and S phenols. The ratios of each kind of phenols were also calculated.

Simple exponential decay constants (k) (day^{-1}) were calculated based on a first order kinetics to examine the susceptibility of lignin phenols and CDOM absorption coefficients $a(350)$, respectively, to photochemical and microbial degradation. Equation (5) was used to fit to derive k,

$$C_t = C_0 \times e^{-kt} \tag{5}$$

For lignin phenols, where C_t is the lignin phenol concentrations ($TDLP_9$) at time t, and C_0 is the initial lignin phenol concentrations ($TDLP_9$). For CDOM absorption coefficients $a(350)$, where C_t is the absorption spectral values of $a(350)$ at time t, and C_0 is the initial absorption spectral values of $a(350)$.

3.2.3. CDOM analysis

CDOM subsamples were collected from the filtrate (5 L) through 1-µm filter and stored frozen in the dark for CDOM analysis. A 5-cm quartz cell was used for incubation samples and CDOM absorbance was measured as described in Chapter 2. The CDOM absorption coefficients $a(250)$ and $a(350)$, and the spectral slope coefficients, $S_{275\text{-}295}$ (the spectral slope coefficients between 275–295 nm) and $S_{350\text{-}400}$ (the spectral slope coefficients between 350–400 nm), and the slope ratio, S_R (the ratio of $S_{275\text{-}295}$ to $S_{350\text{-}400}$), were reported in this study. The ratio of absorption coefficient, E_2/E_3 [the ratio of $a(250)$ to $a(365)$], was also calculated.

3.3. Results

3.3.1. Lignin phenols results

The photochemical and biological decomposition of lignin was investigated in experiments with river water incubated under natural sunlight and in the dark for 62 days (Fig. 3-1). The light treatment includes photochemical and biological processing, whereas the dark treatment only includes biological processes. $TDLP_9$ decreased rapidly (29%) during the first 3 days in the light treatment compared with the dark treatment (5%) (Fig. 3-1A). After 62 days, $TDLP_9$ decreased by 59% in the light treatment and 39% in the dark treatment. The rapid loss of lignin phenols in the light treatment was accompanied by a sharp decrease in the S/V, indicating a preferential removal of syringyl phenols (Fig. 3-1C). During the next 59 days, an additional 30% of lignin phenols were removed in the light treatment, versus 34% in the dark treatment (Table 3-1). Relatively minor differences in P/V and S/V were observed between the light and dark treatments. Slightly higher P/V and lower S/V were found in the light treatment after 62 days (Fig. 3-1B, 1C). However, the (Ad/Al)v increased dramatically in the light treatment and declined slightly in the dark treatment throughout the incubation period (Fig. 3-1F).

3.3.2. CDOM results

There was also a rapid decrease (27%) in $a(350)$ in the light treatment compared with the dark treatment (~0%) during the first 3 days (Fig. 3-1D). During the following

59 days, there was a removal of an additional 40% of *a*(350) in the light treatment and 20% in the dark treatment (Table 3-1). After 62 days, *a*(350) decreased by 68% in the treatment exposed to sunlight and by 18% in the dark treatment (Table 3-1).The $S_{275\text{-}295}$ increased dramatically in the light treatment but only minimally in the dark treatment (Fig. 3-1E). Throughout the incubation period, $S_{350\text{-}400}$ values increased by 21% and 10% in the light and dark treatments, but the slope ratio (S_R) increased by 37% in the light treatment and decreased by 4% in the dark treatment (Table 3-1). The E_2/E_3 ratio increased by 55% and 12% in the light and dark treatment, respectively (Table 3-1). After 62 days, *a*(250) and *a*(365) decreased by 32% and 69% in the treatment exposed to sunlight, and those decreased by 9% and 20% in the dark treatment. The increasing E_2/E_3 value was related to decreasing aromatic contents and molecular size (de Haan 1972; Helms et al, 2008; Peuravuori and Pihlaja, 1997; Spencer et al., 2009, 2012). Therefore, the steady decrease in *a*(250) and *a*(365) in both treatments suggested the aromatic structures in lignin were effectively degraded by microorganisms in the present and absence of ultraviolet radiation.

3.3.3. Correlations between lignin phenols and CDOM parameters

The correlation results between lignin phenols, including $TDLP_9$ and $(Ad/Al)_V$, and CDOM parameters, including *a*(350), $S_{275\text{-}295}$ and E_2/E_3, in this decomposition experiment are showed in Fig. 3-2 and Table 3-2. In this incubation, $TDLP_9$ was highly correlated ($p \leq 0.01$, n = 6) with *a*(350) and parameters $(Ad/Al)_V$, $S_{275\text{-}295}$ and E_2/E_3 in the both treatments (Fig. 3-2A–2D, Table 3-2). CDOM absorption coefficients *a*(350) was also strongly correlated ($p \leq 0.01$, n = 6) with lignin ratio, $(Ad/Al)_V$, and CDOM parameters, $S_{275\text{-}295}$ and E_2/E_3, in the both treatments (Fig. 3-2F–2H, Table 3-2). A significant correlation ($p < 0.01$, n = 6) was observed in $S_{275\text{-}295}$ and E_2/E_3 results in the present and absent of sunlight (Fig. 3-2I, Table, 3-2). However, a strong correlation was between (Ad/Al)v and $S_{275\text{-}295}$ ($p = 0.03$, n = 6), but (Ad/Al)v weakly correlated with E_2/E_3 ($p = 0.1$, n = 6) in the light treatment (Fig 3-2E, 2J, Table 3-2). In contrast, $(Ad/Al)_V$ was highly correlated ($p \leq 0.01$, n = 6) with $S_{275\text{-}295}$ and E_2/E_3, respectively in the dark treatment (Fig. 3-2E, 2J, Table 3-2).

3.3.4. Decay constant of lignin phenols and CDOM absorption coefficients

Simple exponential decay constants (*k*) were calculated for lignin phenols concentrations including $TDLP_9$, S, V and P phenols, respectively, in the light treatment and dark treatments (Table 3-2). The *k* value of $TDLP_9$ in the light treatment ($k = 0.0125$ day^{-1}, $R^2 = 0.81$, $p < 0.05$) was higher than this in the dark treatment ($k = 0.0089$ day^{-1}, $R^2 = 0.92$, $p < 0.01$) (Table 3-3). The similar *k* values were obtained in S and V phenols (in S phenols, $k = 0.0147$ day^{-1} and 0.0102 day^{-1} in the light and dark treatments) (in V phenols, $k = 0.0144$ day^{-1} and 0.0100 day^{-1} in the light and dark treatments) and those were higher than P phenols ($k = 0.0072$ day^{-1} and 0.0055 day^{-1} in the light and dark treatments) (Table 3-3). The calculations for the different families of lignin phenols indicated the following sequence of decay constants S > V > P in the light and dark treatments, in agreement with similar patterns observed in degradation experiments using DOM from the Broad River in South Carolina (Benner and Kaiser, 2011).

Similar calculation was also estimated for CDOM absorption coefficients *a*(350) in the both treatments (Table 3-3). The *k* value of *a*(350) in the light treatment ($k = 0.0163$ day^{-1}) was considerably higher than that ($k = 0.0035$ day^{-1}) in the dark treatment and the $TDLP_9$-*k* values in the light and dark treatment. However, the $TDLP_9$-*k* values in the both treatments were higher than the *a*(350)-*k* value in the dark treatment (Table 3-3).

The decay constants values of lignin phenols were dramatically different in the light treatment after the sharp declining (Table 3-3). The similar $TDLP_9$-*k* values were observed in the both treatments after the first 3 days, *k* values were 0.0098 day^{-1} and 0.0090 day^{-1}, respectively in the light and dark treatments (Table 3-3). However, the *a*(350)-*k* value was higher in the present of solar radiation ($k = 0.0132$ day^{-1}) than that in the absence of solar radiation ($k = 0.0034$ day^{-1}) (Table 3-3).

3.3.5. Contributions of photochemical and biological processes in decomposition experiment

The relative contributions of photochemical and biological processes in the lignin decomposition experiments can be estimated by comparing lignin removal in the light treatment (41.7 ± 3.0 nmol L^{-1}) to that in the dark treatment (28.1 nmol L^{-1}). Photodegradation, photo-enhanced biodegradation and biodegradation occurred in the

light treatment, whereas only biodegradation occurred in the dark treatment. During the 62-day experiments, lignin biodegradation in the dark treatment accounted for 67% of the total lignin degradation observed in the light treatment. Based on this calculation, photodegradation and photo-enhanced biodegradation accounted for 33% of the lignin removal in the light treatment.

3.4. Discussion

3.4.1. Biodegradation and photodegradation of lignin and CDOM

Exposure to solar radiation led to the rapid decomposition of lignin and CDOM in this study. Losses of lignin phenols and CDOM absorption were several times greater in the light than those in the dark during the first three days of the experiments (Fig. 3-1A,1D), which is consistent with the known susceptibility of lignin to photodegradation (Opsahl and Benner, 1998; Stubbins et al., 2010). Following this initial burst of photodegradation and photobleaching, lignin phenol decay constants were similar during the next two months in the light and dark treatments (k = 0.0098 day^{-1} and 0.0090 day^{-1} in the light and dark treatments, respectively) (Table 3-3). Photochemical processes can produce bioavailable photoproducts (Miller and Moran, 1997; Obernosterer and Benner, 2004), but the similar rates of lignin degradation in the light and dark treatments during the ensuing two months indicated photochemical processes had a minor impact on lignin biodegradation after the initial three days of solar exposure. In contrast, alterations of a(350) and $S_{275\text{-}295}$ continued to be much greater in the light treatments, the a(350)-k values was nearly 4-fold higher accompanying with solar radiation compared with that in the dark treatment (Table 3-3). This result suggested some photobleaching was not directly linked with lignin decomposition. The biodegradation decay rate for lignin in the Unosumai River was higher than that observed in the similar decomposition experiments in the Broad and Mississippi rivers (Opsahl and Benner, 1998; Fichot and Benner, 2014), which could be related to more rapid mobilization and transport of lignin and also tDOM in the Unosumai River basin. Therefore, tDOM in this area is relatively fresh compared with that in the above river basins.

Previous studies have observed varying susceptibility to photodegradation among lignin phenols, such as P/V and $(Ad/Al)_V$ ratios increased because of photodegradation (Opsahl and Benner, 1998; Spencer et al., 2009; Benner and Kaiser, 2011). In the present study a relatively small increase in P/V and decrease in S/V were observed in the light treatment, whereas the $(Ad/Al)_V$ increased rapidly in the light treatment. The rapid increase in $(Ad/Al)_V$ was matched by rapid increases in $S_{275\text{-}295}$ and E_2/E_3. Previous studies have linked increases in $S_{275\text{-}295}$ and E_2/E_3 with decreases in the average molecular weight of DOM (de Haan 1972; Helms et al, 2008). Overall these observations indicated the photodegradation of lignin is accompanied by a decrease in its molecular weight, as previously demonstrated during the photodegradation of lignin in Mississippi River water (Opsahl and Benner, 1998). Relatively minor increases in $S_{275\text{-}295}$ and E_2/E_3 were observed in the absence of solar radiation even though the rate of lignin biodegradation and photodegradation were similar after the initial three days of decomposition. Losses of *a*(350) were substantially higher (ca. 10%) than those of lignin phenols in the light treatment, whereas losses of *a*(350) were lower (ca. 20%) than those of lignin phenols in the dark treatments. It appears the pathways of lignin and CDOM degradation are different in the presence and absence of solar radiation. CDOM is primarily responsible for photochemical process because solar radiation bleaches all photoactive components in seawater including terrestrial and marine origin (Benner and Kaiser, 2011; Spencer et al., 2012). In contrast, lignin photodegradation, as well as biodegradation, is related to the structure of the lignin macropolymer rather than an intrinsic difference in monomer lability such as lignin containing aldehydes are preferentially degradated than those containing carboxylic acids during photodegradation (Ertel and Hedges, 1994; Hedges et al., 1988; Opsahl and Benner, 1995, 1998; Shakya et al., 2011).

The decay constant *k* values after the first 3 days also suggested the various pathways in lignin and CDOM results (Table 3-3). Similar $TDLP_9$-*k* values but different *a*(350)-*k* values during the next 59 days indicated biodegradation dominated lignin decomposition, but CDOM index continued to be altered by photobleaching. Although, photochemical process was primarily responsible for losses of the chromophoric and lignin phenols of DOM, and lignin phenols exhibit a robust positive relationship with CDOM absorption coefficients *a*(350) (Hernes and Benner, 2003; Benner and Kaiser,

2011; Fichot and Benner, 2012). This incubation results suggested that the pathway or the reactive compounds of lignin photodegradation are inconsistent with the pathway of CDOM photobleaching.

3.4.2. The relative contributions of photodegradation and biodegradation

The decomposition experiments demonstrated the susceptibility of lignin to microbial and photochemical decomposition. As with previous experimental studies, solar exposure promoted relatively rapid alterations of lignin and CDOM (Opsahl and Benner, 1998; Hernes and Benner, 2003; Spencer et al., 2009; Benner and Kaiser, 2011). The relative contributions of photochemical and biological processes in the transformation and decomposition of lignin and CDOM are dependent on several environmental variables, including solar irradiance, water clarity, microbial community structure, temperature, and physical mixing. On the Louisiana shelf in the northern Gulf of Mexico, biodegradation dominated lignin transformations in the shelf mixed layer and accounted for 60% of total decomposition of lignin (Fichot and Benner, 2014). Photo-enhanced biodegradation accounted for 32% of total lignin decomposition and direct photodegradation accounted for 8% of lignin removal on the Louisiana shelf. Based on the relative contributions of photodegradation and biodegradation in the lignin decomposition experiments, and assuming solar exposure in the light treatments was similar to that in surface seawaters of Otsuchi Bay, biodegradation was accounted for 67% of total lignin removal and photo-enhanced biodegradation plus direct photodegradation were accounted for 33% of total lignin removal.

3.4.3. Possible pathways of tDOM degradation

The environmental condition (e.g., light condition) and tDOM compositions (e.g., labile, semi-labile and refractor tDOM) decide the mechanism of tDOM degradation. In this study, tDOM was classed as two fractions based on photo-reactivity and biological reactivity. In light condition, tDOM is classified into: (1) photo-resistant and biologically refractory fraction, and (2) photo-reactive but partly biologically refractory fraction (including lignin phenols). With solar irradiance, photo-reactive lignin phenols are altered due to photochemical processes, and aromatic contents also decrease. Meanwhile, size

distribution of tDOM shifts from relatively-high-molecular-weight toward relatively-low-molecular-weight, and a part of this low-molecular-weight tDOM could directly remineralize to CO_2 or cycle within microbial food web (Ward et al., 2013). In dark condition of this experiment, tDOM is mostly altered by microbial enzymatic activity, thus, tDOM is classified into: (1) biologically refractory fraction (including lignin phenols), (2) biologically semi-labile fraction (also including lignin phenols), and (3) biologically labile fraction (including amino acid and sugars) following previous studies (Davis and Benner, 2007; Benner and Kaiser, 2011). Biologically labile fraction of tDOM is directly consumed by microbe, and biologically semi-labile tDOM is altered by microbial enzymatic activity coupling with molecular weight decline as indicate as the incubation results. In this incubation experiment, assuming photo-reactivity lignin phenols (ca. 29%) had been completely consumed during the first 3 days, therefore, biologically fraction is ca. 30% and non-active tDOM is ca. 41% of total tDOM in this incubation experiment. Those fractions were consistence with previous Mississippi River water microbial degradation experiment after 620-day incubation (Hernes and Benner, 2003). This previous study data showed ca. 48% of lignin was non-active fraction in this long-term incubation (Hernes and Benner, 2003).

3.5. Conclusion

This decomposition experiment results indicates lignin phenols are photolabile, and photochemical process are preferentially responsible for losses of lignin phenols than biological processes. However, once photosensitive lignin phenols are depleted, biodegradation will dominate in controlling lignin transformation, and the remained tDOM will become fairly refractory in seawater due to lignin is relatively high resistance to biodegradation (Whitehead, 2008). Meanwhile, other chromophore has continuously bleached by solar radiation in natural environment. Therefore: (1) the pathways of lignin and CDOM degradation are different with and without solar radiation, (2) the pathways of photodegradation for lignin phenols and photobleaching for CDOM optical properties are not directly linking. In addition, CDOM optical properties are also influenced by *in-situ* production (Moran et al., 2000; Coble, 2007), and this highlights the significance of

lignin phenols in tDOM study. This study also implies biodegradation was underestimated in previous incubation experiment because of the short incubation time. Our results suggest that the water residence time in *in-situ* environment will be another important factor to estimate the contributions of photochemical and/or biological processes.

Table 3-1 Decomposition experiments of DOM in the Unosumai River water under natural sunlight and dark treatments. Signal data after 41 days in the dark treatment due to one of the two incubated container was broken.

Days	[1]Irradiance dose (MJ m^{-2})	[2]$TDLP_9$ (nM)	P/V	S/V	C/V	$(Ad/Al)_P$	$(Ad/Al)_V$	$(Ad/Al)_S$	$a(350)$ (m^{-1})	$S_{275-295}$ (nm^{-1})	S_R	E_2/E_3
LIGHT TREATMENT												
0	0.00	70.7±4.3	0.54	0.59	0.14	1.16	0.78	0.61	2.01	0.0136	0.88	4.57
3	0.96	50.5±0.9	0.48	0.51	0.11	1.25	1.02	0.66	1.47	0.0169	1.03	5.39
10	1.85	47.7±1.5	0.42	0.54	0.12	1.29	1.14	0.70	1.16	0.0204	1.10	6.34
20	3.59	37.1±1.5	0.48	0.57	0.14	1.36	1.22	0.69	0.93	0.0238	1.29	7.57
41	6.16	30.9±2.8	0.61	0.55	0.14	1.14	1.23	0.64	0.72	0.0272	1.40	9.26
62	8.11	29.0±1.8	0.75	0.53	0.16	1.03	1.14	0.57	0.65	0.0273	1.40	10.3
DARK TREATMENT												
0	0	72.6±1.2	0.48	0.59	0.14	1.15	0.75	0.56	1.95	0.0137	0.87	4.66
3	0	69.4±0.7	0.46	0.55	0.12	1.12	0.76	0.54	1.98	0.0136	0.88	4.60
10	0	71.5±0.3	0.46	0.55	0.12	1.09	0.73	0.51	1.85	0.0137	0.83	4.79
20	0	63.8±1.3	0.51	0.58	0.14	1.09	0.72	0.55	1.74	0.0139	0.83	4.92
41	0	45.7	0.59	0.54	0.12	1.07	0.63	0.47	1.65	0.0145	0.84	5.12
62	0	44.5	0.60	0.57	0.15	1.08	0.65	0.59	1.60	0.0147	0.83	5.31

[1]Irradiance dose was the results between wavelength 315~400 nm during the incubation period.
[2] Error indicates range of duplicate samples.

Table 3-2 Summary of regression analysis between lignin concentrations ($TDLP_9$), composition ratio [$(Ad/Al)_V$] and CDOM parameters [including $a(350)$, $S_{275-295}$ and E_2/E_3].

	$TDLP_9$ (nmol L^{-1})	$a(350)$ (m^{-1})	$(Ad/Al)_V$	$S_{275-295}$ (nm^{-1})
LIGHT TREATMENT				
$TDLP_9$ (nmol L^{-1})				
$a(350)$ (m^{-1})	Slope = 0.011 R^2 = 0.98 $p < 0.01$			
$(Ad/Al)_V$	Slope = 0.010 R^2 = 0.83 $p = 0.01$	Slope = 0.31 R^2 = 0.85 $p = 0.01$		
$S_{275-295}$ (nm^{-1})	Slope = 0.35 R^2 = 0.94 $p = 0.01$	Slope = 10 R^2 = 0.96 $p < 0.01$	Slope = 28 R^2 = 0.75 $p = 0.05$	
E_2/E_3	Slope = 0.13 R^2 = 0.86 $p = 0.01$	Slope = 4.0 R^2 = 0.87 $p < 0.01$	Slope = 9.6 R^2 = 0.54 $p = 0.1$	Slope = 2.5 R^2 = 0.95 $p < 0.01$
DARK TREATMENT				
$TDLP_9$ (nmol L^{-1})				
$a(350)$ (m^{-1})	Slope = 0.033 R^2 = 0.84 $p = 0.01$			
$(Ad/Al)_V$	Slope = 0.0039 R^2 = 0.93 $p < 0.01$	Slope = 0.31 R^2 = 0.86 $p = 0.01$		
$S_{275-295}$ (nm^{-1})	Slope = 0.035 R^2 = 0.96 $p < 0.01$	Slope = 2.7 R^2 = 0.89 $p < 0.01$	Slope = 8.5 R^2 = 0.94 $p < 0.01$	
E_2/E_3	Slope = 0.020 R^2 = 0.87 $p < 0.01$	Slope = 1.7 R^2 = 0.97 $p < 0.01$	Slope = 4.9 R^2 = 0.86 $p = 0.01$	Slope = 1.6 R^2 = 0.95 $p < 0.01$

n = 6 in all correlations.

Table 3-3 Decay constants *k* values of $TDLP_9$, syringyl (S), vanillyl (V) and *p*-hydroxy (P) phenols, and CDOM absorption coefficients *a*(350) throughout the 62-day incubation.

		$TDLP_9$	S phenols	V phenols	P phenols	*a*(350)		$TDLP_9$	*a*(350)
		Through the 62-day incubation, n = 6					After the first 3 days, n = 5		
Light treatment	k (day^{-1})	0.0125	0.0147	0.0144	0.0072	0.0163	k (day^{-1})	0.0098	0.0132
	R^2	0.81	0.87	0.89	0.41	0.84	R^2	0.90	0.90
	p	< 0.05	< 0.01	< 0.01	> 0.1	0.01	p	0.01	0.01
Dark treatment	k (day^{-1})	0.0089	0.0102	0.0100	0.0055	0.0035	k (day^{-1})	0.0090	0.0034
	R^2	0.92	0.89	0.92	0.93	0.92	R^2	0.90	0.90
	p	< 0.01	< 0.01	< 0.01	< 0.01	< 0.01	p	0.01	0.01

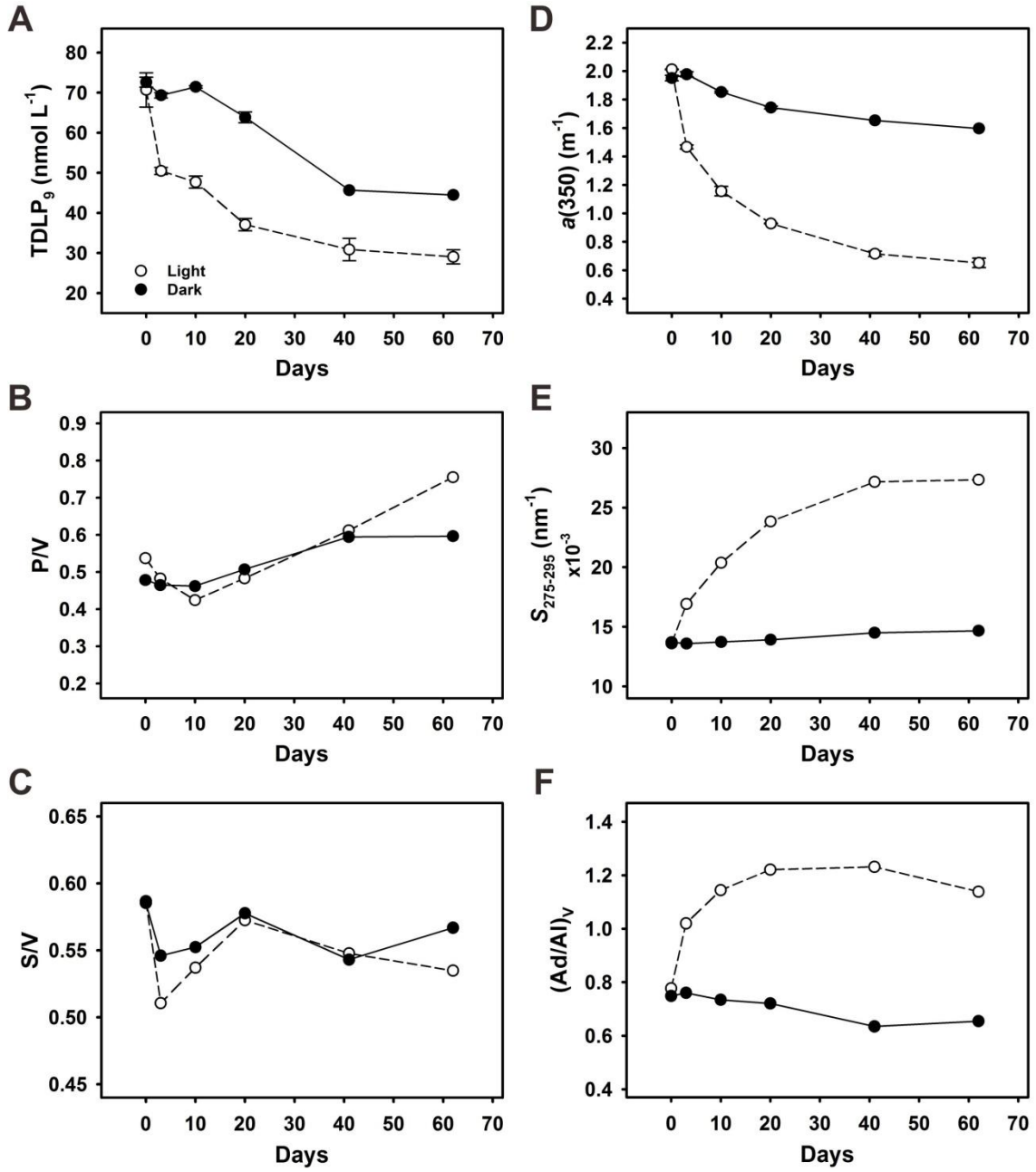

Figure 3-1 Photochemical and biological degradation of DOM in Unosumai River water. Time-course changes in **(A)** lignin phenol concentrations ($TDLP_9$), **(B)** lignin phenol P/V composition, **(C)** lignin phenol S/V composition**, (D)** CDOM absorption coefficient *a*(350), **(E)** spectral slope $S_{275\text{-}295}$, and **(F)** lignin phenol $(Ad/Al)_V$ composition. Experiments were conducted with duplicate samples incubated under natural sunlight (light treatment; photochemical and biological processes; open circles) and duplicate samples wrapped in aluminum foil (dark treatments; biological processes; closed circles). Plots are presented as average value ± range of duplicate samples, and error of lignin phenol composition ratio is < 0.01 of duplicate samples in this decomposition experiment.

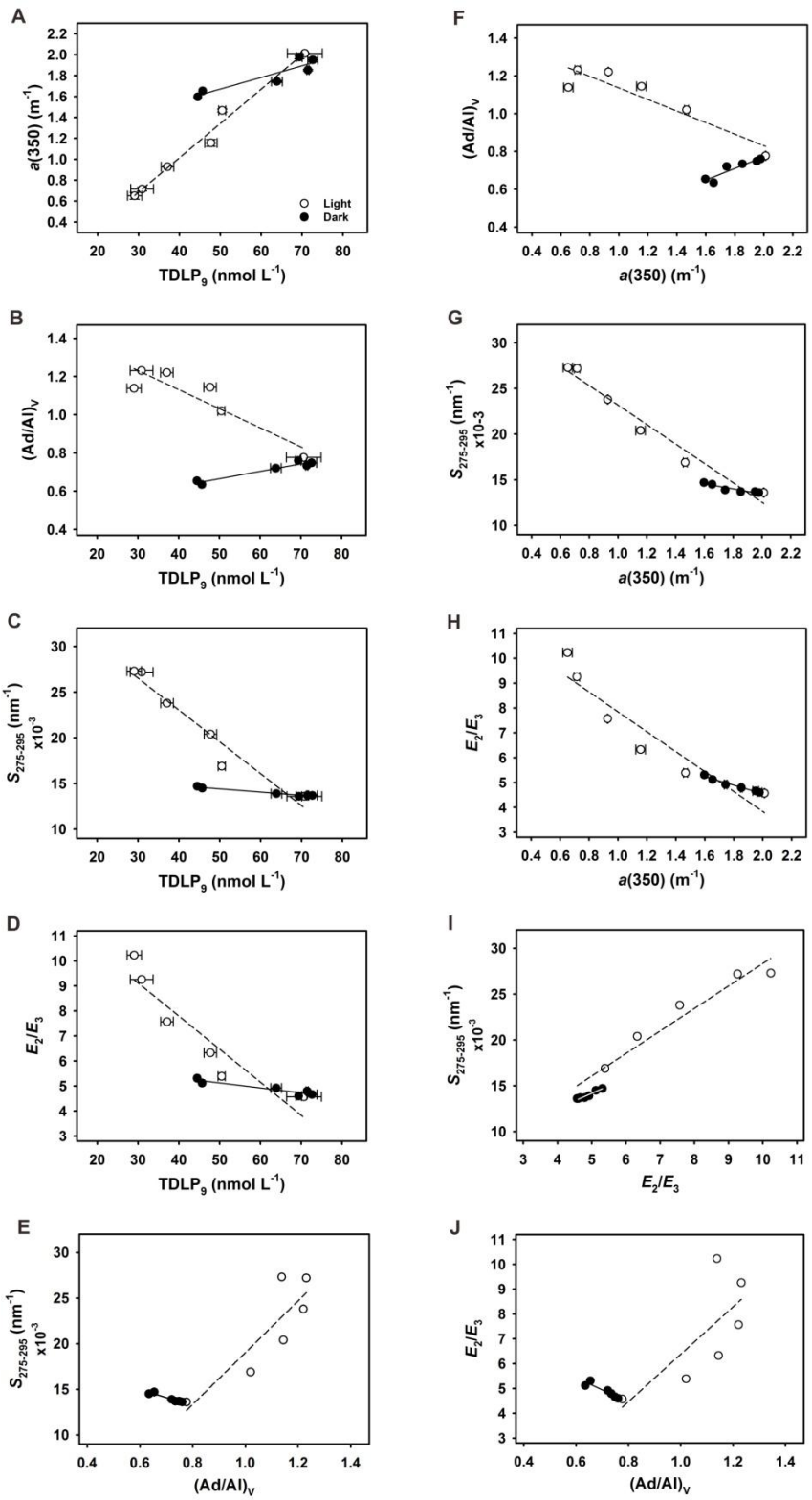

Figure 3-2 Correlation relationship between **(A)** $TDLP_9$ and $a(350)$, **(B)** $TDLP_9$ and $(Ad/Al)_V$, **(C)** $TDLP_9$ and $S_{275\text{-}295}$, **(D)** $TDLP_9$ and E_2/E_3, **(E)** $(Ad/Al)_V$ and $S_{275\text{-}295}$, **(F)** $a(350)$ and $(Ad/Al)_V$, **(G)** $a(350)$ and $S_{275\text{-}295}$, **(H)** $a(350)$ and E_2/E_3, **(I)** E_2/E_3 and $S_{275\text{-}295}$, and **(J)** $(Ad/Al)_V$ and E_2/E_3 in decomposition experiment. Dashed line presents the regression line in light treatment. Solid (or white) line represents the regression line in dark treatment.

Chapter 4
Open-Ocean Environment: tDOM in the Western North Pacific

4.1. Introduction

It limits our knowledge to understand terrigenous dissolved organic matter (tDOM) in open ocean environment due to the limited number of tDOM study in the open ocean. Previous studies pointed out tDOM is a small fraction (0.7–2.4%) of bulk DOM in the Pacific and Atlantic Ocean, and suggested ocean margin is the major site of tDOM transformation due to the short residence time of tDOM (21–132 year) (Hedges et al., 1997; Opsahl and Benner, 1997). However, previous investigations found the chemical characteristic of terrestrial matter in North Pacific Intermediate Water (NPIW) including high contents of dissolved and particulate organic carbon (DOC and POC), humic substance and dissolved iron (Hansel et al., 2002; Hernes and Benner, 2002; Nakatsuka et al., 2004; Nishioka et al., 2007, 2013; Yamashita et al., 2008). Those investigation results highlight the potential of a long-distance transportation of tDOM, in other words, tDOM escapes from degradation processes in coastal regions.

NPIW plays a significant role in the North Pacific Ocean because of its original terrestrial sources. Numbers of NPIW circulations studies suggested that the Sea of Okhotsk is important as a source of NPIW (Talley, 1991; Yasuda et al., 1996, 2001; Yasuda 2004; You, 2003), and large volume of freshwater from the Amur River is inflowing into the Sea of Okhotsk (Simonov and Dahmer, 2008). NPIW is different from other intermediate water characterized by salinity minimum at 26.8σ_θ and that is widely distributed up to the North Pacific subtropical gyre (Yasuda, 2004). Yasuda (2004) suggested NPIW is the water including the salinity minimum layer in the density range of 26.6–27.4σ_θ and that is influenced by low-salinity subarctic waters. Fig. 4-1 shows the NPIW circulation patterns and water modification in the western North Pacific Ocean. The origins of NPIW include: (1) the fresh and low potential vorticity water from the Sea of Okhotsk, and (2) Kuroshio high-salinity water (the old NPIW). After those two waters

met, part of the mixing water flows eastward along the Kuroshio Extension. Part of the modified water flows southwestward, and the rest of the modified waters flows northeastward and enters into the Kuroshio-Oyashio interfrontal zone (Yasuda et al., 1996; You, 2003). In addition, the terrestrial characteristics of NPIW are also investigated in biogeochemical cycles. Iron availability is important for phytoplankton growth in the western subarctic Pacific. Nishioka et al. (2013) investigated the Fe supply process in the western subarctic Pacific. They found the high concentrations of dissolved Fe in the intermediate water layer and that is derived from sediments in the Sea of Okhotsk. Other study pointed out the intermediate water mass was rich in DOC, POC and fluorescent intensity indicated that terrestrial humic substances from the Amur River were evident (Hansell et al., 2002; Nakatsuka et al., 2004; Yamashita and Tanoue, 2008). Hernes and Benner (2002) directly measured lignin phenols in NPIW at Station Aloha, and found lignin concentrations were a factor of two greater than at all other depths. In addition, based on the characteristic of tDOM combined with high level of dissolved Fe (Nishioka et al., 2013), a hypothesis is that tDOM may act as organic lignad with bioactive trace metals in the ocean (Rue and Bruland 1995), and it plays an important role in the marine biogeochemical cycles. However, it still needs the direct evidence, such as lignin phenol, to test this hypothesis.

Lignin phenol is the good indicator of tDOM in the ocean because lignin is the major structure of terrestrial vascular plants (Hedges and Mann, 1979; Meyers-Schulte and Hedges, 1986; Opsahl and Benner, 1997), and that indicates the transformations of tDOM in waters and soils including photodegradation and biodegradation (Opsahl and Benner, 1998; Dickens et al., 2007; Spencer et al., 2009; Benner and Kaiser, 2011; Fichot and Benner, 2012, 2014). Hernes and Benner (2002) measured lignin in the North Pacific Ocean and suggested lignin can serve as a general circulation tracer for tracing riverine input and diagenesis processing of tDOM in the open ocean. They found the maximum lignin concentrations were in NPIW layer, and their lignin results also provided molecular evidence of photochemical oxidation in seawater.

Chromophoric dissolved organic matter (CDOM) has been widely studied in DOM sources and sinks including photobleaching and microbial processes, and even CDOM can used to trace hydrography in marine environment (Coble 2007; Yamashita et

al., 2008, 2013; Swan et al., 2009; Nelson et al., 2010). The global distribution of CDOM in surface waters is superficially similar to the distribution of chlorophyll *a* (Siegel et al., 2002) The highest abundances of CDOM are in coastal regions, on the continental shelf, restricted sea, and river outflows due to terrestrial input in these systems (Stedmon and Nelson, 2015). In the open ocean, CDOM is more abundance at high latitudes and upwelling area, such as coastal and equatorial, indicating the connection to productivity and CDOM-rich deep water. In contrast, the lowest CDOM is in the subtropical gyres causing by low productivity, high stratification, and high level of photobleaching (Stedmon and Nelson, 2015). In the North Pacific, the deep-water CDOM absorption and fluorescence are higher than that in the South Pacific (Yamshita and Tanoue, 2008; Swan et al., 2009; Nelson et al., 2010). The higher values of CDOM in deep water indicate the accumulation of CDOM from the remineralization of sinking particles and comparatively slower overturning circulation (Yamashita and Tanoue, 2009; Nelson et al., 2010).

Previous studies observed a good linkage between lignin phenols and CDOM in the coastal ocean and suggested predicting lignin phenol concentrations by CDOM absorption coefficients (Hernes and Benner, 2003; Fichot and Benner, 2011, 2012; Fichot et al., 2016). However, the correlation between lignin and CDOM in the open ocean could be weak due to the *in-situ* production of CDOM. Additionally, the results of tDOM decomposition experiment in this study (Chapter 3) showed the pathways of lignin and CDOM degradation are different in the presence and absent of sunlight. Considering photodegradation only happens in the surface layer, and biodegradation could dominate tDOM transformation with long-term transport in the open ocean. Therefore, these imply the uncertain to investigate tDOM using CDOM only, especially in the open ocean where tDOM is a low level of bulk DOM.

Dissolved lignin phenols and CDOM optical properties were measured to investigate the sources and transformation of tDOM in the western North Pacific Ocean, especially NPIW. NPIW provides a high potential to study tDOM in marine environment because of the well-identified terrestrial characteristics (Hansel et al., 2002; Hernes and Benner, 2002; Nakatsuka et al., 2004; Nishioka et al., 2007, 2013; Yamashita et al., 2008). Additionally, NPIW transports for a long-distance in a deep layer where solar radiation is minor and at low temperature to reduce the influences of photochemical and microbial

processes. Therefore, the measurement of lignin and CDOM in NPIW can improve our knowledge of tDOM transportation and its transformation in the ocean, and have a better understanding of the global biogeochemical cycles.

4.2. Material and Method

4.2.1. Study area and sampling overview

Observations in the western North Pacific Ocean were carried out during a cruise by the R/V *Hakuho Maru* (KH-12-3, from July to August 2012) along the 160˚E transect from the subarctic to the subtropical regions (Fig. 4-2). One surface sample (station G9, Fig. 4-2) was collected near the mouth of the Amur River by the research vessel Professor Khromov (Far Eastern Hydrometeorogical Research Institute: FERHRI) during the observation in the Sea of Okhotsk in 2006 (Kh06).

4.2.2. Lignin extraction and analysis

Seawater samples (20 L) were collected for lignin analysis at station 1, 2, 5, 7, 8, 9, 11, 12, 14, 15, 16, 17 and 18. Seawater was collected using Niskin bottles mounted on a CTD/CMS from various depths (10–2000 m). Those samples included seawater from the NPIW layers that were close to salinity minimum depth such as 500 m and 750 m. Seawater for lignin analysis was filtered through Whatman® polycarbonate filter (1-µm pore size) and then acidified to ca. pH 2.5 using sulfuric acid. tDOM fraction including lignin phenols was extracted following the method as described in Chapter 2. Total dissolved lignin concentrations (nmol L^{-1}) were calculated as the sum of 6 lignin phenols ($TDLP_6$, including vanillyl and syringyl phenol families) to avoid non-lignin-derived cinnamyl phenols form ester-bound during alkaline CuO oxidation (Opsahl and Benner, 1995; Hernes and Benner, 2003). The ratios of those phenols were also calculated. In additional, this study also presented the concentration of 3,5-dihydroxybenzoic acid (DiOHBA), one of the benzene carboxylic acid and is not substituted with methoxy group. DiOHBA is also released from CuO oxidation and appears to be derived from soils organic carbon (Dickens et al., 2007).

4.2.3. CDOM analysis

CDOM subsamples were collected from all stations and depths during routine casts. Seawater was gravity-filtered directly from Niskin bottle and through pre-combusted Whatma® GF/F filter (0.7-µm pore size) and collected in pre-combusted glass vials (Teflon-lined cap). CDOM subsamples were stored frozen in the dark until CDOM analysis. A 5-cm quartz cell was used for all samples and CDOM absorbance was measured as described in Chapter 2. The CDOM absorption coefficients *a*(350), and the spectral slope coefficients, $S_{275\text{-}295}$, were reported in this study.

4.2.4. Calculation of apparent oxygen utilization

Apparent oxygen utilization (AOU) (µmol L^{-1}) represents one estimate of the O_2 utilized due to biochemical processes relative to a preformed value (Garcia et al., 2013). AOU was calculated using *in-situ* (CTD data) O_2, temperature and salinity, and it was defined as the difference between the O_2 gas solubility and the measured O_2 concentrations and expressed as equation (6) (Garcia et al., 2013):

$$AOU = [O_2^*] - [O_2] \tag{6}$$

where $[O_2]$ is measured O_2 concentration, and $[O_2^*]$ is the O_2 solubility concentration (mL L^{-1}) calculated as a function of *in-situ* temperature (˚C) and salinity, and one atmosphere of total pressure (Garcia et al., 2013). The $[O_2^*]$ values were calculated using equation (7) and (8) following Garcia and Gordon (1992):

$$\ln[O_2^*] = A_0 + A_1T_S + A_2T_S^2 + A_3T_S^2 + A_3T_S^3 + A_4T_S^4 + A_5T_S^5 + S(B_0 + B_1T_S + B_2T_S^2 + B_3T_S^3) + C_0S^2 \tag{7}$$

where S is salinity, and A_0, A_1, A_2, A_3, A_4, A_5, B_0, B_1, B_2, B_3 and C_0 are the constant coefficients of Garcia and Goedon (1992), and those values are shown in Table 4-1. T_S is scaled temperature using equation (8):

$$T_S = \ln[(298.15 - t)(273.15 + t)^{-1}] \tag{8}$$

where t is *in-situ* temperature.

4.3. Results

4.3.1. Dissolved lignin phenols in the western North Pacific Ocean

An inverse pattern was found in salinity and lignin phenol concentrations ($TDLP_6$) results throughout the depth profile in Fig. 4-3. Lignin concentrations ranged from 0.057–0.71 nmol L^{-1} along the 160˚E transect (station 1–11), and those ranged from 0.038–0.26 nmol L^{-1} at station 12–18 (Table 4-2). Throughout the depth profile, lignin concentrations declined slightly with increasing depth in the upper layer (< 200 m), and those increased dramatically at 500–700 m which salinity was close to minimum (34.26 ± 0.16, 1-SD, n = 14, station 7-11), and then lignin concentrations decreased again in deep layer (Fig. 4-3). Along the 160˚E transect (station 1–11), the extremely high $TDLP_6$ value (0.71 nmol L^{-1}) was observed at 500 m at station 5 which was matched with the NPIW layer in previous studies (Talley et al., 1995; Hernes and Benner, 2002), and the minimum $TDLP_6$ value (0.057 nmol L^{-1}) was found at 100 m at station 9 (Table 4-2). Meanwhile, lignin concentrations were not noticeably higher values in the intermediate layer at station 9 and 11 (Figure 4-3; Table 4-2). A substantial decrease (ca. 1-order) in lignin concentrations was in the NPIW layer (750 m) from station 5 to station 11. The similar $TDLP_6$ values (0.040–0.15 nmol L^{-1}) were shown at the different depths at station 14–16 and those were close to the result at station 9 (Table 4-2). A high $TDLP_6$ value (0.26 nmol L^{-1}) was found at 10 m at station 18, and this decreased rapidly by ca. 65% in the subsurface layer and deep seawater (700 m) (Table 4-2). The high lignin concentrations in the surface water at station 18 appeared to be the terrigenous input from Tosa Bay, Japan. Additionally, $TDLP_6$ value was 138.6 nmol L^{-1} at station G9 where salinity was close to 16.

Various patterns of lignin parameters including S/V, $(Ad/Al)_V$ and $(Ad/Al)_S$ throughout the depth profile at each station (Table 4-2). Lignin composition S/V ratios ranged between 0.070–0.66 at station 1–16, and those ranged between 0.30–0.52 at station 17 and 18. The two extremely low values in S/V (0.07 and 0.12) were found at 500 m and 750 m, respectively at station 5, and those were close to the values at 750 m and 2000 m at station 1 (S/V = 0.14 and 0.11 at 750 and 2000 m, respectively) (Table 4-2). Otherwise, S/V ratios ranged between 0.18–0.66 at different depths at other stations, and S/V value was 0.35 at station G9 (Table 4-2). $(Ad/Al)_V$ ratios ranged between 0.21–1.46 at station 1–16, and those ranged between 0.77–1.49 at station 17 and 18, and 0.83 in $(Ad/Al)_V$ ratio at station G9 (Table 4-2). The maximum values of $(Ad/Al)_V$ were 1.46

and 1.49 at 10 m at station 1 and 18, respectively. $(Ad/Al)_S$ ratios ranged between 0.71–2.90 at station 1–16, 0.73–9.59 at station 17 and 18, and the abnormal $(Ad/Al)_S$ value (9.59) with extremely low concentration (0.001 nmol L^{-1}) of syringaldehyde (SAL) was at 500 m at station 18 (Table 4-2). The value of $(Ad/Al)_S$ was 0.70 at station G9 (Table 4-2).

Lignin phenol compositions at 750 m from station 1 to 16 showed the transformation of tDOM along NPIW in the western North Pacific Ocean (Fig. 4-4). $TDLP_6$ decreased from station 1 to 16 but a sharp increasing value at station 5 (Fig. 4-4A). The ratios of S/V in intermediate water at station 1–7 were lower than this at station G9, however, S/V values increased toward station 9, and showed a constant value at station 9–11 (Fig. 4-4B). A similar pattern was found in $(Ad/Al)_V$, $(Ad/Al)_V$ values were lower than station G9 at station 1–5, and increased toward station 9 (Fig. 4-4C). A different pattern was observed in $(Ad/Al)_S$, these values at all station were close to that at station G9 excluding an extremely high vale at station 7 (Fig. 4-4D).

4.3.2 DiOHBA in the western North Pacific

The concentrations of DiOHBA ranged between 0.130–0.329 nmol L^{-1} at station 1–16, and those ranged between 0.148–0.288 nmol L^{-1} at station 17 and 18 (Table 4-2). The patterns of DiOHBA followed lignin concentrations throughout the depth profile (Fig. 4-5). The maximum value of DiOHBA was observed in the intermediate layer especially at station 5 (Fig. 4-5). This result implied organic and/or humic substance released from soil and/or sediment and this was also rich in the intermediate layer. An expectantly high value of DiOHBA was at station G9, and that was 25.9 nmol L^{-1} (Table 4-2).

4.3.3 CDOM and AOU in the western North Pacific Ocean

Salinity and CDOM optical properties delineated the distribution of NPIW along the 160˚E transect are shown in Table 4-3, Fig. 4-6 and Appendix 4-1. The water masses were distinguished as North Pacific Subtropical Mode Water (NPSTMW, 100–500 m), NPIW (500–800 m) and North Pacific Deep Water (NPDW, >2000 m) following the previous studies (Talley and Joyce, 1992; Talley et al., 1995; Sonnerup et al., 1999;

Hanawa and Yoritaka, 2001). A tongue-like of minimum salinity (33.98–34.55) extended southward at intermediate water depth (500–800m) from the subarctic region to the subtropical region and even to tropical region, and which density ranged from 26.10–27.40σθ (Fig. 4-6A). The results of minimum salinity and density in this study are consistent with the definition of NPIW in previous studies (Talley et al., 1995; Yasuda et al., 2001, 2004; Nishioka et al., 2013). A similar tongue-like of the NPIW distribution was observed in CDOM absorption coefficient *a*(350) results, those ranged between 0.028–0.192 m^{-1} (Fig. 4-6B). However, high *a*(350) values were from the surface to deep water (NPDW, 2000 m) in the subarctic area. Hence, high CDOM *a*(350) values were not only found at the intermediate water depth. In additional, a lower *a*(350) values (0.067–0.136 m^{-1}) were found in the subsurface layer (100–500 m) from station 4 to 7, and that corresponded to NPSTMW layer. The location of NPSTMW was consistent with previous CDOM investigation result in the North Pacific (Swan et al., 2009). Extremely low *a*(350) values were observed in the surface layer between station 9 to 11 accompanied with high $S_{275\text{-}295}$ values (Fig. 4-6B, 6C). CDOM spectral slope $S_{275\text{-}295}$ decreased with depth throughout the depth profile at each station, those ranged between 0.0169–0.0572 nm^{-1}. However, the tongue-like distribution in $S_{275\text{-}295}$ was not found along the 160˚E transect (Fig. 4-6C). Similar values of *a*(350) and $S_{275\text{-}295}$ were also found at station 12–18, and those ranged between 0.031–0.186 m^{-1} in *a*(350) and 0.0169–0.0533 nm^{-1} in $S_{275\text{-}295}$. *a*(350) and $S_{275\text{-}295}$ were 7.27 m^{-1} and 0.0166 nm^{-1}, respectively at station G9.

AOU showed a similar distribution with $S_{275\text{-}295}$ along the 160˚E transect (Fig. 4-6D). However, AOU increased from surface layer to deeper layer and those ranged between -13.82–296.49 μmol L^{-1}. The minimum AOU value was found at 20 m at station 1 and the maximum value was at 750 m at station 5. This AOU distribution is consistent with previous AOU investigation in the western Pacific Ocean (Yamashita and Tanoue, 2008).

4.3.3 Relationship between salinity, lignin phenols, CDOM and AOU

In Fig. 4-7–4-10, sampling sites are divided into three groups following the ocean province presented by Longhurst (1995). Salinity and lignin concentrations in the upper

layer and intermediate water indicated the terrestrial source in lignin phenols (Fig. 4-7). High linear relationship (R^2 = 0.87, p < 0.01, n = 20) between salinity and $TDLP_6$ in the upper layer water (< 400 m) at station 1–16 indicated the same terrestrial origins. Another good correlation between salinity and $TDLP_6$ (R^2 = 0.67, p < 0.01, n = 14) was found in the intermediate water at station 7–11 implied the same water origins (Fig 4-7). A non-correlation between salinity and $TDLP_6$ (R^2 = 0.002, p = 0.9, n = 10) was found in the deep water (2000 m) at station 1–16. The slope between salinity and $TDLP_6$ in the upper layer (slope = 0.15) was not statistically different from that (slope = 0.21) in the intermediate layer (F-test, p > 0.05) (Fig. 4-7), suggested the same terrestrial origins of lignin phenols and tDOM in those two water layer.

The different correlations were found between CDOM a(350), salinity and AOU in the upper and intermediate waters, respectively, but a(350) was significantly correlated with lignin concentrations in these two water masses. Salinity was correlated with a(350) in the upper layer water (R^2 = 0.52, p < 0.01, n = 20), but salinity was non-correlated with a(350) in the intermediate layer (R^2 = 0.13, p = 0.23, n = 13) (Fig. 4-8). $TDLP_6$ was significantly correlated with a(350) in the upper layer (R^2 = 0.46, p < 0.01, n = 20) and intermediate layer (R^2 = 0.45, p = 0.01, n = 13) (Fig. 4-9). In addition, a(350) was strongly correlated with AOU in the upper layer (R^2 = 0.36, p < 0.01, n = 20), but that was non-correlated in the intermediate layer (R^2 = 0.15, p = 0.4, n = 7) (Fig. 4-10). However, non-significant relationships was found between $TDLP_6$ and AOU in this study (R^2 = 0.05, p = 0.4, n = 20 in the upper layer and R^2 = 0.02, p = 0.7, n = 7 in the intermediate layer).

4.4. Discussion

4.4.1 Sources of lignin phenols and CDOM

Lignin phenols results indicated the same terrestrial sources of lignin in the upper and intermediate layer. In the upper layer, a strong correlation between salinity and $TDLP_6$ indicated the terrestrial origin (Fig. 4-7). In additional, the good linear relationships between salinity and $TDLP_6$ indicated physical mixing process shaped the

distributions of lignin in those two water layers. The similar S/V ratios inferred the original source was affected by the Amur River (Table 4-2). In addition, lignin results in the upper layer delineated this terrestrial water mass not only north-to-south covered from subarctic to subtropical region, but also western-to-east distributed horizontally until Kuroshio current boundary. Although $TDLP_6$ in intermediate layer was three to four orders lower than the Amur River mouth stations G9. Lignin phenol concentrations in the intermediate layer were correlated with salinity at station 7–16 indicated the same terrestrial origin from the Sea of Okhotsk (Fig. 4-7). The average S/V ratio was 0.38 ± 0.11 (1-SD, n = 20) in the upper layer and 0.35 ± 0.14 (1-SD, n = 18) in the intermediate layer at station 1–16, and those closed to the S/V ratio at station G9 suggested the terrestrial origin and the influence from the Amur River. The S/V in this study was close to that (0.28–0.48) in the large Arctic rivers (Amon et al., 2012) but lower than the values (0.5–1.2) in the tropical and temperature river (Opsahi and Benner, 1997; Shen et al., 2012) indicated the large contributions from gymnosperms vegetation (Hedges and Mann, 1979).

The results in *a*(350) values showed the multiple sources of CDOM. The correlations between *a*(350) against salinity, and *a*(350) against $TDLP_6$ were significantly ($p < 0.01$) in the upper layer. Those results were consistent with other ocean margin and coastal investigations, indicating the linear relationships are between CDOM absorption coefficient and salinity, and lignin concentrations, respectively (Hernes and Benner, 2003; Fichot and Benner, 2012). Therefore, *a*(350) result in the upper layer inferred the terrestrial sources as indicated as lignin result. However, the declination of NPIW by *a*(350) values were inconsistent with density and salinity minimum (Fig. 4-6B). Although the correlation between *a*(350) and $TDLP_6$ was strong ($p = 0.01$) (Fig.4-9), the correlation between *a*(350) and salinity was not significant ($p = 0.23$) in the intermediate water (Fig. 4-8). Those results indicated that physical mixing also shaped CDOM *a*(350) distribution in the upper layer, and *a*(350) was affected by *in-situ* DOM production. The *in-situ* production of DOM was also found in the deep layer, the average value was 0.12 ± 0.02 (1-SD, n = 94) in *a*(350) and that was a refractory DOM fraction based on other florescent DOM study (Yamashita and Tanoue, 2008). In addition, the AOU result also suggested *in-situ* produced bio-refractory DOM in the ocean (Yamashita and Tanoue,

2008). The significant relationship was between AOU and *a*(350), but non-significant relation was between AOU and lignin phenols. Although $TDLP_6$ strongly correlated with *a*(350) (Hernes and Benner, 2003, Fichot and Benner, 2012), *a*(350) data was coupled the message from marine DOM. Therefore the delineation of *a*(350) was not matched with NPIW along the 160˚E transect indicated the influence of marine sources in *a*(350) results. Meanwhile the *a*(350) and AOU results also pointed out that lignin phenols are the irreplaceable tracer of tDOM.

DiOHBA is a benzene carboxylic acid with no methoxy groups and appears to be derived from soil and/or sediments organic (Otto and Simpson, 2006; Dickens et al., 2007). It is robust using DiOHBA as a tracer of soil organic carbon in the marine environment (Dickens et al., 2007). The measurement of DiOHBA pointed out the organic carbon and/or humic substance in NPIW was release from soil and/or sediment organic (Fig. 4-5, Table 4-2). The DiOHBA results inferred a fraction of tDOM would be derived from soil and/or sediment in the Sea of Okhotsk, and those tDOM could be into the intermediate water masses of the western North Pacific Ocean. Our result is consistent with previous dissolved Fe study in this region (Nishioka et al., 2013) suggesting that tDOM act as organic ligand with bioactive trace metal.

Lignin in aerosols was measured in the urban atmosphere, and this provided the evidence of long-range transport of tDOM and lignin underwent photodegradation during transport, and also heighted the importance of primary biology aerosol particles (Shakya et al., 2011). Therefore, lignin in the ocean could input from atmosphere, but it is difficult to know the contribution of aerosols input because aerosol is intermittent sources as like the issue of spatiotemporal heterogeneity in the Fe supply (Nishioka et al., 2013).

4.4.2 Distribution and Transformation of tDOM in NPIW

Lignin phenols results delineated the distribution and transformation of tDOM in the western North Pacific Ocean. Along the 160˚E transect, the typical NPIW stratification identified by lignin phenols was found at station 5 (Fig. 4-3). Lignin phenols decreased slightly with increasing salinity in the upper layer, and then those increased dramatically in the intermediated layer which salinity minimum. Finally, lignin phenols declined rapidly in the deep layer. However, tDOM was strongly affected by diapycnal

mixing as showed by vertical salinity profile at station 1 (Fig. 4-3). The physical mixing processes, including tidal and wind-driven mixing, shape the distribution of chemical and optical characteristic including lignin phenols, CDOM properties and dissolved iron concentrations (Nishioka et al., 2013). Therefore, the distribution of lignin phenols was highly affected by physical mixing in the subarctic of NPIW. In addition, the mechanisms of physical and biogeochemical processes are complicated in margin sea and hence affect its nearly ocean region, such as the Okhotsk-Pacific system, and the factors include freshwater discharge, interior current systems, tidal mixing, local upwelling, interaction of continental shelf, sea ice production and melting, and flow through straits (Nishioka et al., 2014). Those local processes in the western subarctic Pacific might be the reason to explain the maximum $TDLP_6$ value was at station 5 rather than station 1. In this study, lignin is used as an indicator of NPIW, these results suggested the distribution of NPIW covers from subarctic to subtropical region and extends to west until Kuroshio boundary, east of Japan. The horizontal diffusion of NPIW is shown in Fig. 4-4. Lignin phenol compositions including S/V, $(Ad/Al)_V$ and $(Ad/Al)_S$ implied NPIW flows southwestern at station 7–8, therefore, those ratios showed the similar values at station 9–11. Those lignin ratios results were consistent with previous NPIW circulation studies, while the two water currents (low-salinity from north and high-salinity from south) meets east Japan, a part of the modified water flows southwestward and as the recirculation of the subtropical gyre (Yasuda et al., 1996; You, 2003).

The present study suggested tDOM in the western North Pacific Ocean would be affected by photochemical and biological processes. Lignin concentrations in the upper and intermediate layers were ca. three-order lower than that in the Amur River mouth and that implied multiple factors are in controlling tDOM and lignin distributions. The factors include physical mixing and degradation processes. The ratios of lignin phenol compositions including S/V, $(Ad/Al)_V$ and $(Ad/Al)_S$ are the good tracers to indicate the diagesnes of tDOM in the marine environment (Opsahl and Benner, 1998; Spencer et al. 2009; Heners and Benner, 2002). Previous incubation studies pointed out lignin composition S/V ratio decreased and $(Ad/Al)_V$ ratio increased causing by photochemical oxidation, meanwhile, $(Ad/Al)_V$ ratio also increased due to biodegradation as well as $(Ad/Al)_S$ result (Opsahl and Benner, 1995, 1998; Benner and Opsahl, 2001; Spencer et al.,

2009). However, the clear patter caused by photochemical process in S/V ratio was not found in the upper layer, and somewhat an increasing trend in S/V ratio in NPIW from the subarctic to subtropical regions (Fig. 4-4B). The values of $(Ad/Al)_V$ increased after station 7 and those was higher than the value in the Amur River mouth (Fig. 4-4C) and this increasing value is close to the average (ca. 1) values in the tropical and temperature rivers and the large Arctic rivers (Ertel et al., 1986; Opsahl and Benner, 1997; Amon et al., 2012; Shen et al., 2012). In $(Ad/Al)_S$ result, similar values were observed excluding station 7, and those were slightly higher than the value in the Amur River mouth (Fig. 4-4D), the large Arctic rivers (ca. 0.7) and the Mississippi River (ca. 0.8) (Amon et al., 2012; Shen et al., 2012). Although photodegradation and biodegradation increased $(Ad/Al)_V$ ratio, biodegradation was the dominant process of lignin and tDOM in NPIW as indicated in $(Ad/Al)_S$ result. Considering the influence of solar radiation was minor in the intermediate water depth and solar exposure promoted relatively rapid alternations of lignin especially in the early stage of riverine plume dispersal (Chapter 2 and 3). Biodegradation is mainly responsible for lignin and tDOM transformation in NPIW as like tDOM in the coastal area (Ward et al., 2013; Fichot and Benner, 2014). In the upper water column, S/V, $(Ad/Al)_V$ and $(Ad/Al)_S$, show the similar pattern with intermediate layer and inferred the influences causing by biodegradtion and photodegradation (Table 4-2). CDOM spectral slope $S_{275\text{-}295}$ results indicated level of photobleaching was the highest in the upper layer throughout water column especially in the subtropical region (Fig. 4-6C). However, the results in $S_{275\text{-}295}$ did not only indicate tDOM transformation but also included oceanic DOM transformation (Yamashita et al., 2013).

4.5. Conclusion

The present study delineated directly the distributions of NPIW in the western North Pacific including the circulation pathway. Our lignin phenols results highlight: (1) the potential for long-distance transport of tDOM along NPIW, and a fraction of tDOM was removed in the open ocean due to microbial oxidation, (2) tDOM is expectable to act organic ligand for bioactive trace metals in the ocean, (3) although CDOM parameters are

related with lignin phenols, the optical properties are also affected by other *in-situ* factors. Therefore, lignin phenols play an important role in tDOM study.

Table 4-1 Constant coefficients for apparent oxygen utilization (AOU) calculation, those are presented in equation (7). Data are from Garcia and Gordon (1992).

Constant coefficients	Combined fit (μmol L^{-1})
A_0	5.80818
A_1	3.20684
A_2	4.11890
A_3	4.93845
A_4	1.01567
A_5	1.41575
B_0	-7.01211×10^{-3}
B_1	-7.25958×10^{-3}
B_2	-7.93334×10^{-3}
B_3	-5.54491×10^{-3}
C_0	-1.32412×10^{-3}

Table 4-2 Dissolved lignin phenol concentrations ($TDLP_6$), composition ratios [S/V, $(Ad/Al)_V$ and $(Ad/Al)_S$], and 3,5-dihydroxybenzoic acid (DiOHBA) concentration in the western North Pacific Ocean.

Station	Depth (m)	Salinity	$TDLP_6$ (nmol L^{-1})	S/V	$(Ad/Al)_V$	$(Ad/Al)_S$	DiOHBA (nmol L^{-1})
Stn. 1	10	32.66	0.35	0.36	1.46	0.86	0.303
	100	33.11	0.31	0.19	0.90	1.12	0.244
	200	33.76	0.23	0.28	1.18	1.15	0.305
	750	34.34	0.44	0.14	0.28	0.95	0.329
	2000	34.61	0.31	0.11	0.24	1.10	0.238
Stn. 2	100	33.15	0.44	0.26	0.86	0.92	0.261
	400	34.02	0.16	0.36	1.11	1.02	0.205
	750	34.28	0.24	0.29	0.70	0.78	0.298
	2000	34.60	0.14	0.24	0.47	0.99	0.272
Stn. 5	10	34.39	0.088	0.40	0.97	0.75	0.218
	100	34.66	0.079	0.43	1.16	1.08	0.221
	200	34.62	0.064	0.35	0.59	1.51	0.185
	500	34.06	0.71	0.070	0.21	0.86	0.130
	750	34.11	0.63	0.12	0.28	0.65	0.322
	2000	34.59	0.10	0.30	0.88	1.40	0.269
Stn. 7	100	34.75	0.061	0.44	1.21	1.99	0.214
	500	34.13	0.17	0.22	1.14	2.90	0.226
	750	34.10	0.17	0.27	0.95	2.86	0.297
	2000	34.61	0.072	0.39	1.11	1.97	0.228
Stn. 8	100	34.95	0.068	0.49	1.03	1.21	0.290
	500	34.12	0.17	0.30	0.83	0.75	0.259
	750	34.17	0.17	0.34	0.86	0.77	0.288
	2000	34.61	0.078	0.49	1.35	0.88	0.256
Stn. 9	10	34.92	0.073	0.42	0.74	1.03	0.220
	100	35.19	0.057	0.33	0.74	1.49	0.242
	200	34.84	0.089	0.18	1.07	1.47	0.214
	500	34.13	0.12	0.29	1.02	1.87	0.218
	750	34.27	0.13	0.43	1.05	0.71	0.272
	2000	34.61	0.092	0.30	0.82	0.88	0.248
Stn. 11	100	34.94	0.061	0.33	0.71	1.49	0.242
	500	34.55	0.079	0.48	0.93	0.72	0.215
	750	34.53	0.078	0.45	0.99	1.18	0.245
	2000	34.63	0.082	0.30	0.88	1.43	0.235
Stn. 12	10	34.74	0.11	0.48	0.93	0.88	0.264
	100	35.04	0.10	0.66	0.70	0.71	0.267
	200	34.72	0.051	0.47	1.49	1.32	0.190

(*Continues*)

Table 4-2 (*Continued*)

Station	Depth (m)	Salinity	$TDLP_6$ (nmol L^{-1})	S/V	$(Ad/Al)_V$	$(Ad/Al)_S$	DiOHBA (nmol L^{-1})
Stn. 14	100	34.99	0.040	0.36	0.91	2.11	0.210
	500	34.19	0.083	0.45	1.24	1.35	0.206
	750	34.18	0.14	0.41	0.89	1.00	0.257
	2000	34.60	0.080	0.53	1.19	0.97	0.223
Stn. 15	100	34.82	0.045	0.43	0.99	1.42	0.163
	500	34.39	0.075	0.54	1.44	1.11	0.197
	750	34.20	0.14	0.42	1.04	1.05	0.289
	2000	34.60	0.085	0.49	1.27	1.01	0.253
Stn. 16	100	34.79	0.047	0.39	0.92	1.26	0.204
	500	34.45	0.074	0.58	1.34	1.12	0.201
	750	34.20	0.15	0.43	1.02	0.95	0.288
	2000	34.60	0.10	0.51	1.26	0.79	0.289
Stn. 17	10	34.11	0.068	0.45	0.94	1.31	0.235
	100	34.75	0.040	0.38	0.77	1.70	0.209
	200	34.77	0.038	0.30	0.91	2.83	0.172
	500	34.22	0.081	0.31	1.23	5.50	0.148
	750	34.30	0.13	0.33	1.00	3.16	0.288
	1000	34.41	0.11	0.41	0.97	0.73	0.253
Stn. 18	10	33.23	0.26	0.52	1.49	0.81	0.233
	100	34.52	0.070	0.38	1.07	1.99	0.241
	200	34.38	0.078	0.44	1.11	0.79	0.217
	500	34.29	0.087	0.30	1.06	9.59	0.222
	700	34.33	0.13	0.43	0.97	0.74	0.271
Stn. G9	0	16	138.6	0.35	0.83	0.70	25.9

Table 4-3 CDOM absorption coefficient at 350 nm [*a*(350)] and spectral slope 275–295 nm ($S_{275\text{-}295}$) in the western North Pacific Ocean. Those CDOM data are used to compare with lignin results (Table 4-2), others CDOM data are shown in Appendix 4-1.

Station	Depth (m)	Salinity	*a*(350) (m^{-1})	$S_{275\text{-}295}$ (nm^{-1})
Stn. 1	10	32.66	0.16	0.0312
	100	33.11	0.14	0.0275
	200	33.76	0.19	0.0202
	750	34.34	0.17	0.0182
	2000	34.61	0.14	0.0188
Stn. 2	100	33.15	0.15	0.0280
	400	34.02	0.15	0.0209
	750	34.28	0.17	0.0181
	2000	34.60	0.12	0.0187
Stn. 5	10	34.39	0.07	0.0446
	100	34.66	0.08	0.0369
	200	34.62	0.07	0.0379
	500	34.06	0.13	0.0254
	750	34.11	0.14	0.0208
	2000	34.59	0.14	0.0175
Stn. 7	100	34.75	0.09	0.0364
	500	34.13	0.11	0.0264
	750	34.10	0.14	0.0210
	2000	34.61	0.13	0.0178
Stn. 8	100	34.95	0.09	0.0395
	500	34.12	0.12	0.0265
	750	34.17	0.15	0.0197
	2000	34.61	0.13	0.0185
Stn. 9	10	34.92	0.04	0.0529
	100	35.19	0.09	0.0367
	200	34.84	0.09	0.0333
	500	34.13	0.10	0.0262
	750	34.27	0.14	0.0191
	2000	34.61	0.12	0.0186
Stn. 11	100	34.94	0.07	0.0408
	500	34.55	0.11	0.0215
	750	34.53	0.12	0.0200
	2000	34.63	0.13	0.0183

(Continues)

Table 4-3 (*Continued*)

Station	Depth (m)	Salinity	$a(350)$ (m^{-1})	$S_{275-295}$ (nm^{-1})
Stn. 12	10	34.74	0.04	0.0505
	100	35.04	0.08	0.0386
	200	34.72	0.07	0.0369
Stn. 14	100	34.99	0.11	0.0353
	500	34.19	0.10	0.0270
	2000	34.60	0.11	0.0192
Stn. 15	100	34.82	0.09	0.0361
	500	34.39	0.09	0.0303
	750	34.20	0.13	0.0224
	2000	34.60	0.10	0.0199
Stn. 16	100	34.79	0.13	0.0335
	500	34.45	0.10	0.0281
	750	34.20	0.12	0.0232
	2000	34.60	0.18	0.0169
Stn. 17	10	34.11	0.05	0.0440
	100	34.75	0.08	0.0322
	200	34.77	0.09	0.0270
	500	34.22	0.10	0.0225
Stn. 18	10	33.23	0.05	0.0440
	100	34.52	0.08	0.0322
	200	34.38	0.09	0.0270
	500	34.29	0.10	0.0225
	700	34.33	0.12	0.0206
Stn. G-9	0	16	7.27	0.0166

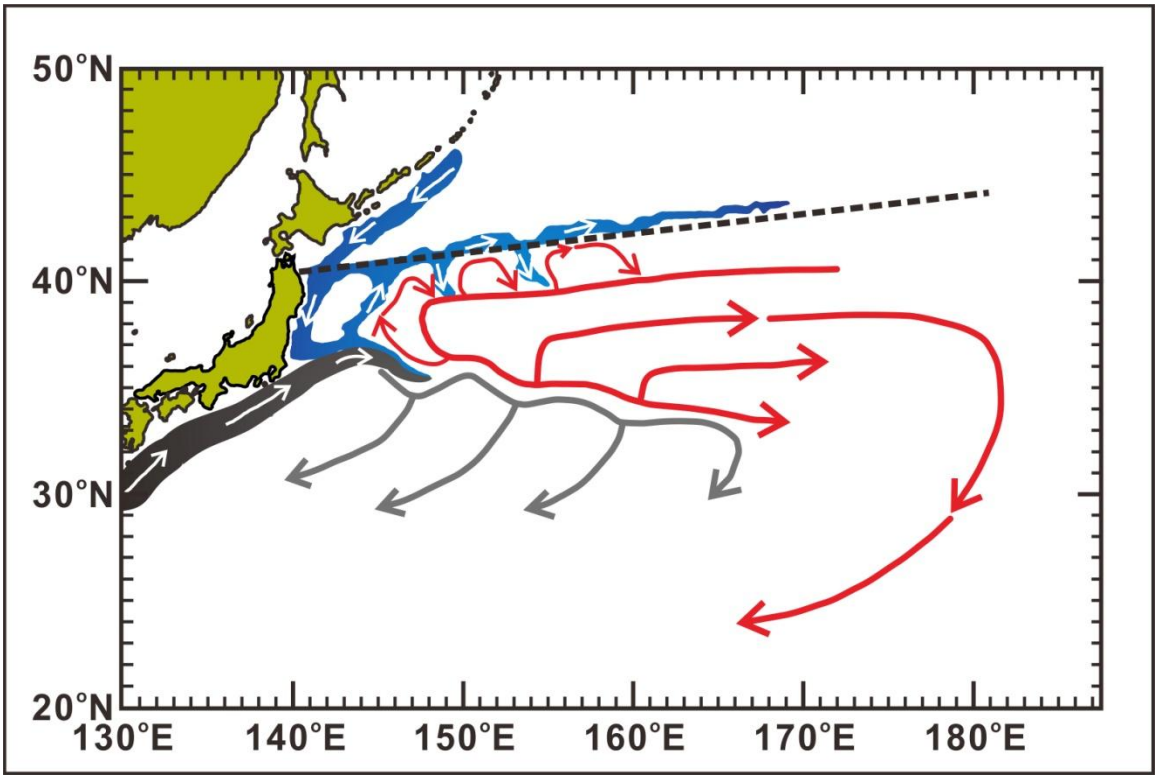

Fig. 4-1 Schematic representation for the NPIW circulation patterns and water modification in the western North Pacific Ocean. The dashed line presents the boundary separating wind-driven gyres estimated from the wind-stress field. The origins of NPIW include the fresh and low potential vorticity water from the Sea of Okhotsk (blue shadowy area) and Kuroshio high-salinity water (the old NPIW) (black shadowy area). Those two waters met east Japan, part of the mixing water flows eastward along the Kuroshio Extension and producing the modified water. Part of the modified water flows southwestward (black solid arrows), and the rest of the modified waters flows northeastward and enters into the Kuroshio-Oyashio interfrontal zone (red solid arrows). Modified from Yasuda et al., 1996.

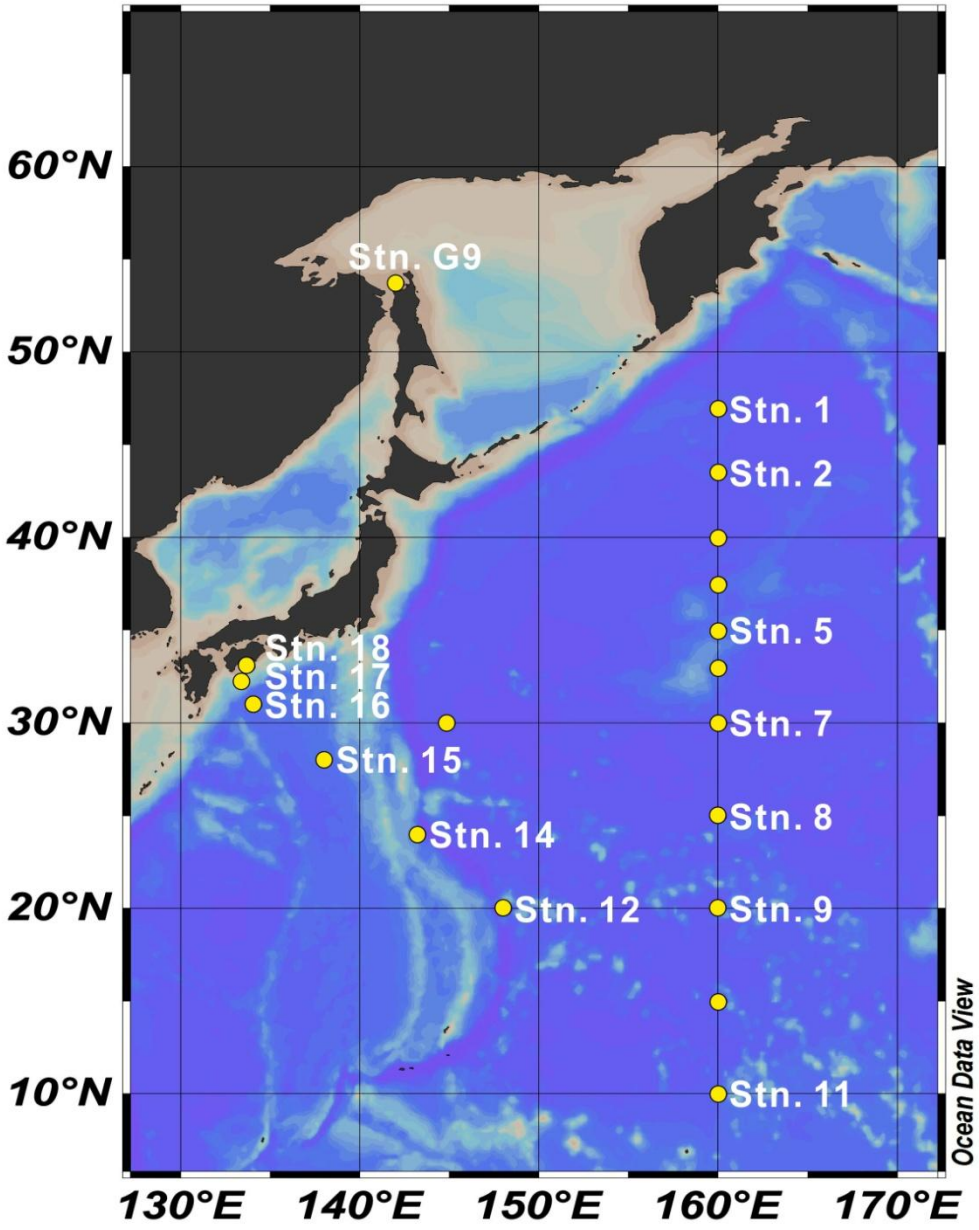

Fig. 4-2 Map of locations sampled for lignin phenols analysis and survey for CDOM distribution during the R/V *Hakuho Maru* cruise KH-12-3 (station 1–18) and the R/V *Professor Khromov* cruise Kh06 (station G9).

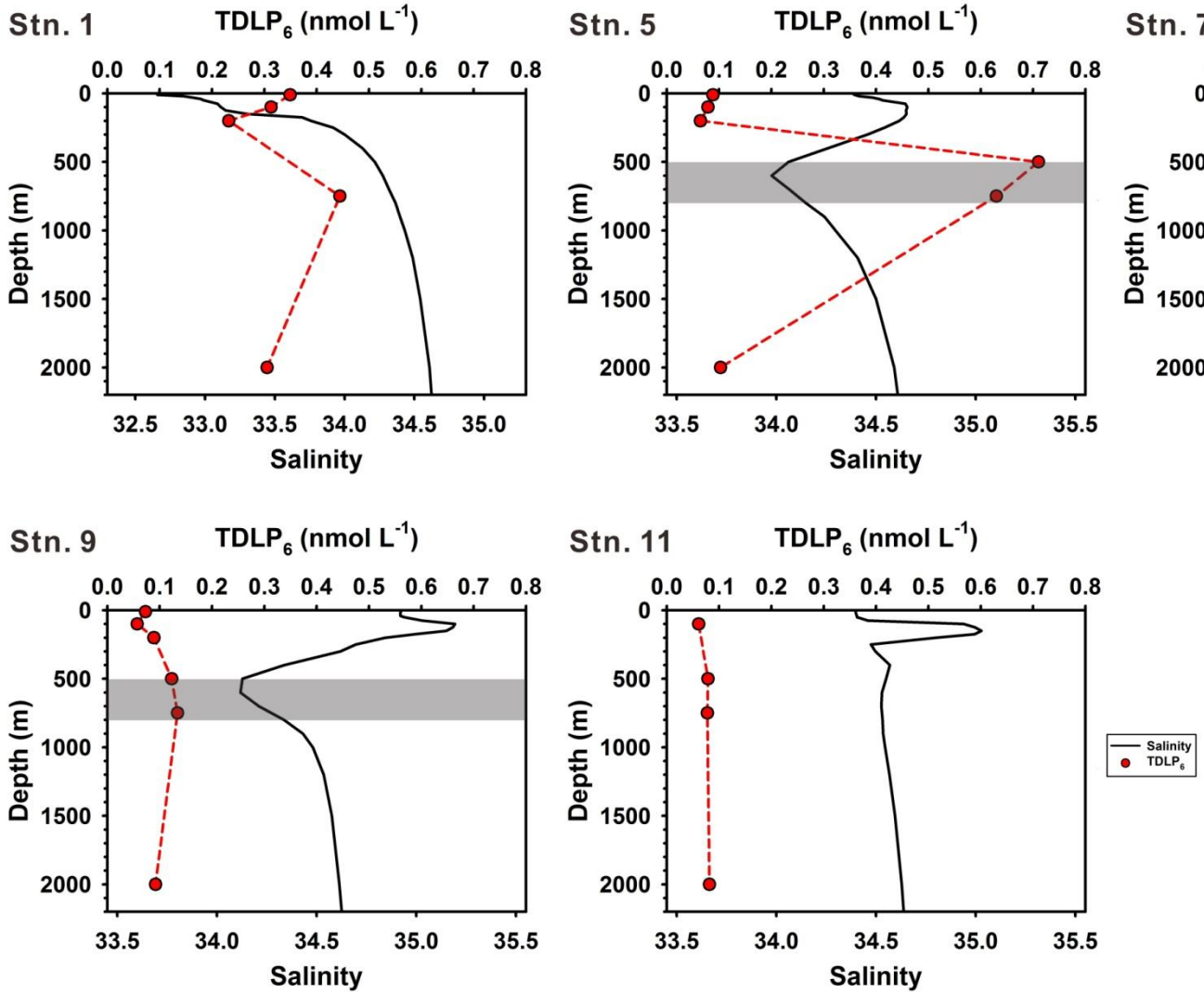

Fig. 4-3 Vertical profiles of salinity and lignin phenol concentrations ($TDLP_6$) at station 1, 5, 7, 9 and 11. The shadowy area is the depth at 500–800 m that is defined as NPIW layer.

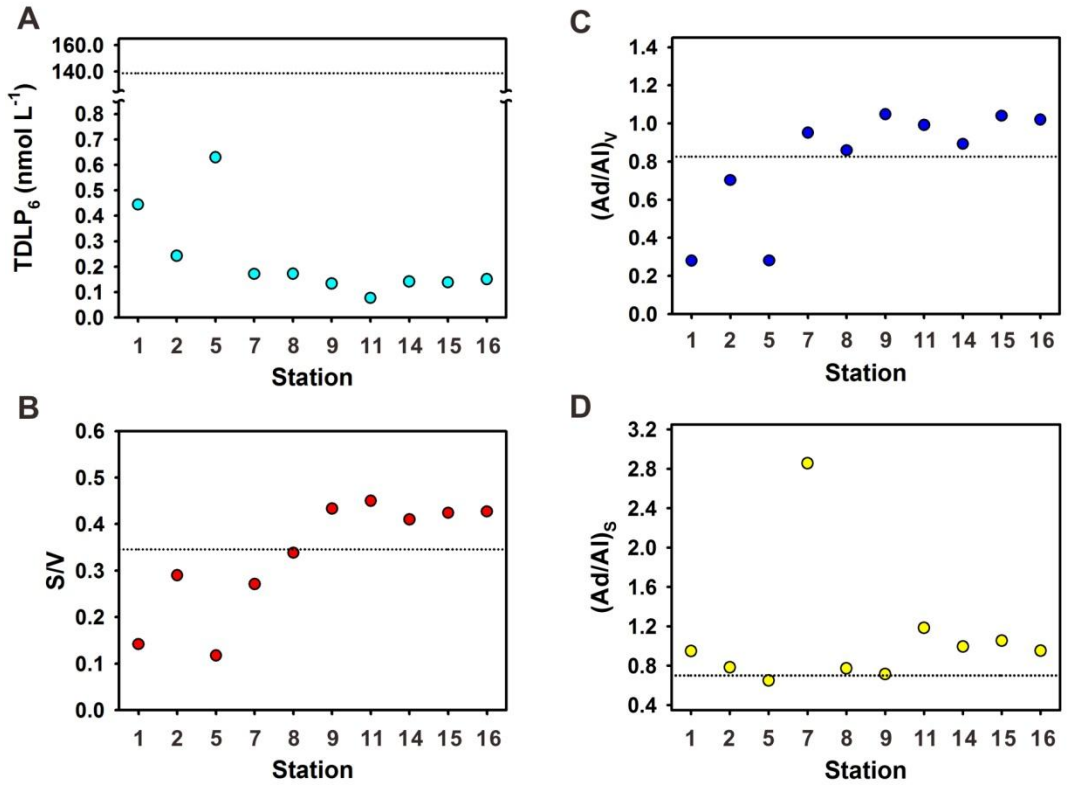

Fig. 4-4 Lignin phenol concentrations and compositions **(A)** lignin phenol concentrations ($TDLP_6$), **(B)** molar ratio of syringyl to vanillyl phenols (S/V), **(C)** molar ratio of vanillin acid to vanillin phenols [$(Ad/Al)_V$], and **(D)** molar ration of syringic acid to syringaldehyde [$(Ad/Al)_S$] at 750 m depth at station 1 to 16. Dotted lines are $TDLP_6$ and these lignin phenol compositions ratios at station G9.

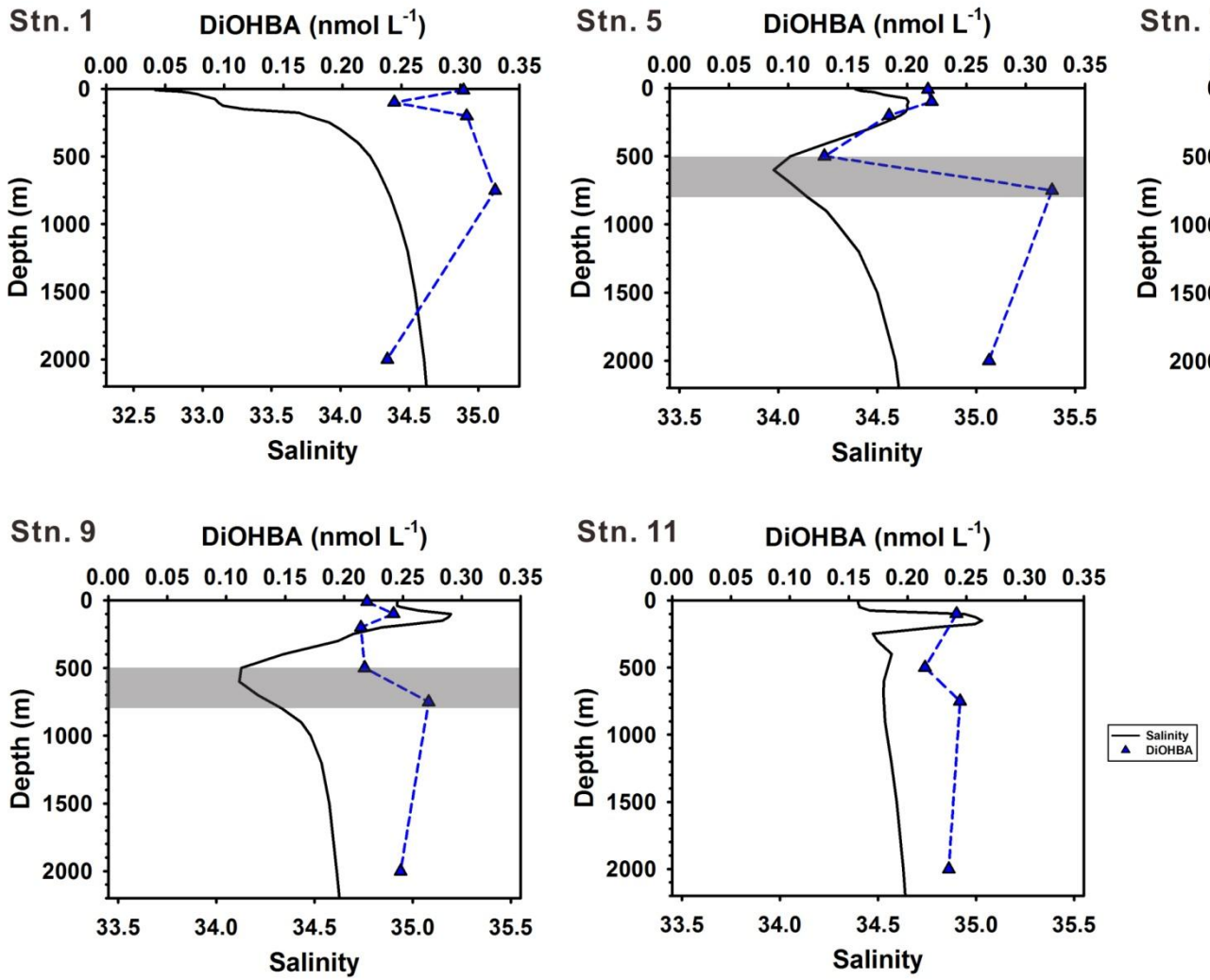

Fig. 4-5 Vertical profiles of salinity and 3,5-dihydroxybenzoic acid concentrations (DiOHBA) at station 1, 5, 7, 9 and 11. The shadowy area is the depth at 500–800 m that is defined as NPIW layer.

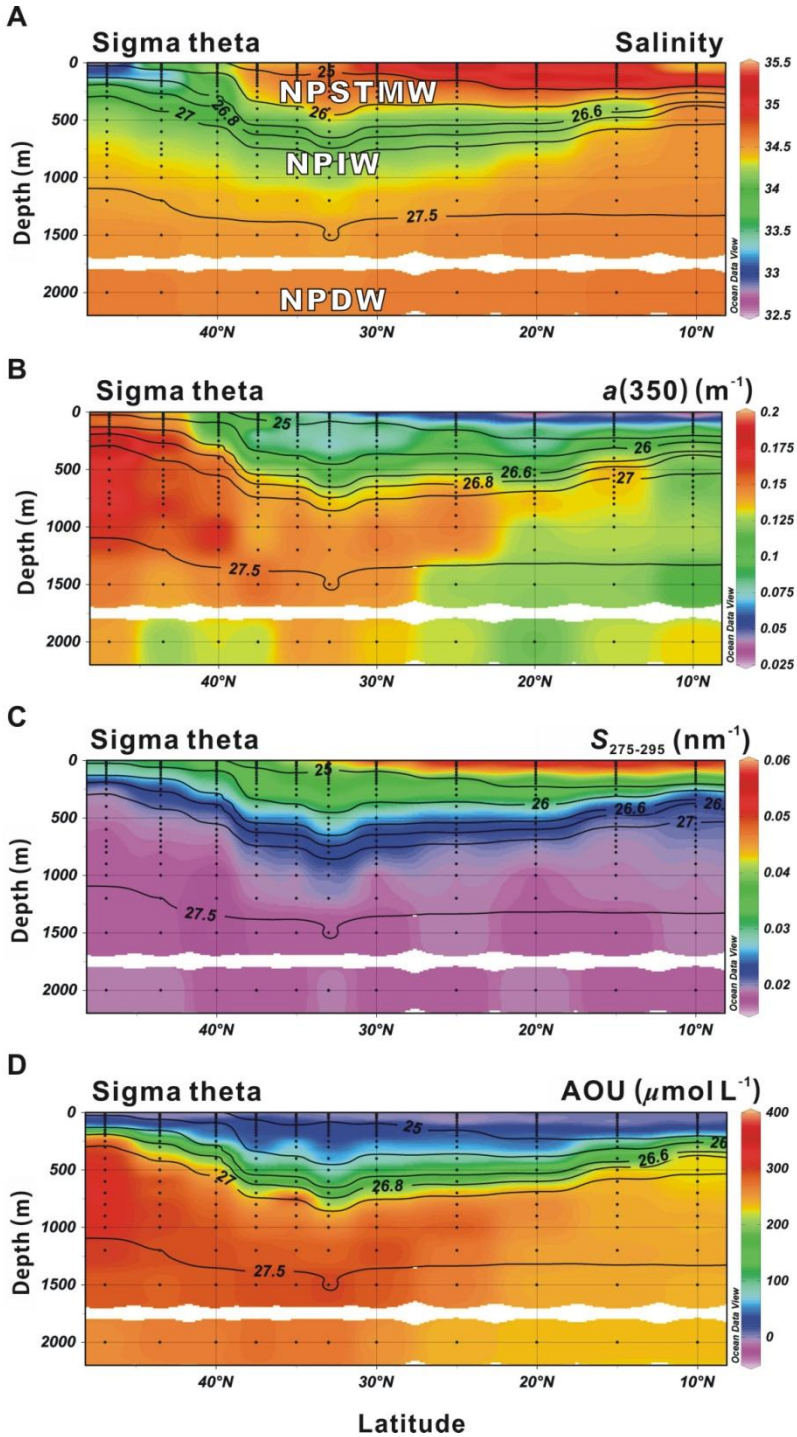

Fig. 4-6 Contour maps of density range 25–27.5σ_θ isopynal surface (solid lines and numbers) and **(A)** salinity, **(B)** CDOM absorption coefficients [*a*(350)], **(C)** the spectral slope coefficient of CDOM absorption coefficient spectrum between 275–295 nm ($S_{275\text{-}295}$), and **(D)** apparent oxygen utilization (AOU) along the 160˚E transect. Abbreviations for water masses in this figure: NPSTMW, North Pacific Subtropical Mode Water; NPIW, North Pacific Intermediate Water; NPDW, North Pacific Deep Water.

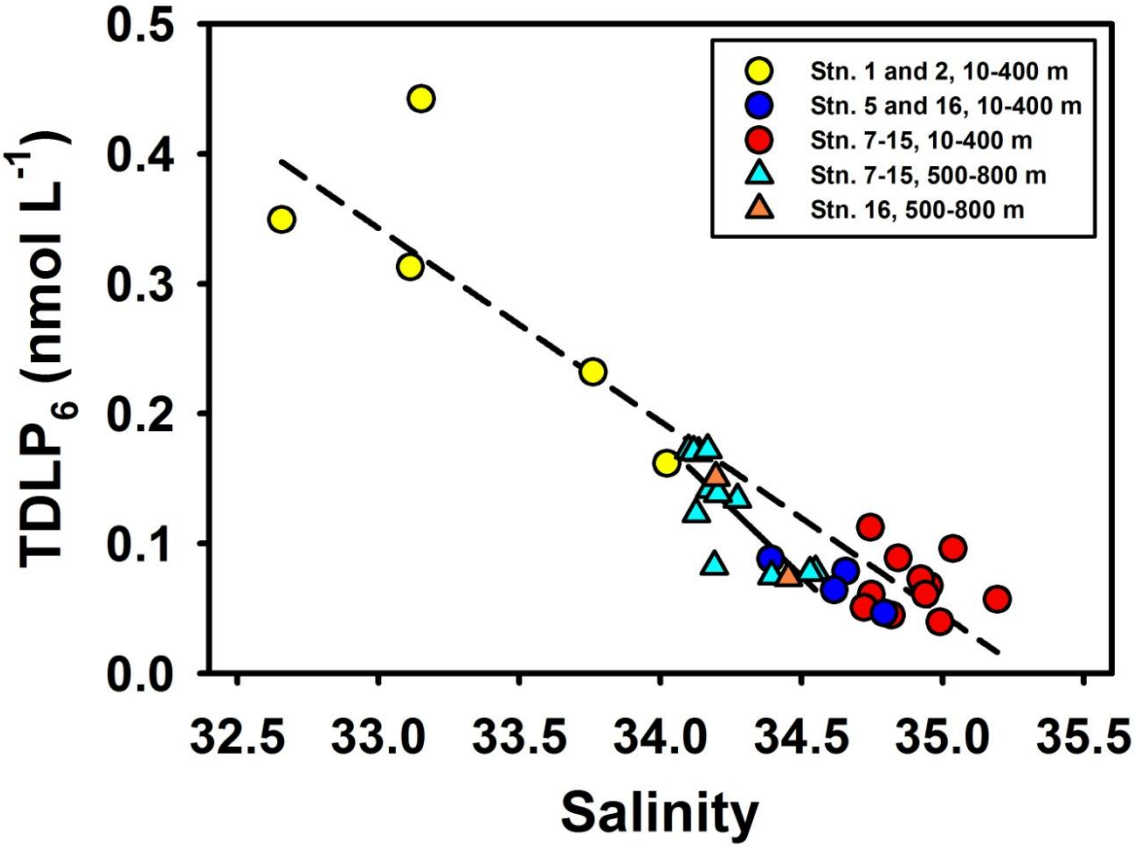

Fig. 4-7 Relationships between salinity and lignin phenol concentrations ($TDLP_6$) in the upper layer (10–400 m) from station 1–16 (yellow, blue and red circles, and dashed line, y = -0.15x+5.25, R^2 = 0.87, p < 0.01, n = 20), and intermediate water (500–800 m, including station 7–16) (cyan and orange triangle, and solid line, y = -0.21+7.34, R^2 = 0.67, p < 0.01, n = 14).

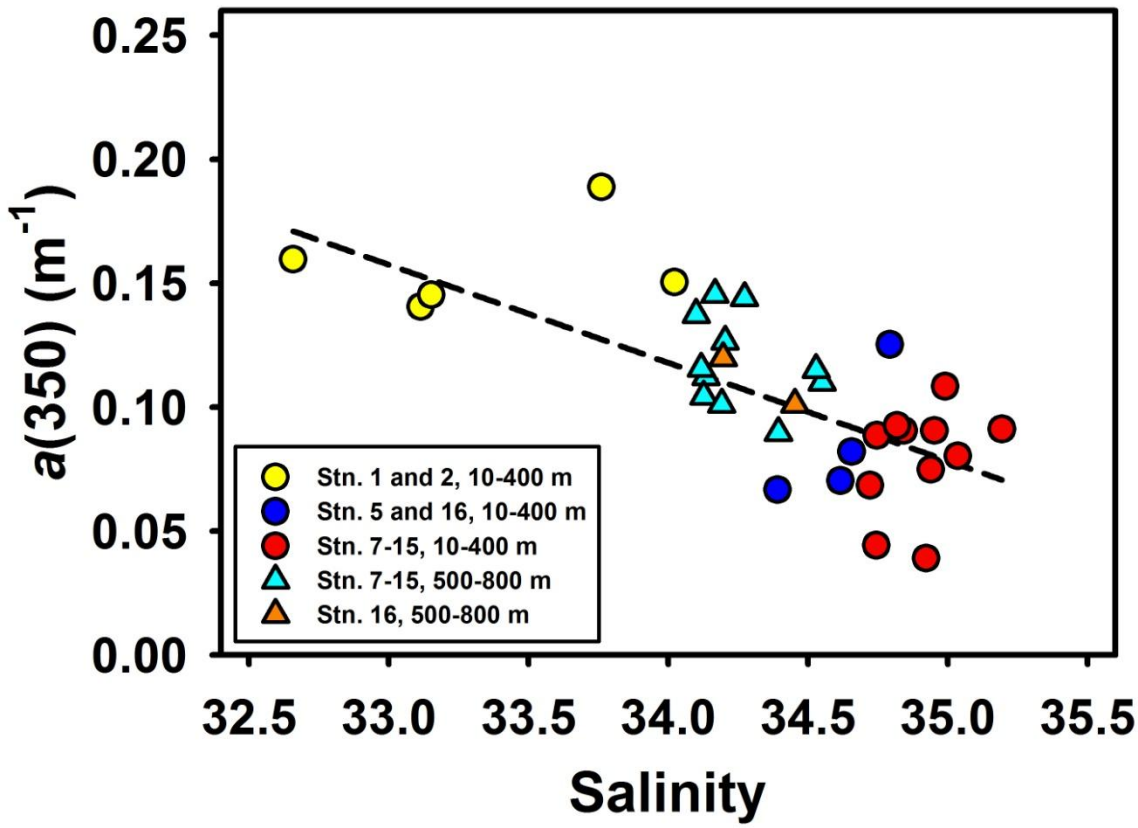

Fig. 4-8 Relationships between salinity and CDOM absorption coefficients [*a*(350)] in the upper layer (10–400 m, including station 1–16) (yellow, blue and red circles, and dashed line, y = 0.04x+1.46, R^2 = 0.52, p < 0.01, n = 20) and intermediate water (500–800 m, including station 7–16) (cyan and orange triangle, y = 0.04x+1.46, R^2 = 0.13, p = 0.23, n = 13).

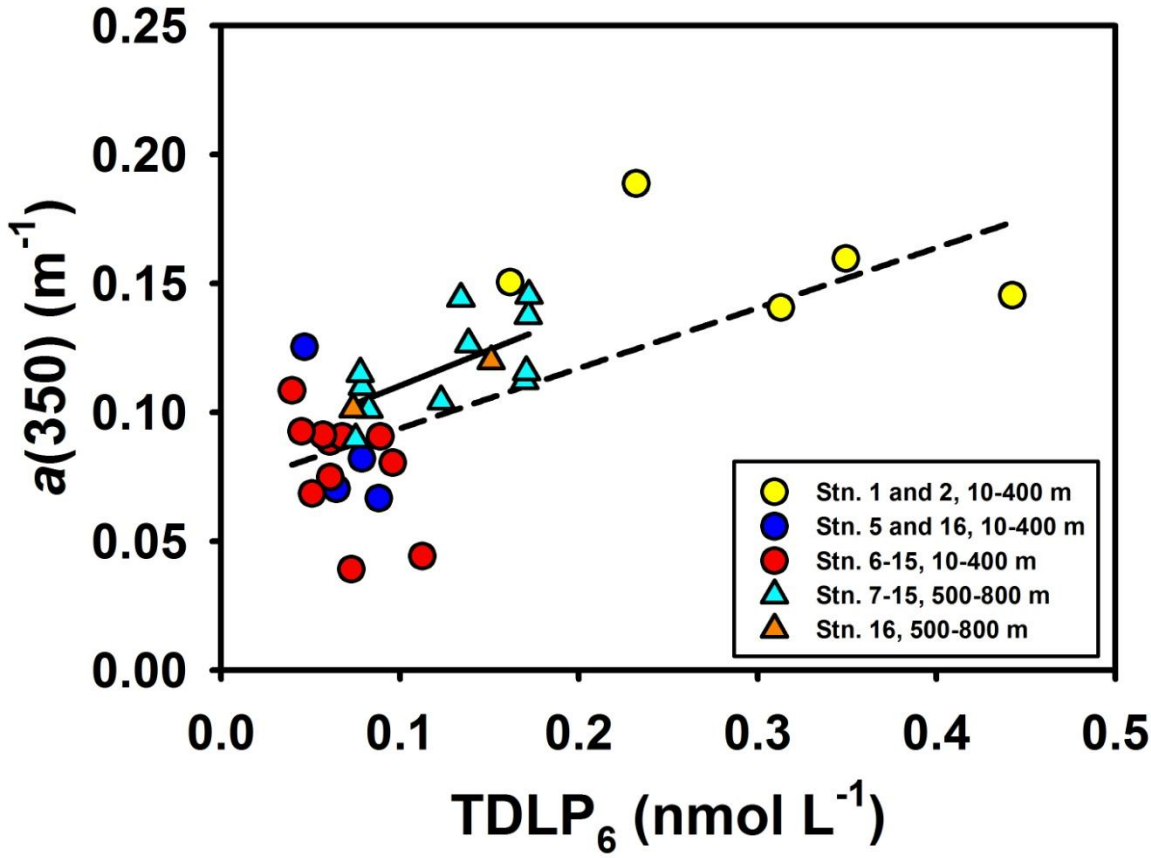

Fig. 4-9 Relationships between lignin phenol concentrations ($TDLP_6$) and CDOM absorption coefficients[*a*(350)] in the upper layer (10–400 m, including station 1–16) (yellow, blue and red circles and dashed line, y = 0.23x+0.07, R^2 = 0.46, p < 0.01, n = 20) and intermediate water (500–800 m, including station 7–16) (cyan and orange triangle and solid line, y = 0.28x+0.08, R^2 = 0.45, p = 0.01, n = 13).

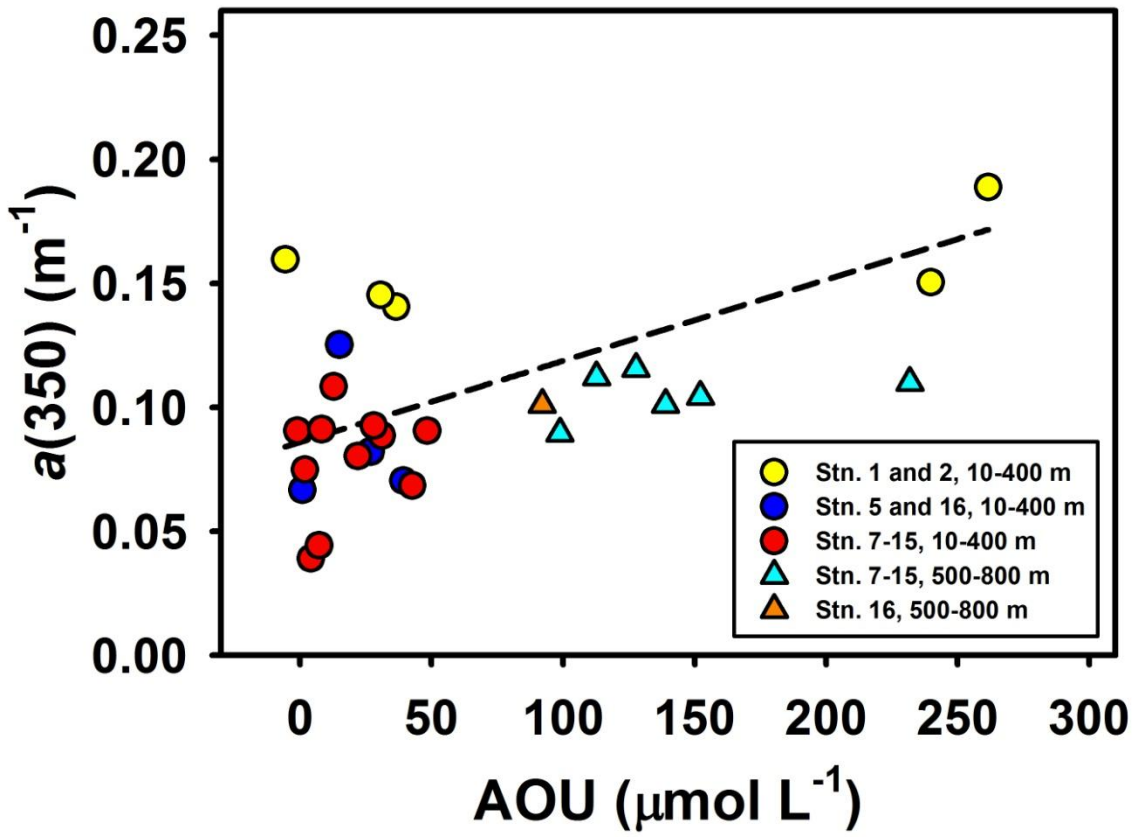

Fig. 4-10 Relationships between CDOM absorption coefficients[*a*(350)] and apparent oxygen utilization (AOU) in the upper layer (10–400 m, including station 1–16) (yellow, blue and red circles and dashed line, y = 1107.8x-68.2, R^2 = 0.36, p < 0.01, n = 20) and intermediate water (500–800 m, including station 7–16) (cyan and orange triangle and solid line, y = 7×10^{-5}x + 0.1, R^2 = 0.15, p = 0.4, n = 7).

Chapter 5
General Discussions

In this study, tDOM distribution was investigated from the terrestrial to marine environments using lignin and CDOM as terrestrial indicators and discussed the transformations of tDOM. The results in the study suggested that the removal mechanism of tDOM is various depending on the environmental conditions.

5.1. Major findings of the present study

5.1.1. tDOM transformations

In this study, the transformations of tDOM are various and this is controlled by the environmental conditions (Fig. 5-1). Several environmental variables including solar irradiance, water clarity, microbial community structure and temperature all can affect the transformation and decomposition of lignin and CDOM. Lignin concentrations and CDOM *a*(350) decreased from river source. Lignin ratios, P/V and $(Ad/Al)_V$ increased, S/V decreased and CDOM spectral slope, $S_{275\text{-}295}$, increased with salinity in Otsuchi Bay. Those results suggested tDOM are mainly removed by photodegradation. Considering lignin is photosensitive, photodegradation should be preferred rather than biodegradation in the terrestrial environment (Chapter 2, 3). Therefore, in terrestrial environment, photodegradation is the dominant process for tDOM alternation, with biodegradation of lesser importance (Fig. 5-1).

In the coastal environment, the conservative behavior of lignin concentrations and CDOM parameters, including *a*(350) and $S_{275\text{-}295}$, pointed out physical mixing of river water and seawater is in controlling the concentrations and distributions of tDOM (Chapter 2). Photodegradation of fresh lignin phenols and tDOM can be significant in the early stages of plume dispersal and mixing with surface waters (Chapter 2, 3). The influence of biodegradation is not obvious in the early stages and this is according to the

loss of lignin and CDOM *a*(350) result in the incubation experiment (Chapter 3). Therefore, in coastal environment, physical mixing of river water and seawater shape the distribution of tDOM. Potodegradation highly affects tDOM alternation than biodegradation in seawater (Fig. 5-1). In addition, the change in $S_{275\text{-}295}$ indicated molecular weight of tDOM has altered from high molecular weight (HMW) to low molecular weight (LMW) from terrestrial to marine environments (Fig. 5-1). The signature of tDOM has shifted toward marine DOM, hence, LMW-tDOM is expected to be fairly refractory.

However, biodegradation dominates the transformations of lignin phenols and tDOM in the open-ocean environment and the influences of photodegradation is minor. Once photosensitized lignin phenol is depleted, microbial degradation will be primarily responsible for tDOM alternation (Chapter 3). Additionally, in the western North Pacific Ocean result, lignin $(Ad/Al)_S$ ratio increased from river source to southward during tDOM transport and this inferred biodegradation of tDOM in the open ocean (Chapter 4). Hence, tDOM in the open ocean environment is primarily removed by biodegradation (Fig. 5-1). The influence of photodegradation is very minor, and this only happens in surface layer. The lignin decomposition experiment with river water for two months suggested biodegradation accounted for 67% of total lignin removal and photo-enhanced biodegradation plus direct photodegradation accounted for 33% of total lignin removal.

5.1.2. Relationships between dissolved lignin phenols and CDOM

The incubation results suggested the pathways of lignin and CDOM degradation are different in the presence and absence of solar radiation (Chapter 3). Lignin phenols were quickly removed by photodegradation and then underwent microbial oxidation, whereas CDOM optical properties were mainly sacrificed for photobleaching. In addition, the removal fractions of lignin phenols and CODM *a*(350) were different during the two months incubation. Although lignin phenol concentrations are highly related with CDOM absorption coefficients and spectral slope (Hernes and Benner, 2003; Fichot and Benner, 2011, 2012), the degradation pathways of them are different. CDOM optical properties are primarily responsible for photobleaching processes (Helms et al., 2008; Yamashita et al., 2013), and lignin phenols are photosensitive (Opsahl and Benner, 1998; Benner and

Kaiser, 2011), however, the mechanism of photo-reaction is different between optical properties and chemical characteristic. In addition, CDOM parameters are also affected by *in-situ* biological production, and this could mislead the final results. Swan et al. (2009), for example, investigated CDOM *a*(325) and AOU in the Pacific Ocean and found no clear signature in the CDOM distribution in NPIW layer. Their CDOM results suggested NPIW represents a case where ventilation and advection compete with remineralization processes, because NPIW is the main ventilation pathway of the North Pacific (the formation and circulation of NPIW, Fig. 4-1). However, Swan et al. (2009) ignored the contribution of tDOM in NPIW and also underestimated the fraction of tDOM in bulk DOC in the ocean.

5.1.3. Long-distance transportation of tDOM in the open-ocean

The present study in the western North Pacific Ocean pointed out the long-distance transportation of tDOM (Chapter 4). The results suggested that tDOM can transport for long distance is due to: (1) large volume of freshwater input to the ocean, (2) the sinking water mass. Large volume of freshwater input can ensure the high level concentrations of terrestrial matter in the ocean. However, only a few rivers in the word, such as the Amur River, Amazon River, Congo River and Mississippi River, can provide the large volume of freshwater. Additionally, the distribution of water depth is another key factor, such as the distribution of NPIW is at intermediated layer. Once fresh riverine tDOM sinks quickly into deep sea where no sunlight and low temperature, tDOM is protected from photochemical reaction and biological processes and transports for a long-distance such as NPIW in the western North Pacific Ocean. This result also implying other terrestrial matter combined with tDOM can transport for a long distance in the ocean. Especially the present results strongly support the hypothesis that tDOM play a role as the organic ligands to transport terregenous bioactive metals in the ocean. Dissolved lignin phenol concentrations were high in NPIW layer and accompanied with the high level of dissolved Fe (Nishioka et al., 2007, 2013). Nishioka et al. (2013) pointed out the rich dissolved Fe in NPIW was released from sediments in the Sea of Okhotsk, and this study in the western North Pacific Ocean also suggested a high level of tDOM

was released from soil and/or sediment. The present study provides the evidence that the iron is transported as complexation with tDOM in the ocean.

5.2. Novelty of this study and future perspectives

In this study, lignin phenol concentrations and CDOM optical properties were measured to investigate the distributions and transformations of tDOM in the marine environment. The results suggested tDOM distributes over terrestrial to coastal and even to open-ocean environments. The transformations of tDOM are including physical mixing, photodegradationa and biodegradation. In small spatial scale environment, physical mixing plays an important role in controlling tDOM concentrations and distributions, and accompanied with photodegradation and biodegradation. In Otsuchi Bay, photochemical transformations of fresh riverine tDOM can be significant in the early stages of plume dispersal and mixing with surface waters in the bay. The short water residence times in Otsuchi Bay (~0.5–1 month; Fukuda et al., 2015; Sakamoto et al., 2016) indicate the potential for substantial export of tDOM and associated nutrients and trace elements from Otsuchi Bay to offshore waters. tDOM decomposition experiment for two months suggested biodegradation dominants tDOM transformations rather than photodegradation. Some previous studies have concluded that photodegradation is dominant removal processes of tDOM and this is the first incubation result consistent with recent observations in rivers and river-influenced ocean margins which showed biodegraation would be more important (Ward et al., 2013, Fichot and Benner, 2014).

The results of the lignin distributions in the wide area of the western North Pacific Ocean highlight the potential for the long-distance transport of tDOM as well as other terrestrial mater. Furthermore, the comparison between lignin and CDOM results in the western North Pacific Ocean also indicates more unique indicator of tDOM is lignin phenols rather than CDOM parameters, because the *in-situ* production also influences CDOM optical properties in the marine environments. In addition, these results provide more evidence to the hypothesis, tDOM acts organic ligands for bioactive trace metals in the ocean. This highlights although tDOM is very minor of bulk DOM in the ocean

(Opsahl and Benner, 1997; Hedges, 1992), it still plays an important role in the global carbon cycles. To further investigate the linkages between dissolved trace metals and tDOM can help us have a better understanding of the marine biogeochemical cycles.

In the present study, the water residence time was an unclear factor in the coast and open-ocean environment. Low lignin concentrations in the Otsuchi River implied the potential of longer residence time of tDOM in the Otsuchi River and underwent higher level of degradation than other two rivers. However, it is difficult to distinguish the relatively longer residence time of tDOM in these three rivers according to the lignin ratio results in this study. Non-reactive tDOM was much abundant and coupled with lower molecular weight with longer residence time in the incubation results, and this was consistent with tDOM investigation in Otuchi Bay and also in the open ocean. Therefore, water residence time may play an important role to understand tDOM in the ocean.

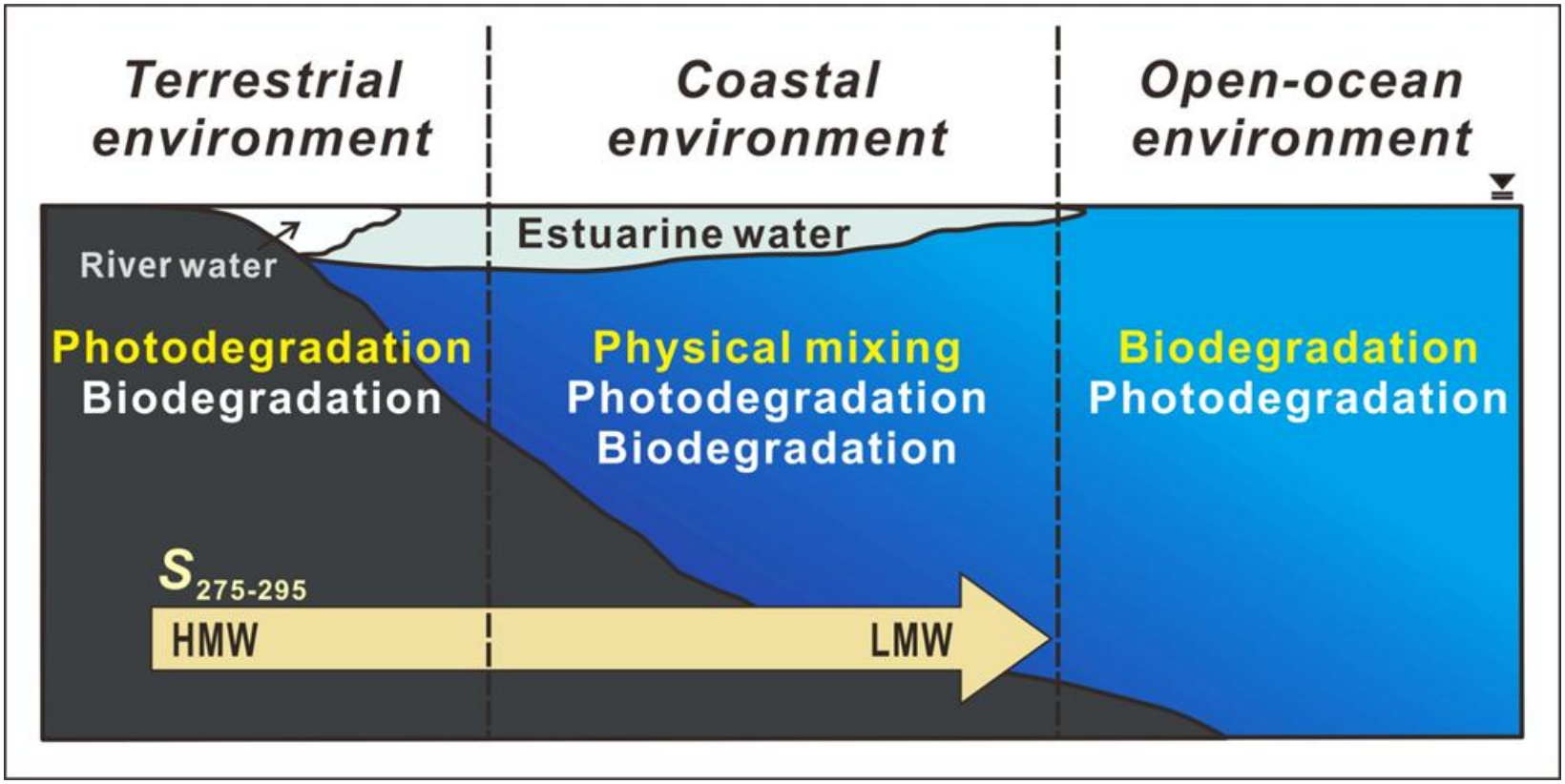

Fig. 5-1 Schematic diagram indicating various transformations of tDOM, and those depend on the environmental conditions. Lignin phenols and tDOM are primarily responsible for photodegradation than biodegradation in the terrestrial environment. In the coastal environment, physical mixing is in controlling the distribution of lignin phenols and tDOM. Photodegradation is significant in the early stages of plume dispersal and mixing with surface waters, and biodegradation has a small effect in this stage. Biodegradation dominates lignin phenols and tDOM transformations in the open-ocean environment and the influence from photodegradation is minor. In addition, tDOM molecular weight has altered from high molecular weight (HMW) to low molecular weight (LMW) from the terrestrial to open-ocean environments, and LMW-tDOM is expected to be fairly refractory in the ocean.

Reference

Aitkenhead, J. A., and McDowell, W. H. (2000). Soil C:N ratio as a preiditor of annual riverine DOC flux at local and global scales. *Global Biogeochem. Cycles* 14, 127-138. doi: 10.1029/1999GB900083

Amon, R. M. W., Rinehart, A. J., Duan S, Louchouarn, P., Prokushkin, A., Guggenberger, G., Bauch, D., Stedmon, C., Raymond, P. A., Holmes, R. M., McClelland, J. W., Peterson, B. J., Walker, S. A., and Zhulidov, A. V. (2012). Dissolved organic matter sources in large Arctic rivers. *Geochim. Cosmochim. Acta* 94, 217-237. doi: 10.1016/j.gca.2012.07.015

Anbo, A., Otobe, H., and Takagi, M. (2005). River water flowing into Otsuchi Bay. *Otsuchi Mar. Res. Cent. Rep.* 30, 4-8. (in Japanese)

Baker, M. A., Valett, H. M., and Dahm, C. N. (2000). Organic carbon supply and metabolism in a shallow groundwater ecosystem. *Ecology* 81, 3133-3148. doi: 10.1890/0012-9658(2000)081[3133:OCSAMI]2.0.CO;2

Benner, R., Pakulski, J. D., McCarthy, M., Hedges, J. I., and Hatcher, P. G. (1992). Bulk chemical characteristics of dissolved organic matter in the ocean. *Science* 255, 1561-1564. doi: 10.1126/science.255.5051.1561

Benner, R., and Opsahl, S. (2001). Molecular indicators of the sources and transformations of dissolved organic matter in the Mississippi river plume. *Org. Geochem.* 32, 597-611. doi: 10.1016/S0146-6380(00)00197-2

Benner, R., and Kaiser, K. (2011). Biological and photochemical transformations of amino acids and lignin phenols in riverine dissolved organic matter. *Biogeochemistry* 102, 209-222. doi: 10.1007/s10533-010-9435-4

Blough, N. V., and Del Vecchio, R. (2002). “Chromophoric DOM in the coastal environment,” in: *Biogeochemistry of marine dissolved organic matter*. Hansell, D. A. and Carlson, C. A. (Eds.), Academic Press, San Diego, pp. 509-546.

Blum, J. D., Gazis, C. A., Jacobson, A. D., and Chamberlian, C. P. (1992). Carbonate versus silicte weathering fluxes of Sr from a high Himalayan watershed. *Mineralogical Magazine* 62A, 174-175. doi: 10.1180/minmag.1998.62A.1.93

Bouillon, S., Yambélé, A., Gillikin, D. P., Teodoru, C., Darchambeau, F., Lambert, T., and Borges, A. V. (2014). Contrasting biogeochemical characteristics of the Oubangui River

and tributaries (Congo River basin). *Scientific Reports* 4, 5402. doi: 10.1038/srep05402

Carlson, C. A., and Hansell, D. A. (2015). "DOM sources, sinks, reactivity, and budgests," in: *Biogeochemistry of marine dissolved organic matter.* ed. D. A. Hansell and C. A. Carlson. (San Diego, California: Academic Press), 65-126.

Coastal Oceanography of Japanese Island (1985). (Tokyo: Tokai University Press). (in Japanese)

Coble, P. G. (1996). Characterization of marine and terrestrial DOM in seawater using excitation-emission matrix spectroscopy. *Mar. Chem.* 51, 325-346. doi: 10.1016/0304-4203(95)00062-3

Coble, P. G. (2007). Marine optical biogeochemistry: the chemistry of ocean color. *Chem. Rev.* 107, 402-418. doi: 10.1021/cr050350+

Dai, M. H., Yin, Z. Q., Meng, F. F., Liu, Q. and Cai, W. J. (2012). Spatial distribution of riverine DOC inputs to the ocean: an updated global synthesis. *Curr. Opin. Environ. Sustain.* 4, 170-178. doi: 10.1016/j.cosust.2012.03.003

de Haan, H. (1972). Molecule size distribution of soluble humic compounds from different natural waters. Feshwat. Biol. 2: 235-241.

Del Vecchio, R., and Blough, N. V. (2002). Photobleaching of chromophoric dissolved organic matter in natural waters: kinetics and modeling. Mar. Chem. 78, 231-253. doi: 10.1016/S0304-4203(02)00036-1

Dickens, A. F., Gudeman, J. A., Gélinas, Y., Baldock, J. A., Tinner, W., Hu, F. S., and Hedges, J. I. (2007). Sources and distribution of CuO-derived benzene carboxylic acids in soils and sediments. *Org. Geochem.* 38, 1256-1276. doi: 10.1016/j.orggeochem.2007.04.004

Evans, G., and Prego, R. (2003). Rias, estuaries and incised valleys: is a ria an estuary? *Marine Geology* 196, 171-175. doi: 10.1016/S0025-3227(03)00048-3

Fichot, C. G., and Benner, R. (2011). A novel method to estimate DOC concentrations from CDOM absorption coefficients in coastal waters. *Geophys. Res. Lett.* 38, L03610. doi: 10.1029/2010gl046152

Fichot, C. G., and Benner, R. (2012). The spectral slop coefficient of chromophoric dissolved organic matter ($S_{275\text{-}295}$) as a tracer of terrigenous dissolved organic carbon in river-influenced ocean margins. *Limnol. Oceanogr.* 57, 1453-1466. doi: 10.4319/lo.2012.57.5.1453

Fichot, C. G., Kaiser, K., Hooker, S. B., Amon, R. M. W., Babin, M., Bélanger, S., Walker, A.

A., and Benner, R. (2013). Pan-Arctic distributions of continental runoff in the Arctic Ocean. *Sci. Rep.* 3, 1053. doi: 10.1038/srep01053

Fichot, C. G., and Benner, R. (2014). The fate of terrigenous dissolved organic carbon in a river-influenced ocean margin. *Global Biogeochem. Cycles* 28, 300-318. doi: 10.1002/2013GB004670

Fichot, C. G., Benner, R., Kaiser, K., Shen, S., Amon, R. W. M., Ogawa, H., and Lu, C.-J. (2016). Predicting dissolved lignin phenol concentrations in the coastal ocean from chromophoric dissolved organic matter (CDOM) absorption coefficients. *Front. Mar. Sci.* 3:7. doi: 10.3389/fmars.2016.00007

Fukuda, H., Ogawa, H., Sohrin, R., Yamasaki, A., and Koike, I. (2007). Sources of dissolved organic carbon and nitrogen in Otsuchi Bay on the Sanriku ria coast of Japan in the spring. *Coastal Mar. Sci.* 31, 19-29.

Fukuda, H., Katayama, R., Yang, Y., Takasu, H., Nishibe, Y., Tsuda, A., and Nagata, T. (2015). Nutrient status of Otsuchi Bay (northeastern Japan) following the 2011 off the Pacific coast of Tohoku Earthquake. *J. Oceanogr.* 72, 39-52. doi: 10.1007/s10872-015-0296-2

Furuya, K., Takahashi, K., and Iizumi, H. (1993). Wind-dependent formation of phytoplankton spring bloom in Otsuchi Bay, a ria in Sanriku, Japan. *J. Oceanogr.* 49, 459-457. doi: 10.1007/BF02234960

Garcia, H. E., and Gordon L. I. (1992). Oxygen solubility in seawater: better fitting equations. *Limnol. Oceanogr.* 37, 1307-1312. doi: 10.4319/lo.1992.37.6.1307

Garcia, H. E., Boyer, T. P., Locarnini, R. A., Antonov, J. I., Mishonov, A. V., Baranova, O. K., Zweng, M. M., Regan, J. R., and Johnson, D. R. (2013) Dissolved oxugen, apparent oxygen utilizationn, and oxygen saturation. *World Ocean Atlas 2013, NOAA Atlas NESDIS 75.*

Hanawa. K., and Yoritaka, H. (2001). North Pacific subtropical mode waters observed in long XBT cross sections along 32.5˚N line. *J. Oceanogr.* 57. 679-692. doi: 10.1023/A:1021276224519

Hansell, D. A., and Carlson, C. A. (2001). Marine dissolved organic matter and the carbon cycle. *Oceanography* 14, 41-49. doi: 10.5670/oceanog.2001.05

Hansell, D. A., Carlson, C. A., and Suzuki, Y. (2002). Dissolved organic carbon export with North Pacific Intermediate Water formation. *Global Biogeochem. Cycles* 16, 1,7-1-7-8. doi: 10.1029/2000GB001361

Hedges, J.I., and Mann, D. C. (1979). The characterization of plant tissues by their lignin

oxidation products. *Geochim. Cosmochim. Acta* 43, 1803-1807. doi: 10.1016/0016-7037(79)90028-0

Hedges, J. I., Blanchette, R. A., Weliky, K., and Devol, A. H. (1988). Effects of fungal degradatin on CuO oxidation products of lignin: a controlled laboratory study. *Geochim. Cosmochim. Acta.* 52, 2717-2726. doi: 10.1016/0016-7037(88)90040-3

Hedges, J. I. (1992). Global biogeochemical cycles: process and problems. *Marine Chemistry* 39, 67-93. doi: 10.1016/0304-4203(92)90096-S

Hedges, J. I., Keil, R. G., and Benner, R. (1997). What happens to terrestrial organic matter in the ocean?. *Org. Geochem.* 27, 195-212. doi: 10.1016/S0146-6380(97)00066-1

Helms, J. R., Stubbins, A., Ritchie, J. D., Minor, E. C., Kieber, D. J., and Mopper, K. (2008). Absorption spectral slopes and slope ratios as indicators of molecular weight, source, and photobleaching of chromophoric dissolved organic matter. *Limnol. Oceanogr.* 53, 955-969. doi: 10.4319/lo.2008.53.3.0955

Hernes, P. J., and Benner, R. (2002). Transport and diagenesis of dissolved and particulate terriigenous organic matter in the North Pacific. *Deep-Sea Res. Pt. I* 49, 2119-2132. doi: 10.1016/S0967-0637(02)00128-0

Hernes, P. J., and Benner, R. (2003). Photochemical and microbial degradation of dissolved lignin phenols: Implication for the fate of terrigenous dissolved organic matter in marine environments. *J. Geophys. Res.* 108, 1453-1466. doi: 10.1029/2002JC001421

Kaiser, K., and Benner, R. (2011). Characterization of lignin by gas chromatography and mass spectrometry using a simplified CuO oxidation method. *Anal. Chem.* 84, 459-464. doi: 10.1021/ac202004r

Kawamiya, M., Kishi, M. J., Ahmed, M. D. K., and Sugimoto, R. (1996). Cause and consequences of phytoplankton blooms in Otsuchi Bay, Japan. *Cont. Shelf Res.* 16, 1683-1698. doi: 10.1016/0278-4343(96)00007-6

Kazama, M., and Noda, T. (2012). Damage statistics (summary of the 2011 off the Pacific coast of Tohoku earthquake damage). *Soils and Foundations* 52, 780-792. doi: 10.1016/j.sandf.2012.11.003

Kicheol, S., Nakano, T., Mori, S., and Ikeda, K. (2015). Distribution of chemical and isotope components in the stream water of Otsuchi town, northeastern Japan. Abstract retrieved from Abstract in Japan Geoscience Union Meeting.

Longhurst, A. (1995). Sesonal cycles of pelagic production and consumption. Prog. Oceanogr.

36, 77-167. doi: 10.1016/0079-6611(95)00015-1

Louchouarn, P., Opsahl, S., and Benner, R. (2000). Isolation and quantification of dissolved lignin from natural waters using solid-phase extraction and GC/MS. *Anal. Chem.* 72, 2780-2787. doi: 10.1021/ac9912552

Lou, T., and Xie, H. (2006). Photochemical alternation of the molecular weight of dissolved organic matter. *Chemosphere* 65, 2333-2342. doi: 10.1016/j.chemosphere.2006.05.001

Mann, P. J., Spencer, R. G. M., Dinga, B. J., Poulsen, J. R., Hernes, P. J., Fiske, G., Salter, M. E., Wang, Z. A., Hoering, K. A., Six, J., and Holmes, R. M. (2014). The biogeochemistry of carbon across a gradient of streams and rivers with the Congo Basin. *J. Geophys. Res.* 119, 687-702. doi: 10.1002/2013JG002442

McNally, A. M., Moddy, E. C., McNeill K. (2005). Kientics and mechanism of the sensitized photodegradation of lignin model compounds. *Photochem Photobiol Sci.* 4, 268-274. doi: 10.1039/b416956e

Meybeck, M. (1993). Riverine transport of atmospheric carbon-sourcesm global typology and budget. *Water Air Soil Pollut.* 70, 443-463. doi: 10.1007/978-94-011-1982-5_31

Meyers-Schulte, K. J., and Hedges, J. I. (1986). Molecular evidence for a terrestrial component of organic matter dissolved in ocean water. *Nature* 321, 61-63. doi: 10.1038/321061a0

Miller, L. M., and Moran, M. A. (1997). Interaction of photochemical and microbial processes in the degradation of refractory dissolved organic matter from a coastal marine environment. *Limnol. Oceanogr.* 42, 1317-1324. doi: 10.4319/lo.1997.42.6.1317

Miller, W. L., and Zepp, R. G. (1995). Photochemical production of dissolved inorganic carbon from terrestrial organic matter: Significance to the oceanic organic carbon cycle. *Geophys. Res. Lett.* 22, 417-420. doi: 10.1029/94GL03344

Mopper, K., and Kieber, D. J. (2002). "Photochemistry and the cycling of carbon, sulfur, nitrogen and phosphorus," in *Biogeochemistry of marine dissolved organic matter*, ed. D. A. Hansell and C. A. Carlson (San Diego, California: Academic Press), 455-508.

Moran, M. A., Sheldon, W. M. JR., and Zepp, R. G. (2000). Carbon loss and optical property changes during long-term photochemical and biological degradation of estuarine dissolved organic matter. *Limnol. Oceanogr.* 45, 1254-1264. doi: 10.4319/lo.2000.45.6.1254

Nakano, T., Saitoh, Y., Kobayashi, T., Mori, S., Shin, K., and Mizutani, H. (2010). "Stronium isotope ratios in water as an index of habitat and foraging sites of aquatic organisms," in *Earth, life, and isotopes.* ed. N. Ohkouchi, I. Tayasu, and K. Koba (Kyoto: Kyoto

University press), 71-84.

Nakatsuka, T., Toda, M., Kawamura, K., and Wakatsuchi, M. (2004). Dissolved and particulate organic carbon in the Sea of Okhotsk: transport from continental shelf to ocean interior. *J. Geophys. Res.* 109, C09S14. doi: 10.1029/2003JC001909

Nelson, N. B., Siegel, D. A., and Michaels, A. F. (1998). Seasonal dynamica of colored dissolved material in the Sargasso *Sea. Deep-Sea Res. Pt.* I 45, 931-957. doi: 10.1016/S0967-0637(97)00106-4

Nelson, N. B., Siegel, D. A., Carlson, C. A., and Swan, C. M. (2010). Tracing global biogeochemical cycles and meridional overturning circulation using chromophoric dissolved organic matter. *Geophys. Res. Lett.* 37, L03610. doi: 10.1029/2009GL042325.

Nishioka, J., Ono, T., Saito, H., Nakatsuka, T., Takeda, A., Yoshimura, T., Suzuki, K., Kuma, K., Nakabayashi, S., Tsumune, D., Mitsudera, H., Johnson, W. K., and Tsuda, A. (2007). Iron supply to the western subarctic Pacific: importance of iron export from the Sea of Okhotsk. *J. Geophys. Res.* 112, C10012. doi: 10.1029/2006JC004055

Nishioka, J., Nakatsuka, T., Watanabe, Y. W., Yasuda, I., Kuma, K., Ogawa, H., Ebuchi, N., Scherbinin, A., Volkov, Y. N., Shiraiwa, T., and Wakatsuchi, M. (2013). Intensive mixing along an island chain controls oceanic biogeochemical cycles. *Global Biogeochem. Cycles* 27, 920-929. doi: 10.1002/gbc.20088

Nishioka, J., Yasuda, I., Liu, H., Nakatsuka, T., and Volkov, Y. N. (2014). Biogeochemical and physical processes in the Sea of Okhotsk and the linkage to the Pacific Ocean. *Processes in Oceano.* 126, 1-7. doi: 10.1016/j.pocean.2014.04.027

Obernosterer, I., and Benner, R. (2004). Competition between biological and photochemical processes in the mineralization of dissolved organic carbon. *Limnol. Oceanogr.* 49, 117-124. doi: 10.4319/lo.2004.49.1.0117

Ogawa, H., and Tanoue, E. (2003). Dissolved organic matter in oceanic waters. *J. Oceanogr.* 59, 129-147. doi: 10.1023/A:1025528919771

Opsahl, S., and Benner, R. (1997). Distribution and cycling of terrigenous dissolved organic matter in the ocean. *Nature* 386, 480-482. doi: 10.1038/386480a0

Opsahl, S., and Benner, R. (1998). Photochemical reactivity of dissolved lignin in river and ocean water. *Limnol. Oceanog*r. 43, 1297-1304. doi: 10.4319/lo.1998.43.6.1297

Otobe, H., Onishi, H., Inada, M., Michida, Y., and Terazaki, M. (2009). Estimation of water circulation in Otsuchi Bay, Japan inferred from ADCP observation. *Coastal Mar. Sci.* 33,

78-86.

Otto, A., and Simpson, M. J. (2006). Evaluation of CuO oxidation parameters for determining the source and stage of lignin degradation in soil. *Biogeochemistry* 80, 121-142. doi: 10.1007/s10533-006-9014-x

Raymond, P. A., and Spencer, R. G. M. (2015). "Riverine DOM," in: *Biogeochemistry of marine dissolved organic matter.* ed. D. A. Hansell and C. A. Carlson. (San Diego, California: Academic Press), 509-533.

Rue, E. L., and Bruland, K. W. (1995). Complexation of iron(III) by natural organic ligands in the central North Pacific as determined by a new competitive ligand equilibration/adsorptive cathodic stripping voltammetric method. *Marine Chemistry* 50, 117-138. doi: 10.1016/0304-4203(95)00031-L

Sakamoto, T. T., Urakawa, L. S., Hasumi, H., Ishizu, M., Itoh, S., Komatsu, T. and Tanaka, K. (2016). Numerical simulation of Pacific water instructions into Otsuchi Bay, northeast of Japan, with a nested-grid OGCM. *J. Oceanogr.* doi: 10.1007/s10872-015-0344-y

Santos, L., Santos, E. B. H., Dias, J. M., Cunha, A., and Almeida, A. (2014). Photochemical and microbial alternations of DOM spectroscopic properties in the estuarine system Ria de Aveiro. *Photochem. Photobiol. Sci.* 13, 1146-1159. doi: 10.1039/c4pp00005f

Schlesinger, W. H., and Melack, J. M. (1981). Transport of organic carbon in the world's river. *Tellus* 33, 172-187.

Shakya. K. M., Louchouarn, P., and Geiffin, R. J. (2011). Lignin-derived phenols in Houston aerosols: implications for natural bachground sources. *Environ. Sci. Technol.* 45, 8268-8275. doi: 10.1021/es201668y

Shen, Y., Fichot, C. G., and Benner, R. (2012). Floodplain influence on dissolved organic matter export from the low Mississippi-Atchafalaya River system to the Gulf of Mexico. *Limnol. Oceanogr.* 57, 1149-1160. doi: 10.4319/lo.2012.57.4.1149

Shen, Y., Chapelle, F. H., Strom, E. W., and Benner, R. (2015). Origins and bioavailability of dissolved organic matter in groundwater. *Biogeochemistry* 122, 61-78. doi: 10.1007/s10533-014-0029-4

Siegel, D. A., Maritorena, S., Nelson, N. B., Hansell, D. A., and Lorenzi-Kayser, M. (2002). Global distribution and dynamics of colored dissolved and detrital irganic materials. *J. Geophys. Res.* 107. 3228. doi: 10.1029/2001JC000965

Simonov, E. A., and Dahmer, T. D. (2008). *Amur-Heilong River basin reader*. Ecosystem Ltd.,

Hong Kong, pp. 426.

Sonnerup, R. E., Quay, P.D., and Bullister, J. L. (1999). Thermocline ventilation and oxygen utilization rates in the subtropical North Pacific based on CFC disrtibutions during WOCE. Deep-Sea Res. Pt. I 46, 777-805. doi: 10.1016/S0967-0637(98)00092-2

Spencer. R. G., Aiken, G. R., Wickland, K. P., Striegl, R. G., and Hernes, P. J. (2008). Seasonal and spatial variability in dissolved organic matter quantity and composition from the Yukon River basin, Alaska. *Global Biogeochem. Cycles* 22, GB4002. doi: 10.1029/2008GB003231

Spencer, R. G. M., Stubbins, A., Hernes, P. J., Baker, A., Mopper, K., Aufdenkampe, A. K., Dyda, R. Y., Mwamba, V. L., Mangangu, A. M., Wabakanghanzi, J. N., and Six, J. (2009). Photochemical degradation of dissolved organic matter and dissolved lignin phenols from the Congo River. *J. Geophys. Res.* 114, G03010. doi: 10.1029/2009JG000968

Spencer, R. G. M., Butler, K. D., and Aiken, G. R. (2012). Dissolved organic carbon and chromophoric dissolved organic matter properties of rivers in the USA. *J. Geophys. Res.* 117, G03001. doi: 10.1029/2011JG001928

Stedmon, C. A., and Markager, S. (2003). Behaviour of the optical properties of coloured dissolved organic matter under conservative mixing. *Estuarine, Coastal and Shelf Science* 57, 973-979. doi: 10.1016/S0272-7714(03)00003-9

Stedmon, C. A., and Nelson, N. B. (2015). "The optical properties of DOM in the ocean," in: *Biogeochemistry of marine dissolved organic matter.* ed. D. A. Hansell and C. A. Carlson. (San Diego, California: Academic Press), 481-508.

Stubbins, A., Spencer, R. G. M., Chen, H., Hatcher, P. G., Mopper, K., Hernes, P. J., Mwamba, V. L., Mangangu, A. M., Wabakanghanzi, J. N., and Six, J. (2010). Illuminated darkness: molecular signatures of Congo River dissolved organic matter and its photochemical alteration as revealed by ultrahigh precision mass spectrometry. *Limnol. Oceanogr.* 55, 1467-1477. doi: 10.4319/lo.2010.55.4.1467

Suzuki, R., and Ishimaru, T. (1990). An improved method for the determination of phytoplankton chlorophyll using N, N-dimethylformamide. *J. Oceanogr. Soc. Japan* 46, 190-194. doi: 10.1007/BF02125580

Swan, C. M., Siegel, D. A., Nelson, N. B., Carison, C. A., and Nasir, E. (2009). Biogeochemical and hydrographic controls on chromophoric dissolved organic matter distribution in the Pacific Ocean. *Deep-Sea Res. Pt. I* 56, 2175-2192. doi: 10.1016/j.dsr.2009.09.002

Talley, L. D. (1991). An Okhotsk Sea water anomaly: implications for ventilation in the North

Pacific. *Deep-Sea Res. Pt. I* 38, S171-S190. doi: 10.1016/S01980149(12)80009-4

Talley, L. D., and Joyce, T. M. (1992). The double silica maximum in the North Pacific. *J. Phys. Res.* 97, 5465-5480. doi: 10.1029/92JC00037

Talley, L. D., Nagata, Y., Fujimura, M., Iwao, T., Kono, T., Inagake, D., Hirai, M., and Okuda, K. (1995). North Pacific intermediate water in the Kuroshio/Oyashio mixed water region. *J. Phys. Oceanogr.* 25, 475-501. doi: 10.1175/1520-0485(1995)025<0475:NPIWIT>2.0.CO;2

Tanaka, K., Komatsu, K., Itoh, S., Yanagimoto, D., Ishizu, M., Hasumi, H., Sakamoto, T. T., Urakawa, S., and Michida, Y. (2015). Baroclinic circulation and its high frequency variability in Otsuchi Bay on the Sanriku ria coast, Japan. *J. Oceanogr.* doi: 10.1007/s10872-015-0338-9

The questionnaire survery report for temporary housing residents in Otsuchi area, Japan (2012). (Iwate: Iwate University press). (in Japanese)

Walker, S. A., Amon, R. M. W., and Stedmon, C. A. (2013). Variations in high-latitude riverine fluorescent dissolved organic matter: a comparison of large Arctic rivers. *J. Geophys. Res. Biogeosci.*118, 1689-1702. doi: 10.1002/2013JG002320

Ward, N. D., Keil, R. G., Medeirod, P. M., Brito, D. C., Cunha, A. C., Dittmar, T., Yager, P. L., Krusche, A. V., and Richey, J. E. (2013). Degradation of terrestrially derived macromolecules in the Amazon River. *Nat. Geosci.* 6, 530-533. doi: 10.1038/NGEO1817

Whitehead, K. (2008). "Marine organic geochemistry," in: *Chemical oceanography and the marine carbon cycle.* ed. S. R. Emerson and J. I. Hedges. (New York: Cambridge University Press), 261-302.

Yamashita, Y., and Tanoue, E. (2008). Production of bio-refractory fluorescent dissolved organic matterin the ocean interior. *Nat. Geosci.* 1. 579-582. doi: 10.1038/ngeo279

Yamashita, Y., and Tanoue, E. (2009). Basin scale distribution of chromophoric dissolved organic matter in the Pacific Ocean. *Limnol. Oceanogr.* 54, 598-609. doi: 10.4319/lo.2009.54.2.0598

Yamashita, Y., Kloeppel, B. D., Knoepp, J., Zausen, G. L., and Jaffé, R. (2011). Effects of watershed history on dissolved organic matter characteristics in headwater streams. *Ecosystems* 14, 1110-1122. doi: 10.1007/s10021-011-9469-z

Yamashita, Y., Nosaka, Y., Suzuki, K., Ogawa, H., Takahashi, K., and Saito, H. (2013). Photobleaching as a factor controlling spectral characteristics of chromophoric dissolved organic matter in open ocean. *Biogeosciences* 10, 7207-7217. doi: 10.5194/bg-10-7207-

2013

Yasuda, I., Okuda, K., and Shimizu, Y. (1996). Distribution and modification of North Pacific intermediate water in the Kuroshio-Oyashio interfrontal zone. *J. Phys. Oceanogr.* 26, 448-465. doi: 10.1175/15200485(1996)026<0448:DAMONP>2.0.CO;2

Yasuda, I., Hiroe, Y., Komatsu, K., Kawasaki, K., Joyce, T. M., Bahr, F., and Kawasaki, Y. (2001). Hydrographic structure and transport of Oyashio south of Hokkaido and the formation of North Pacific intermediate water. *J. Geophys. Res.* 106 (C4), 6931-6942. doi: 10.1029/1999JC000154

Yasuda, I. Y. (2004). North Pacific intermediate water: process in SAGE (subarctic Gyre Experiment) and related projects. *J. Oceanogr.* 60, 385-395. doi: 10.1023/B:JOCE.0000038344.25081.42

You, Y. (2003). The pathway and circulation of North Pacific intermediate water. *Geophys. Res. Lett.* 30, 2291. doi: 10.1029/2003GL018561

中野 孝教（2016）大槌の水のつながりを考える．谷口 真人編 震災と地域の自然・文化ー大槌発・未来へのグランドデザイン．昭和堂，pp.52-70.

Appendix

Appendix 2-1 Dissolved lignin phenol concentrations ($TDLP_{11}$) and composition ratios ($(Ad/Al)_P$ and $(Ad/Al)_S$), and CDOM parameters included absorption coefficient at 250 nm ($a(250)$), slope ratio (S_R) and ratio of absorption at 250 and 365 nm (E_2/E_3) in the rivers.

Month	Sampling site	[1]$TDLP_{11}$ (nmol L^{-1})	$(Ad/Al)_P$	$(Ad/Al)_S$	$a(250)$ (m^{-1})	S_R	E_2/E_3
Nov 2012	Otsuchi River	7.09	1.38	0.53	1.79	0.99	7.23
	Kozuchi River	14.3	1.13	0.64	2.97	1.14	5.52
	Unosumai River	30.8	1.11	0.59	4.24	0.85	5.27
Mar 2013	Otsuchi River	7.24	1.62	0.78	1.19	0.65	3.78
	Kozuchi River	14.0	1.26	0.70	1.71	0.92	4.51
	Unosumai River	34.7	1.01	0.61	3.61	0.82	4.24
May 2013	Otsuchi River	7.61	1.69	0.70	1.69	0.96	4.19
	Kozuchi River	13.6	1.00	0.66	1.87	1.04	5.12
	Unosumai River	39.5	1.13	0.61	4.70	0.99	4.36
July 2013	Otsuchi River	41.2	1.12	0.65	3.30	0.83	5.43
	Kozuchi River	62.9	1.23	0.67	4.85	0.82	4.90
	Unosumai River	87.0	1.11	0.63	7.08	0.83	4.78
Nov 2013	Otsuchi River	18.3	1.46	0.58	2.06	1.05	4.33
	Kozuchi River	24.7	1.07	0.50	2.76	1.00	4.23
	Unosumai River	39.1	1.09	0.59	4.31	0.92	4.36

[1]$TDLP_{11}$: sum of syringyl phenols, vanillyl phenols, cinnamyl phenols and *p*-hydroxy phenols.

Appendix 2-2 Dissolved lignin phenol concentrations ($TDLP_{11}$) and composition ratios [$(Ad/Al)_P$ and $(Ad/Al)_S$], and CDOM parameters [$a(250)$, $S_{275\text{-}295}$, S_R and E_2/E_3] included surface and subsurface water in Otsuchi Bay.

Month	Sampling site	Depth (m)	$TDLP_{11}$ (nmol L^{-1})	$(Ad/Al)_P$	$(Ad/Al)_S$	$a(250)$ (m^{-1})	$S_{275\text{-}295}$ (nm^{-1})	S_R	E_2/E_3
Sep 2012	L1	1	4.73	1.97	0.48	2.55	0.0313	2.25	10.0
	L2	1	4.79	2.01	0.53	2.56	0.0306	2.25	9.58
	L3	1	5.30	1.61	0.53	2.53	0.0305	2.16	9.66
	L4	1	5.66	1.56	0.48	2.59	0.0289	2.05	9.00
	L5	1	6.23	1.51	0.54	2.55	0.0294	2.08	9.20
	L6	1	6.59	1.36	0.56	2.71	0.0286	2.03	8.72
Nov 2012	L0	1	1.53	2.26	0.62	1.62	0.0319	2.16	11.0
	L1	1	1.95	2.40	0.57	1.68	0.0302	2.02	10.8
	L5	1	2.71	1.66	0.57	1.70	0.0299	2.01	12.5
	L6	1	2.93	1.84	0.59	1.69	0.0295	1.84	13.0
Mar 2013	L0	1	5.03	1.71	0.75	No data	No data	No data	No data
	L0	10	No data	No data	No data	1.67	0.0279	2.11	10.1
	L0	45	No data	No data	No data	1.68	0.0284	2.03	11.3
	L1	1	5.15	1.80	0.68	No data	No data	No data	No data
	L3	1	5.77	1.65	0.72	No data	No data	No data	No data
	L3	10	No data	No data	No data	1.58	0.0289	2.12	12.5
	L3	20	No data	No data	No data	1.03	0.0278	2.22	10.6
	L3	35	No data	No data	No data	1.63	0.0285	2.11	11.4
	L5	1	6.06	1.68	0.70	1.61	0.0283	2.10	11.1
	L5	10	No data	No data	No data	1.65	0.0282	2.24	11.2
	L5	18	No data	No data	No data	1.61	0.0274	1.94	10.8
	L6	1	5.61	1.63	0.68	No data	No data	No data	No data
May 2013	L0	1	7.82	1.78	0.59	No data	No data	No data	No data
	L0	10	No data	No data	No data	1.49	0.0300	2.01	11.9
	L0	45	No data	No data	No data	1.48	0.0301	2.01	12.0
	L0	78	5.45	1.95	0.83	No data	No data	No data	No data

(*Continues*)

Appendix 2-2 (*Continued*)

Month	Sampling site	Depth (m)	$TDLP_{11}$ (nmol L^{-1})	$(Ad/Al)_P$	$(Ad/Al)_S$	$a(250)$ (m^{-1})	$S_{275-295}$ (nm^{-1})	S_R	E_2/E_3
May 2013	L1	1	6.77	1.74	0.63	1.92	0.0299	1.85	11.4
	L1	5	No data	No data	No data	1.78	0.0300	1.88	11.2
	L1	10	No data	No data	No data	1.62	0.0300	1.89	11.2
	L1	44	No data	No data	No data	1.52	0.0299	1.95	12.0
	L3	1	7.58	1.54	0.65	1.64	0.0297	1.82	11.6
	L3	5	No data	No data	No data	1.64	0.0298	1.82	11.0
	L3	20	No data	No data	No data	1.81	0.0300	1.85	12.0
	L3	35	6.46	1.74	0.76	1.72	0.0302	1.94	12.5
	L5	1	9.57	1.44	0.60	1.97	0.0302	1.76	11.9
	L5	10	No data	No data	No data	1.84	0.0301	1.85	11.8
	L5	18	No data	No data	No data	1.76	0.0301	1.86	11.8
	L6	1	12.6	1.32	0.70	1.93	0.0281	1.73	10.4
	L6	7	7.35	1.63	0.69	1.80	0.0287	1.73	10.8
	L8	1	11.7	1.36	0.69	1.88	0.0265	1.62	9.34
July 2013	L0	1	7.10	1.85	0.73	1.87	0.0297	1.68	11.3
	L0	10	No data	No data	No data	1.76	0.0321	1.87	13.3
	L0	45	No data	No data	No data	1.61	0.0317	1.90	12.6
	L0	78	2.62	2.36	0.85	1.44	0.0303	1.90	11.9
	L1	1	22.1	1.38	0.66	2.70	0.0237	1.42	7.84
	L1	5	No data	No data	No data	1.95	0.0288	1.69	10.7
	L1	10	No data	No data	No data	1.69	0.0331	1.93	14.6
	L1	20	No data	No data	No data	1.66	0.0331	1.89	13.9
	L1	44	No data	No data	No data	1.66	0.0302	1.77	12.0
	L3	1	21.1	1.29	0.64	2.71	0.0231	1.35	7.67
	L3	5	No data	No data	No data	2.13	0.0260	1.61	9.04
	L3	10	No data	No data	No data	1.86	0.0296	1.86	11.1
	L3	20	No data	No data	No data	1.79	0.0305	1.91	11.5

(*Continues*)

Appendix 2-2 (*Continued*)

Month	Sampling site	Depth (m)	$TDLP_{11}$ (nmol L^{-1})	$(Ad/Al)_P$	$(Ad/Al)_S$	$a(250)$ (m^{-1})	$S_{275-295}$ (nm^{-1})	S_R	E_2/E_3
July 2013	L3	35	4.83	2.06	0.75	1.81	0.0293	1.93	10.6
	L5	1	26.6	1.19	0.60	2.84	0.0226	1.35	7.49
	L5	5	No data	No data	No data	2.14	0.0265	1.63	9.21
	L5	10	No data	No data	No data	1.78	0.0284	1.81	10.3
	L5	18	No data	No data	No data	1.83	0.0293	1.95	10.7
	L6	1	25.1	1.19	0.67	3.04	0.0213	1.23	7.16
	L6	5	No data	No data	No data	2.41	0.0243	1.49	8.16
	L6	7	15.5	1.41	0.70	2.26	0.0253	1.60	8.55
	L8	1	22.9	1.16	0.67	2.39	0.0237	1.39	8.10
Nov 2013	L3	1	9.07	1.40	0.66	2.08	0.0281	1.88	9.65
	L3	5	6.45	1.49	0.66	1.99	0.0296	1.92	10.4
	L3	10	4.80	1.66	0.75	1.86	0.0318	2.07	12.1
	L3	20	4.10	1.79	0.77	1.77	0.0329	2.09	13.1
	L3	35	4.32	1.83	0.65	1.77	0.0327	2.04	12.9

Appendix 2-3 CDOM parameters results include $a(250)$, $a(350)$, $S_{275\text{-}295}$, $S_{350\text{-}400}$, S_R and E_2/E_3 in November 2014.

Sampling site	Salinity	$a(250)$ (m^{-1})	$a(350)$ (m^{-1})	$S_{275\text{-}295}$ (nm^{-1})	$S_{350\text{-}400}$ (nm^{-1})	S_R	E_2/E_3
Otsuchi River	0	1.63	0.45	0.0095	0.0112	0.85	4.42
Kozuchi River	0	2.82	0.85	0.0122	0.0128	0.96	4.09
Unosumai River	0	4.31	1.19	0.0118	0.0141	0.83	4.52
U1	28.52	1.88	0.24	0.0275	0.0161	1.71	10.2
U2	32.82	1.71	0.19	0.0308	0.0163	1.89	12.0
U3	15.52	2.82	0.61	0.0159	0.0162	0.98	5.95
U4	25.34	2.27	0.40	0.0209	0.0163	1.28	7.13
U5	27.92	2.07	0.33	0.0236	0.0173	1.36	8.15
U6	26.71	2.14	0.35	0.0223	0.0173	1.28	7.98
U7	27.76	2.08	0.32	0.0231	0.0177	1.30	8.36
U8	29.42	1.96	0.28	0.0250	0.0179	1.40	9.27
L0	33.81	1.62	0.16	0.0321	0.0159	2.02	12.8
L1	33.95	1.67	0.18	0.0310	0.0148	2.09	11.7
L3	33.87	1.60	0.16	0.0325	0.0160	2.03	12.9
L5	33.86	1.66	0.18	0.0317	0.0150	2.11	11.9
L6	33.74	1.64	0.17	0.0319	0.0155	2.07	11.8
L8	33.57	1.74	0.22	0.0300	0.0162	1.85	10.1

Appendix 4-1 CDOM absorption coefficient at 350 nm [*a*(350)] and spectral slope 275-295 nm ($S_{275\text{-}295}$) in the western North Pacific Ocean.

Station	Depth (m)	Salinity	*a*(350) (m^{-1})	$S_{275\text{-}295}$ (nm^{-1})
Stn. 1	0	no data	0.16	0.0321
	5	32.66	0.16	0.0317
	10	32.66	0.16	0.0312
	20	32.85	0.16	0.0305
	30	32.91	0.17	0.0284
	40	32.97	0.15	0.0290
	50	32.99	0.15	0.0291
	75	33.09	0.15	0.0279
	100	33.11	0.14	0.0275
	150	33.31	0.17	0.0251
	200	33.76	0.19	0.0202
	250	33.92	0.19	0.0194
	300	34.00	0.18	0.0190
	400	34.13	0.18	0.0188
	500	34.22	0.17	0.0189
	600	34.27	0.16	0.0179
	750	34.34	0.17	0.0182
	1000	34.43	0.16	0.0183
	1500	34.54	0.15	0.0181
	2000	34.61	0.14	0.0188
Stn. 2	0	no data	0.12	0.0346
	5	33.73	0.11	0.0348
	10	33.79	0.12	0.0334
	20	33.88	0.13	0.0323
	30	33.81	0.14	0.0314
	40	33.77	0.18	0.0291
	50	33.35	0.14	0.0302
	75	33.05	0.14	0.0291
	100	33.15	0.15	0.0280
	150	33.30	0.14	0.0268
	200	33.44	0.17	0.0242
	250	33.59	0.16	0.0231

(*Continues*)

Appendix 4-1 (*Continued*)

Station	Depth (m)	Salinity	$a(350)$ (m^{-1})	$S_{275-295}$ (nm^{-1})
Stn. 2	300	33.66	0.17	0.0222
	400	34.02	0.15	0.0209
	500	34.08	0.16	0.0196
	550	-	0.16	0.0190
	600	34.13	0.15	0.0193
	650	-	0.16	0.0192
	700	34.26	0.15	0.0190
	750	34.28	0.17	0.0181
	800	34.29	0.17	0.0179
	1000	34.39	0.15	0.0181
	1500	34.52	0.14	0.0181
	2000	34.60	0.12	0.0187
Stn. 3	0	no data	0.12	0.0353
	5	34.11	0.11	0.0349
	10	34.11	0.12	0.0343
	20	34.11	0.12	0.0339
	30	34.18	0.11	0.0342
	40	34.33	0.12	0.0334
	50	34.25	0.11	0.0337
	75	34.27	0.11	0.0306
	100	34.13	0.11	0.0307
	150	33.90	0.11	0.0300
	200	33.82	0.11	0.0288
	250	33.82	0.12	0.0286
	300	33.81	0.14	0.0246
	400	33.92	0.15	0.0219
	500	33.98	0.16	0.0203
	550	-	0.15	0.0199
	600	34.12	0.15	0.0195
	650	-	0.15	0.0188
	700	34.20	0.15	0.0188
	750	-	0.16	0.0181

(*Continues*)

Appendix 4-1 (*Continued*)

Station	Depth (m)	Salinity	$a(350)$ (m^{-1})	$S_{275-295}$ (nm^{-1})
Stn. 3	800	34.27	0.15	0.0184
	1000	34.36	0.17	0.0171
	1500	34.50	0.15	0.0170
	2000	34.58	0.13	0.0179
Stn. 4	0	no data	0.07	0.0422
	5	34.31	0.08	0.0400
	10	34.36	0.07	0.0402
	20	34.38	0.10	0.0357
	30	34.51	0.12	0.0342
	40	34.55	0.11	0.0346
	50	34.59	0.11	0.0341
	75	34.59	0.09	0.0329
	100	34.55	0.14	0.0314
	150	34.56	0.08	0.0357
	200	34.46	0.07	0.0359
	250	34.42	0.08	0.0338
	300	34.35	0.08	0.0327
	400	34.24	0.09	0.0299
	500	34.06	0.12	0.0265
	550	-	0.14	0.0239
	600	33.99	0.14	0.0230
	650	-	0.13	0.0225
	700	34.06	0.14	0.0214
	750	-	0.15	0.0204
	800	34.15	0.14	0.0200
	1000	34.29	0.14	0.0189
	1500	34.49	0.15	0.0175
	2000	34.58	0.13	0.0176
Stn. 5	0	no data	0.06	0.0452
	5	34.39	0.06	0.0446
	10	34.39	0.07	0.0446
	20	34.42	0.07	0.0419
	30	34.48	0.10	0.0371

(*Continues*)

Appendix 4-1 (*Continued*)

Station	Depth (m)	Salinity	$a(350)$ (m^{-1})	$S_{275-295}$ (nm^{-1})
Stn. 5	40	34.51	0.08	0.0374
	50	34.53	0.10	0.0364
	75	34.65	0.08	0.0368
	100	34.66	0.08	0.0369
	150	34.65	0.07	0.0370
	200	34.62	0.07	0.0379
	250	34.54	0.09	0.0331
	300	34.46	0.08	0.0325
	400	34.26	0.09	0.0300
	500	34.06	0.13	0.0254
	550	-	0.12	0.0251
	600	33.98	0.13	0.0239
	650	-	0.14	0.0220
	700	34.06	0.15	0.0215
	750	34.11	0.14	0.0208
	800	34.15	0.15	0.0201
	1000	34.30	0.15	0.0188
	1500	34.50	0.15	0.0179
	2000	34.59	0.14	0.0175
Stn. 6	0	no data	0.05	0.0482
	5	34.70	0.05	0.0483
	10	34.66	0.06	0.0470
	20	34.52	0.06	0.0450
	30	34.52	0.07	0.0422
	40	34.59	0.10	0.0378
	50	34.61	0.11	0.0356
	75	34.72	0.09	0.0366
	100	34.73	0.07	0.0382
	150	34.71	0.07	0.0380
	200	34.70	0.08	0.0372
	250	34.68	0.07	0.0379
	300	34.65	0.07	0.0357
	400	34.53	0.08	0.0326

(*Continues*)

Appendix 4-1 (*Continued*)

Station	Depth (m)	Salinity	a(350) (m^{-1})	S275-295 (nm^{-1})
Stn. 6	500	34.34	0.10	0.0311
	550	-	0.10	0.0291
	600	34.14	0.11	0.0285
	650	-	0.12	0.0251
	700	34.02	0.14	0.0242
	750	-	0.14	0.0228
	800	34.04	0.13	0.0224
	1000	34.23	0.14	0.0197
	1500	34.47	0.14	0.0179
	2000	34.57	0.14	0.0186
Stn. 7	0	no data	0.05	0.0516
	5	34.86	0.04	0.0529
	10	34.87	0.04	0.0524
	20	35.10	0.04	0.0516
	30	35.14	0.05	0.0503
	40	34.94	0.06	0.0444
	50	34.93	0.10	0.0377
	75	34.81	0.11	0.0333
	100	34.75	0.09	0.0364
	150	34.71	0.08	0.0371
	200	34.68	0.08	0.0357
	250	34.62	0.07	0.0353
	300	34.51	0.08	0.0330
	400	34.33	0.09	0.0311
	500	34.13	0.11	0.0264
	600	34.03	0.13	0.0233
	650	-	0.14	0.0227
	700	34.05	0.13	0.0225
	750	34.10	0.14	0.0210
	850		0.14	0.0196
	1000	34.32	0.15	0.0183
	1500	34.52	0.14	0.0177
	2000	34.61	0.13	0.0178

(*Continues*)

Appendix 4-1 (*Continued*)

Station	Depth (m)	Salinity	$a(350)$ (m^{-1})	$S_{275-295}$ (nm^{-1})
Stn. 8	0	-	0.04	0.0558
	5	35.37	0.03	0.0572
	10	35.37	0.06	0.0509
	30	35.22	0.04	0.0541
	40	35.19	0.06	0.0488
	50	35.16	0.05	0.0490
	75	35.08	0.07	0.0429
	100	34.95	0.09	0.0395
	150	34.86	0.10	0.0354
	200	34.69	0.11	0.0325
	250	34.63	0.09	0.0335
	300	34.51	0.09	0.0325
	400	34.27	0.11	0.0287
	500	34.12	0.12	0.0265
	550	-	0.13	0.0238
	600	34.05	0.13	0.0222
	650	-	0.13	0.0212
	700	34.12	0.15	0.0201
	750	34.17	0.15	0.0197
	800	34.21	0.15	0.0189
	1000	34.36	0.15	0.0185
	1500	34.55	0.13	0.0188
	2000	34.61	0.13	0.0185
Stn. 9	0	no data	0.03	0.0540
	5	34.92	0.03	0.0543
	10	34.92	0.04	0.0529
	20	34.92	0.03	0.0528
	30	34.92	0.04	0.0546
	40	34.92	0.03	0.0538
	50	34.94	0.04	0.0502
	75	35.03	0.07	0.0415
	100	35.19	0.09	0.0367
	150	35.15	0.09	0.0345

(*Continues*)

Appendix 4-1 (*Continued*)

Station	Depth (m)	Salinity	$a(350)$ (m^{-1})	$S_{275-295}$ (nm^{-1})
Stn. 9	200	34.84	0.09	0.0333
	250	34.70	0.07	0.0353
	300	34.62	0.08	0.0334
	400	34.34	0.08	0.0299
	500	34.13	0.10	0.0262
	550	-	0.12	0.0235
	600	34.12	0.12	0.0226
	650	-	0.13	0.0206
	700	34.21	0.14	0.0199
	750	34.27	0.14	0.0191
	800	34.34	0.13	0.0191
	1000	34.48	0.12	0.0184
	1500	34.58	0.12	0.0183
	2000	34.61	0.12	0.0186
Stn. 10	0	no data	0.04	0.0520
	5	34.90	0.04	0.0537
	10	34.91	0.05	0.0522
	20	34.91	0.04	0.0553
	30	34.91	0.04	0.0527
	40	34.91	0.04	0.0542
	50	34.91	0.05	0.0507
	75	35.04	0.07	0.0444
	100	35.07	0.07	0.0442
	150	35.21	0.10	0.0345
	200	34.96	0.11	0.0337
	250	34.56	0.11	0.0316
	300	34.31	0.12	0.0287
	400	34.18	0.13	0.0231
	500	34.28	0.14	0.0207
	550	-	0.14	0.0200
	600	34.40	0.13	0.0203
	650	-	0.13	0.0199

(*Continues*)

Appendix 4-1 (*Continued*)

Station	Depth (m)	Salinity	$a(350)$ (m^{-1})	$S_{275-295}$ (nm^{-1})
Stn. 10	700	34.46	0.14	0.0193
	750	-	0.13	0.0192
	800	34.49	0.13	0.0190
	1000	34.53	0.13	0.0188
	1500	34.58	0.12	0.0184
	2000	34.63	0.13	0.0182
Stn. 11	0	no data	0.04	0.0503
	5	34.40	0.03	0.0537
	10	34.40	0.04	0.0531
	20	34.40	0.04	0.0525
	30	34.40	0.04	0.0526
	40	34.40	0.03	0.0534
	75	34.46	0.06	0.0433
	100	34.94	0.07	0.0408
	150	35.03	0.10	0.0338
	200	34.80	0.10	0.0322
	250	34.47	0.11	0.0253
	300	34.50	0.13	0.0221
	400	34.57	0.12	0.0212
	500	34.55	0.11	0.0215
	550	-	0.12	0.0213
	600	34.53	0.12	0.0208
	650	-	0.11	0.0208
	700	34.53	0.12	0.0202
	750	34.53	0.12	0.0200
	800	34.53	0.13	0.0194
	1000	34.54	0.13	0.0189
	1500	34.59	0.11	0.0192
	2000	34.63	0.13	0.0183
Stn. 12	0	no data	0.05	0.0512
	5	no data	0.04	0.0553
	10	34.74	0.04	0.0505
	30	34.76	0.05	0.0524

(*Continues*)

Appendix 4-1 (*Continued*)

Station	Depth (m)	Salinity	$a(350)$ (m^{-1})	$S_{275-295}$ (nm^{-1})
Stn. 12	40	34.81	0.04	0.0515
	50	34.99	0.05	0.0497
	75	35.09	0.06	0.0429
	100	35.04	0.08	0.0386
	150	34.86	0.09	0.0367
	200	34.72	0.07	0.0369
	250	34.68	0.10	0.0326
	300	34.60	0.08	0.0343
	400	34.35	0.09	0.0306
	500	34.17	0.12	0.0252
	550	-	0.12	0.0240
	600	34.13	0.13	0.0228
	650	-	0.14	0.0220
	700	34.23	0.13	0.0209
	750	-	0.15	0.0200
	800	34.32	0.13	0.0198
	1000	34.48	0.13	0.0195
	1500	34.57	0.12	0.0194
	2000	34.61	0.11	0.0201
Stn. 13	0	no data	0.05	0.0496
	5	no data	0.04	0.0513
	10	34.37	0.05	0.0510
	20	34.38	0.04	0.0502
	30	34.44	0.07	0.0436
	40	34.54	0.07	0.0420
	50	34.62	0.10	0.0362
	75	34.73	0.11	0.0345
	100	34.74	0.09	0.0365
	150	34.73	0.07	0.0393
	200	34.72	0.08	0.0382
	250	34.69	0.06	0.0392
	300	34.65	0.07	0.0348

(*Continues*)

Appendix 4-1 (*Continued*)

Station	Depth (m)	Salinity	$a(350)$ (m^{-1})	$S_{275-295}$ (nm^{-1})
Stn. 13	400	34.47	0.08	0.0318
	500	34.25	0.11	0.0292
	550	-	0.11	0.0268
	600	34.09	0.12	0.0255
	650	-	0.12	0.0242
	700	34.03	0.13	0.0232
	750	-	0.14	0.0222
	800	34.10	0.19	0.0198
	1000	34.27	0.15	0.0192
	1500	34.49	0.14	0.0184
	2000	34.59	0.12	0.0187
Stn. 14	0	no data	0.04	0.0526
	5	no data	0.03	0.0534
	10	34.61	0.04	0.0526
	20	34.61	0.05	0.0512
	30	34.61	0.04	0.0517
	40	34.87	0.07	0.0437
	50	34.92	0.06	0.0444
	75	34.95	0.08	0.0408
	100	34.99	0.11	0.0353
	150	34.84	0.10	0.0350
	200	34.76	0.10	0.0340
	250	34.71	0.08	0.0359
	300	34.65	0.09	0.0338
	400	34.41	0.09	0.0309
	500	34.19	0.10	0.0270
	550	-	0.12	0.0247
	600	34.14	0.12	0.0233
	650	-	0.14	0.0224
	700	34.16	0.14	0.0216
	800	34.19	0.14	0.0200
	1000	34.40	0.16	0.0181

(*Continues*)

Appendix 4-1 (*Continued*)

Station	Depth (m)	Salinity	$a(350)$ (m^{-1})	$S_{275-295}$ (nm^{-1})
Stn. 14	1500	34.53	0.13	0.0180
	2000	34.60	0.11	0.0192
Stn. 15	0	no data	0.05	0.0470
	5	34.40	0.05	0.0491
	10	34.39	0.05	0.0492
	20	34.38	0.04	0.0491
	30	34.44	0.07	0.0437
	40	34.58	0.09	0.0399
	50	34.71	0.11	0.0364
	75	34.80	0.10	0.0357
	100	34.82	0.09	0.0361
	150	34.80	0.07	0.0391
	200	34.78	0.08	0.0374
	250	34.73	0.07	0.0365
	300	34.70	0.07	0.0362
	400	34.59	0.09	0.0318
	500	34.39	0.09	0.0303
	550	-	0.11	0.0274
	600	34.25	0.11	0.0266
	650	-	0.11	0.0251
	700	34.19	0.13	0.0228
	750	34.20	0.13	0.0224
	800	34.22	0.12	0.0218
	1000	34.34	0.13	0.0196
	1500	34.52	0.13	0.0190
	2000	34.60	0.10	0.0199
Stn. 16	0	no data	0.05	0.0476
	5	34.27	0.04	0.0525
	10	34.26	0.08	0.0446
	20	34.26	0.09	0.0413
	30	34.26	0.05	0.0487
	40	34.43	0.16	0.0337
	50	34.58	0.07	0.0406

(*Continues*)

Appendix 4-1 (*Continued*)

Station	Depth (m)	Salinity	$a(350)$ (m^{-1})	$S_{275-295}$ (nm^{-1})
	75	34.80	0.09	0.0366
	100	34.79	0.13	0.0335
	150	34.80	0.11	0.0343
	200	34.79	0.11	0.0335
	250	34.75	0.15	0.0288
	300	34.71	0.14	0.0285
	400	34.61	0.11	0.0291
	500	34.45	0.10	0.0281
Stn. 16	550	-	0.09	0.0287
	600	34.31	0.13	0.0249
	650	-	0.12	0.0248
	700	34.18	0.12	0.0241
	750	34.20	0.12	0.0232
	800	34.21	0.13	0.0218
	1000	34.34	0.18	0.0181
	1500	34.51	0.13	0.0190
	2000	34.60	0.18	0.0169
	0	no data	0.05	0.0451
	5	34.12	0.05	0.0452
	10	34.11	0.05	0.0440
	20	34.16	0.10	0.0370
	30	34.17	0.13	0.0325
	40	34.31	0.16	0.0283
	50	34.53	0.15	0.0302
Stn. 17	75	34.72	0.08	0.0328
	100	34.75	0.08	0.0322
	150	34.83	0.08	0.0312
	200	34.77	0.09	0.0270
	250	34.71	0.09	0.0267
	300	34.66	0.09	0.0252
	400	34.46	0.11	0.0226
	500	34.22	0.10	0.0225

(*Continues*)

Appendix 4-1 (*Continued*)

Station	Depth (m)	Salinity	$a(350)$ (m^{-1})	$S_{275-295}$ (nm^{-1})
Stn. 17	600	34.23	0.11	0.0219
	700	34.27	0.12	0.0206
Stn. 18	0	no data	0.05	0.0451
	5	33.17	0.05	0.0452
	10	33.23	0.05	0.0440
	20	33.36	0.10	0.0370
	30	33.71	0.13	0.0325
	40	34.04	0.16	0.0283
	50	34.29	0.15	0.0302
	75	34.51	0.08	0.0328
	100	34.52	0.08	0.0322
	150	34.48	0.08	0.0312
	200	34.38	0.09	0.0270
	250	34.33	0.09	0.0267
	300	34.31	0.09	0.0252
	400	34.29	0.11	0.0226
	500	34.29	0.10	0.0225
	600	34.29	0.11	0.0219
	700	34.33	0.12	0.0206
Stn. G-9	0	16	7.27	0.0166